

SCHOOL OF  
CIVIL ENGINEERING  
  
INDIANA  
DEPARTMENT OF HIGHWAYS

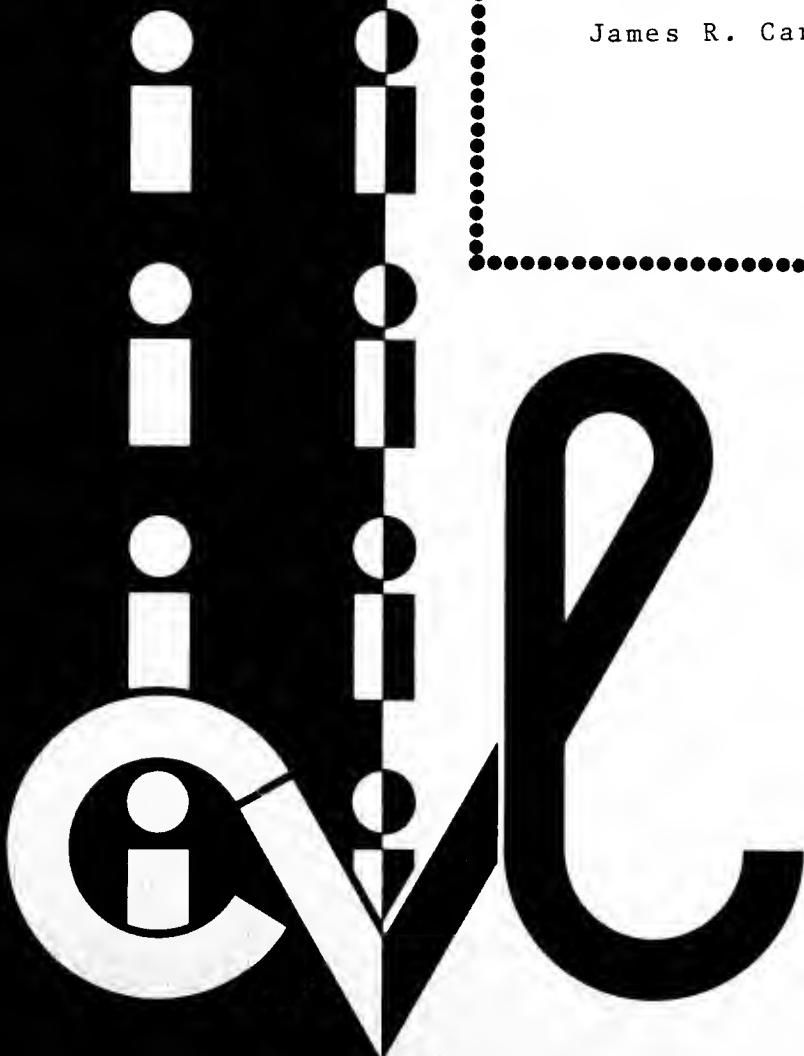
JOINT HIGHWAY RESEARCH PROJECT

JHRP-86-21

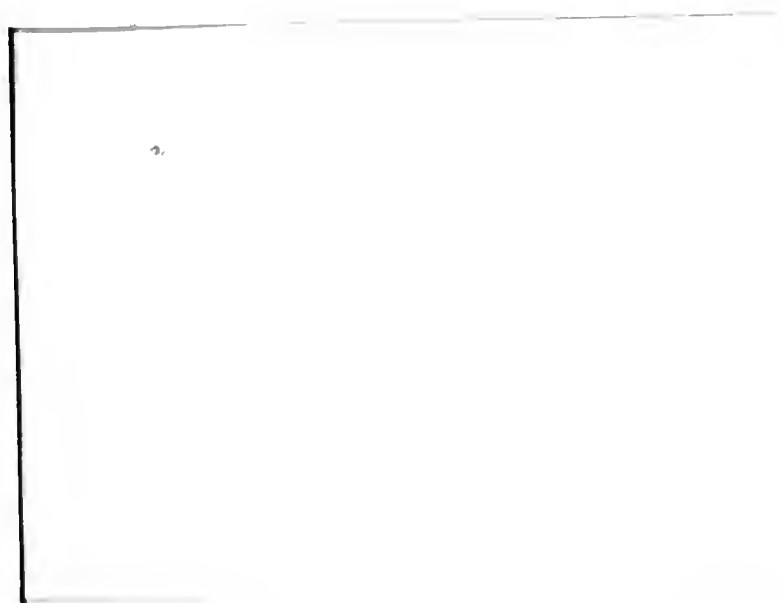
Informational Report

SLOPE STABILITY ANALYSIS CONSIDERING  
TIEBACKS AND OTHER CONCENTRATED LOAD

James R. Carpenter



PURDUE UNIVERSITY



JOINT HIGHWAY RESEARCH PROJECT

JHRP-86-21

Informational Report

SLOPE STABILITY ANALYSIS CONSIDERING  
TIEBACKS AND OTHER CONCENTRATED LOADS

James R. Carpenter

Digitized by the Internet Archive  
in 2011 with funding from  
LYRASIS members and Sloan Foundation; Indiana Department of Transportation

Information Report

SLOPE STABILITY ANALYSIS CONSIDERING TIEBACKS  
AND OTHER CONCENTRATED LOADS

To: H. L. Michael, Director  
Joint Highway Research Project

December 10, 1986

File: 6-14-11

From: C. W. Lovell  
Research Engineer  
Joint Highway Research Project

The attached report contains the background information for the tieback option present in STABL4 and PC STABL4. These programs were developed as an implementation package for the FHWA, and are currently in use by many engineers. However, this document is the only one explaining the theory and assumptions involved, and is accordingly a valuable reference.

This report also contains a description of the development of STABL5 and PC STABL5. The User Manual for STABL5 and PC STABL5 has already been published as JHRP 86/14.

Respectfully submitted,



C. W. Lovell  
Research Engineer

CWL:cr

cc: A.G. Altschaeffl	D.E. Hancher	P.L. Owens
J.M. Bell	R.A. Howden	B.K. Partridge
M.E. Cantrall	M.K. Hunter	G.T. Satterly
W.F. Chen	J.P. Isenbarger	C.F. Scholer
W.L. Dolch	J.F. McLaughlin	K.C. Sinha
R.L. Eskew	K.M. Mellinger	C.A. Venable
J.D. Fricker	R.D. Miles	T.D. White
		L.E. Wood



Informational Report

SLOPE STABILITY ANALYSIS CONSIDERING TIEBACKS  
AND OTHER CONCENTRATED LOADS

by

James R. Carpenter  
Graduate Instructor in Research

School of Civil Engineering  
Purdue University  
West Lafayette, Indiana 47907

for the

Joint Highway Research Project  
Purdue University  
West Lafayette, Indiana 47907

File: 6-14-11

December 1986



## ACKNOWLEDGEMENTS

I want to thank my major professor, Professor C.W. Lovell, for his friendship, guidance and support during the preparation of this thesis, and for providing me with the opportunity to work on such interesting and rewarding research. My sincere thanks and appreciation is extended to Professor Jean-Lou Chameau for providing me with access to his microcomputer and for his helpful suggestions during the preparation of this thesis. Thanks is also extended to Professor Milton Harr for his advice and for reviewing this thesis.

I also wish to thank Mr. Dana Humphrey for sharing his knowledge of microcomputers and for providing useful input on implementation of STABL on the microcomputer, and Mr. Sunil Sharma for sharing his knowledge of slope stability.

Thanks is also expressed to Mr. Thomas C. Anderson and Mr. David E. Weatherby of Schnabel Foundation Company for their practical suggestions concerning tieback structures and for providing several case histories on the performance of tiedback walls and slopes.

Thanks also go to Wendy Nather who typed portions of the text and to Rudy Gonzembach who drafted the figures.

The financial support for this research project was provided by the Federal Highway Administration and the Indiana Department of Highways through the Joint Highway Research Project, Purdue University, West Lafayette, Indiana.

Finally, I especially want to thank my wife, Theresa, and my parents, for their continuous support, encouragement, patience, and understanding, during my study at Purdue.

## TABLE OF CONTENTS

	Page
LIST OF FIGURES . . . . .	vii
LIST OF ABBREVIATIONS AND SYMBOLS . . . . .	xi
HIGHLIGHT SUMMARY . . . . .	.xvii
CHAPTER I. INTRODUCTION. . . . .	1
Problem Statement . . . . .	1
Purpose of Study. . . . .	6
Organization of Report. . . . .	9
CHAPTER II. EXISTING STABILITY ANALYSES FOR TIEDBACK STRUCTURES . . . . .	11
Support of Excavations. . . . .	11
Krantz Method. . . . .	18
Rankine-Ostermayer Method. . . . .	22
French Code of Practice Method . . . . .	24
Broms Method . . . . .	29
Littlejohn Method. . . . .	31
Ostermayer Method. . . . .	31
Finite Element Method. . . . .	33
Summary. . . . .	36
Stabilization of Landslides . . . . .	37
Slope Stability Program Method . . . . .	40
CHAPTER III. LOAD DISTRIBUTION METHOD - STABL4 . . . . .	46
Theory. . . . .	47
Implementation in STABL4. . . . .	52
Distribution of Load to Failure Surface . . . . .	68
Distribution of Normal and Tangential Stresses . . . . .	68
Restrictions on Distribution . . . . .	74
Applications. . . . .	76
Uniform Line Loads . . . . .	76
Distributed Loads. . . . .	76
Braced Excavations . . . . .	79
Buried Tiedback Structures . . . . .	80
Reinforced Earth Walls/Fabric Reinforced Walls . . . . .	80

Limitations . . . . .	82
CHAPTER IV. PARAMETRIC STUDIES USING THE LDM . . . . .	84
Effect of Point of Application on Factor of Safety. . . . .	84
Load Inclination versus Factor of Safety. . . . .	89
Load Magnitude versus Factor of Safety. . . . .	92
Purely Cohesive Soils. . . . .	92
c - $\phi$ Soils. . . . .	94
Effect of Multiple Tieback Structures on Factor of Safety. . . . .	100
CHAPTER V. MICROCOMPUTER IMPLEMENTATION OF STABL4 - PCSTABL4. . . . .	108
Implementation Process. . . . .	109
Plotting Routines - PLOTSTBL. . . . .	113
Program Characteristics . . . . .	115
Versions. . . . .	115
CHAPTER VI. ADDITION OF SPENCER'S METHOD OF SLICES - STABL5 AND PCSTABL5. . . . .	117
Stability Equations. . . . .	118
STABL Method of Solution - Linear Approximation Method. . . . .	127
Line of Thrust . . . . .	133
Spencer Options in STABL . . . . .	136
CHAPTER VII. SUMMARY, CONCLUSIONS AND RECOMMENDATIONS . . . . .	139
Summary . . . . .	139
Conclusions . . . . .	142
Recommendations . . . . .	145
LIST OF REFERENCES. . . . .	147
References Cited. . . . .	147
General References. . . . .	151
APPENDIX	
Derivation of Simplified Bishop Factor of Safety. . . . .	153

## LIST OF FIGURES

Figure	Page
1. Permanently Tiedback Wall Used to Prevent a Landslide in Fairfax County, VA (After Weatherby, 1982) . . . . .	2
2. Tiedback H-Beam and Lagging Sheeting System for a Cut-and-Cover Station in Philadelphia (After Weatherby, 1982). . . . .	3
3. Tiered Permanently Tiedback Bored Pile Wall With Masonry Finish Near Innsbruck, Austria (After Weatherby, 1982). . . . .	4
4. Permanently Tiedback Wall Used to Stabilize a Fill Slide Near Spruce Pine, NC (After Weatherby, 1982) . . . . .	5
5. Permanently Tiedback Concrete Elements Used to Support a Rock Slope Near Alpnach-Stad, Switzerland (After Weatherby, 1982). . . . .	7
6. Tie-downs Used to Increase the Slope Stability of a Dam . . . . .	8
7. Components of a Tiedback Retaining Structure (After Cheney, 1984). . . . .	12
8. Soil Mass Analyzed for Overall Stability Analysis (After Schnabel, 1982). . . . .	14
9. Modes of Tiedback Wall Stability and Instability.	15
10. Determination of Overall Stability by Krantz Method (After Anderson, 1983). . . . .	19
11. Determination of Overall Stability by Ranke-Ostermayer Method (After Cheney, 1984) . . . . .	23
12. Overall Stability for Two Independent Anchors (After French Code of Practice, 1972). . . . .	25

13.	Overall Stability for Two Anchors (After French Code of Practice, 1972) . . . . .	26
14.	Overall Stability with Complex Failure Surface (After French Code of Practice, 1972) . . . . .	28
15.	Determination of Overall Stability by Broms Method (After Broms, 1968) . . . . .	30
16.	Determination of Overall Stability by Littlejohn Method (After Littlejohn, 1972) . . . . .	32
17.	Determination of Overall Stability by Ostermayer Method (After Ostermayer, 1977) . . . . .	34
18.	Determination of Stability by Finite Element Method (After Hobst and Zajic, 1983; and, Bendel and Weber, 1966) . . . . .	35
19.	Landslide Stabilization Using Tiebacks . . . . .	38
20.	Distribution of Stress Along Potential Failure Surface (After Sangrey, 1982) . . . . .	41
21.	Normal Stress Distribution on Failure Surface Considering a Concentrated Load . . . . .	43
22.	Flamant's Distribution of Stress . . . . .	49
23.	Application of Flamant's Solution to Tiedback Slopes . . . . .	51
24.	Intersection of Tieback Anchor with Trial Failure Surface . . . . .	53
25.	Development of Tieback Anchor Capacity . . . . .	55
26.	Tieback Input Parameters . . . . .	56
27.	Transfer of Tieback Load to Potential Failure Surface . . . . .	58
28.	Slice Forces Considered In STABL4 Using Load Distribution Method . . . . .	65
29.	Distribution of Normal Stress to Potential Failure Surface . . . . .	69
30.	Distribution of Tangential Stress to Potential Failure Surface . . . . .	72

31.	Distribution of Tieback Stress to Potential Failure Surface for Two Tiebacks. . . . .	73
32.	Limit of Stress Distribution to Potential Failure Surface Due to Tieback Load . . . . .	75
33.	Restriction of Stress Distribution to Potential Failure Surface Due to Tieback Load . . . . .	77
34.	Modelling Distributed Loads with Concentrated Loads Using Load Distribution Method. . . . .	78
35.	Modelling Buried Tiedback Structures. . . . .	81
36.	Effect of Point of Application on Factor of Safety. . . . .	86
37.	Load Line of Action Through Center of Rotation. .	88
38.	Slope Model for Load Inclination versus Factor of Safety Study. . . . .	90
39.	Load Inclination versus Factor of Safety. . . . .	91
40.	Slope Model for Load versus Factor of Safety Studies . . . . .	93
41.	Load versus Factor of Safety for Purely Cohesive Soil Slopes . . . . .	95
42.	Load versus Factor of Safety for $c - \phi$ Soil Slopes. . . . .	97
43.	Effect of Increased Normal Component on Factor of Safety for $c - \phi$ Soil Slopes. . . . .	98
44.	Slope Model for Multiple Tiedback Structures Study . . . . .	101
45.	Total Tieback Load versus Factor of Safety. . . .	103
46.	Total Tieback Load versus Factor of Safety - Potential Failure Surface #1. . . . .	105
47.	Total Tieback Load versus Factor of Safety - Potential Failure Surface #2. . . . .	107
48.	Slice Forces Considered for Spencer's Method of Slices. . . . .	120

49.	Slice Forces Considered in Derivation of Stability Equations for Spencer's Method of Slices. . . . .	121
50.	Variation of $F_m$ and $F_f$ with $\theta$ . . . . .	126
51.	Determination of $F_f$ and $F_m$ for a Given Value of $\theta$ by the Linear Approximation Method. . . . .	130
52.	Determination of the FOS and $\theta$ Satisfying Complete Equilibrium Using the Linear Approximation Method. . . . .	132
53.	Line of Thrust. . . . .	135
Appendix		
Figure		
A-1.	Slice Forces Considered for Derivation of Simplified Bishop Method of Slices Using Load Distribution Method . . . . .	154

## LIST OF ABBREVIATIONS AND SYMBOLS

Abbreviations

DOS	- Disk Operating System
FOS, FS	- Factor of Safety
HP	- Hewlett-Packard trade name
HP-7470A	- Hewlett-Packard two-pen plotter
IBM	- International Business Machines trade name
LAM	- Linear Approximation Method
LDM	- Load Distribution Method
MS-DOS	- Microsoft brand of personal computer disk operating system
8087	- Intel 8087 Math Co-Processor

Symbols

$A_c$	- cylindrical surface area of soil-anchor bond
ALPHA	- inclination of the base of a slice
ALPHA1	- angle formed by the line of action of the force PRAD and the normal to the base of a slice
$A_1$	- term used by STABL to calculate the factor of safety by the Simplified Bishop and Simplified Janbu methods of slices
$A_2$	- term used by STABL to calculate the factor of safety by the Simplified Bishop and Simplified Janbu methods of slices
$A_3$	- term used by STABL to calculate the factor of safety by the Simplified Bishop method of slices

$A_4$	- term used by STABL to calculate the factor of safety by the Simplified Bishop method of slices
$A_5$	- term used by STABL to calculate the factor of safety by the Simplified Bishop method of slices
$A_6$	- term used by STABL to calculate the factor of safety by the Simplified Bishop method of slices
$c$	- Mohr-Coulomb failure envelope intercept - cohesion intercept
$c'$	- effective cohesion
$C'_a$	- available cohesion force on the base of a slice
CORR	- correction factor for a row of tiebacks
$d_a$	- diameter of grouted anchor
DEV	- angle between horizontal and center of the base of a slice
DIST	- distance between the point of application of tieback load and center of the base of a slice
$dx$	- width of a slice
$E_a$	- active earth pressure force
$f_a$	- available unit soil-anchor bond stress
$f(x)$	- arbitrary interslice angle scaling function
$F$	- friction force
$F_f$	- factor of safety with respect to force equilibrium
$F_{int}$	- intersection of the $F_m$ and $F_f$ curves approximated by straight lines
$F_m$	- factor of safety with respect to moment equilibrium
$F_1$	- factor of safety with respect to tieback #1
$F_2$	- factor of safety with respect to tieback #2
$h$	- height of a slice

$h_{eq}$	- height of the horizontal earthquake force above the base of a slice
$H$	- horizontal distance between tiebacks
$I, INCLIN$	- inclination of a tieback
$k_h$	- horizontal pseudo-static earthquake coefficient
$k_v$	- vertical pseudo-static earthquake coefficient
$l_a$	- length of a grouted anchor
$L$	- free (unbonded) length of a tieback
$L_l$	- line of thrust height above the midpoint of the base of a slice, on the left side of the slice
$L_r$	- line of thrust height above the midpoint of the base of a slice, on the right side of the slice
$m$	- number of tieback loads
$M_1$	- sliding mass #1
$M_2$	- sliding mass #2
$n$	- number of slices in a sliding mass
$N$	- normal force on the base of a sliding mass
$P$	- tieback or concentrated load applied to the ground surface; passive earth pressure force
$P, P_a, P_l$	- active earth pressure force
$P_{a1}$	- active earth pressure force on sliding mass #1
$P_{a2}$	- active earth pressure force on sliding mass #2
$P_A$	- resultant earth pressure force
$P_p$	- passive earth pressure force
$PNORM$	- normal force on the center of the base of a slice caused by a tieback load
$PRAD$	- radial force on the center of the base of a slice caused by a tieback load

PSUM	- sum of the radial forces acting on the center of the bases of the sliding mass in the direction of the tieback load
PTAN	- tangential force on the center of the base of a slice caused by a tieback load
QF	- resultant interslice force on a slice
$r_u$	- pore pressure parameter
R	- radius - distance between circular failure surface and center of rotation; distance to point in question
$R, R_a, R_1$	- resisting force
$R_n$	- nominal resisting force
$R_2$	- resisting force on sliding mass #2
$S_c$	- friction force
$S_\phi$	- resisting force
$S_u$	- undrained soil strength
$S_1$	- term used in the stability equations for Spencer's method of slices
$S_2$	- term used in the stability equations for Spencer's method of slices
$S_3$	- term used in the stability equations for Spencer's method of slices
T	- tieback force
$T_{des}$	- design tieback force
$T_{exist}$	- existing tieback force
$T_{poss}$	- possible tieback force
$T_{max}$	- maximum tieback force
$T_1$	- tieback force on sliding mass #1; total tieback force on retaining structure #1
$T_2$	- tieback force on sliding mass #2; total tieback force on retaining structure #2

$T'_1$	- maximum tieback force on sliding mass #1
$T'_2$	- maximum tieback force on sliding mass #2
$T'_{12}$	- maximum tieback force for sliding masses #1 and #2
TLOAD	- equivalent tieback line load
TNORM	- total normal force on the center of the base of a slice caused by all rows of tiebacks
TTAN	- total tangential force on the center of the base of a slice caused by all rows of tiebacks
TTHETA	- angle between line of action of tieback and the center of the base of a slice
u	- pore water pressure
$U_1$	- horizontal pore water force on the left side of a slice
$U_r$	- horizontal pore water force on the right side of a slice
V	- vertical reaction force
$W, W_1$	- weight of sliding mass
$W_a$	- weight of active sliding mass
$W_2$	- weight of sliding mass #2
x	- x coordinate of point of application of tieback load
y	- y coordinate of point of application of tieback load
$z_0$	- depth to zero active effective stress
z	- interslice side force
$z_1$	- interslice force on the left side of a slice
$z_r$	- interslice force on the right side of a slice
$\alpha$	- inclination of the base of a slice
$\beta$	- inclination of the top of a slice

$\delta$	- inclination of a surcharge load acting on the top of a slice
$\Delta N'$	- effective normal force acting on the base of a slice
$\Delta Q$	- surcharge load acting on the top of a slice
$\Delta S_r$	- available resisting shear force acting on the base of a slice
$\Delta T$	- tieback force acting on top of slice (Spencer's)
$\Delta U_\alpha$	- water force acting on the base of a slice
$\Delta U_\beta$	- water force acting on the top of a slice
$\Delta W$	- weight of a slice
$\gamma$	- unit weight
$\lambda$	- Morgenstern and Price method interslice angle scaling function
$\phi$	- slope of the Mohr-Coulomb failure envelope - friction angle
$\phi'$	- effective friction angle
$\phi'_a$	- available effective friction angle
$\phi'_m$	- mobilized effective friction angle
$\phi'_n$	- nominal friction angle
$\pi$	- pi
$\sigma'_1$	- effective major principal stress
$\sigma'_3$	- effective minor principal stress
$\sigma_r$	- radial stress
$\Sigma$	- summation
$\theta$	- angle between the line of action of a concentrated load and the point in question; slope of the resultant interslice side forces
$\theta_{int}$	- slope of the resultant interslice side forces calculated by the intersection of the linear approximation of the $F_m$ and $F_f$ curves

## HIGHLIGHT SUMMARY

A method has been developed to assess the internal and external stability of tiedback structures using a limiting equilibrium method. The method is called the Load Distribution Method (LDM) and is contained in the slope stability programs, STABL4, PCSTABL4, STABL5 and PCSTABL5. A discussion of the methods available previously for assessing the stability of tiedback structures precedes the presentation of the model used in the development of the Load Distribution Method.

The Load Distribution Method attempts to account for the diffusion of stresses throughout a soil mass caused by a tieback load by distributing the load to the potential failure surface, and hence all slices of the sliding mass, rather than accounting for the applied load only on the slice on which it acts. The stress distribution utilized in the LDM assumes that the problem conforms to a semi-infinite elastic half space; however, tiedback slopes or retaining walls do not necessarily conform to this assumption. Parametric studies were performed during development of the

LDM to determine the reasonableness of applying the assumptions used in the method of solution to tiedback slopes and retaining walls. These studies revealed that the method generally gives reasonable results; however, at large applied loads and for some slope models, the method may not yield conservative solutions since the problem modelled does not totally conform to a semi-infinite elastic half space.

The LDM is especially useful for assessing the stability of tiedback structures used for landslide control and may be used to determine the length, inclination and load of tiebacks required for slope stabilization. Parametric studies are presented which demonstrate the effects of such tieback characteristics on the stability of tiedback structures and slopes. In addition, recommendations for further research are presented so that the stress distribution used in the LDM may be modified to account for problems which do not conform to the semi-infinite elastic half space assumption.

STABL4 has been implemented on a microcomputer (PCSTABL4) and plotting routines have been developed for a microcomputer compatible plotter. The implementation process is discussed along with the characteristics of the microcomputer version.

Finally, Spencer's method of slices has been incorporated in STABL5 and PCSTABL5. A new iterative method called the Linear Approximation Method (LAM) has been

developed which rapidly and accurately determines the factor of safety by Spencer's method of slices, while avoiding problems with non-convergence. A User's Manual for STABL5 and PCSTABL5 has been written as a separate document.



## CHAPTER I. INTRODUCTION

### Problem Statement

The use of tiebacks in geotechnical engineering and construction for support of excavations and landslide control has increased substantially within the last 10 to 15 years. As a result, the need for a reliable and practical method of analyzing the internal and overall (external) stability of slopes and retaining walls subjected to tieback and anchor loads has become evident.

Tiebacks are routinely used for both temporary and permanent support of excavated slopes. Figure 1 shows an excavation where permanent tiebacks have been utilized to stabilize a potential failure surface, while Figure 2 illustrates the use of temporary tiebacks for support of an excavation. Tiedback or anchored retaining structures for temporary and permanent support of excavations may consist of soldier piles with wood lagging, sheetpiling, drilled concrete pile walls (Figure 3), or concrete diaphragm walls constructed using the slurry trench method.

The use of tiebacks for stabilization of embankments and slopes is illustrated in Figure 4. Tiedback retaining structures for stabilization of embankments and slopes may

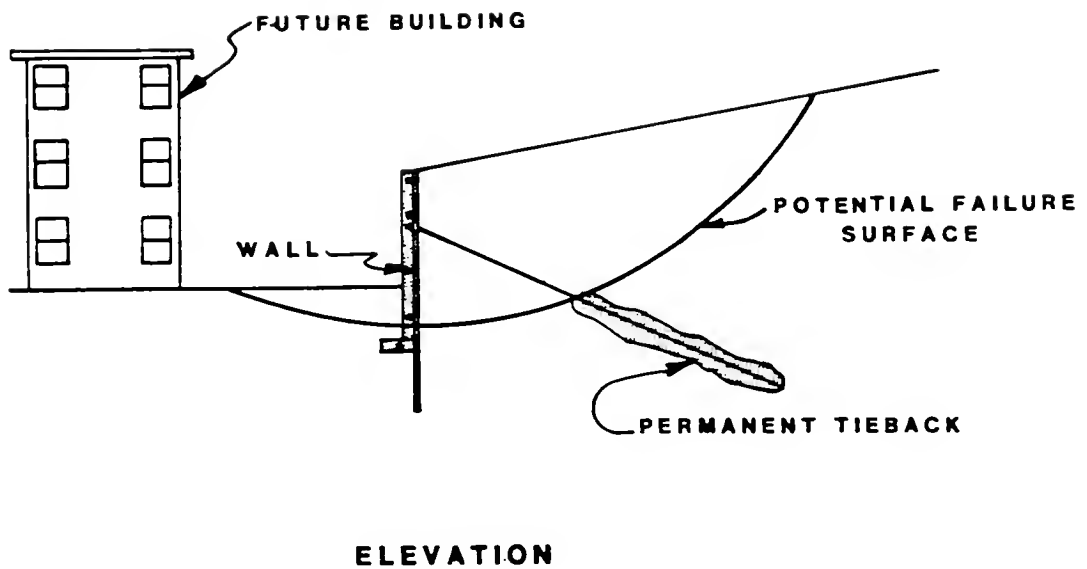


FIGURE 1. Permanently Tiedback Wall Used to Prevent a Landslide in Fairfax County, VA (After Weatherby, 1982)

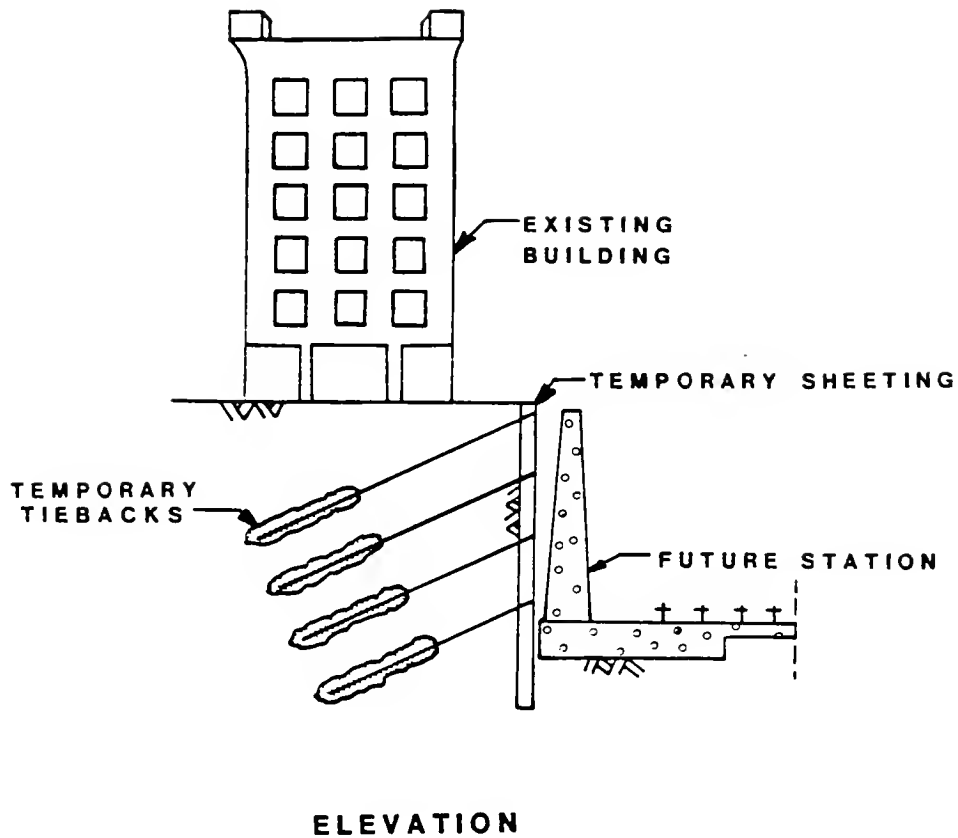


FIGURE 2. Tiedback H-Beam and Lagging Sheetling System for a Cut-and-Cover Station in Philadelphia (After Weatherby, 1982)

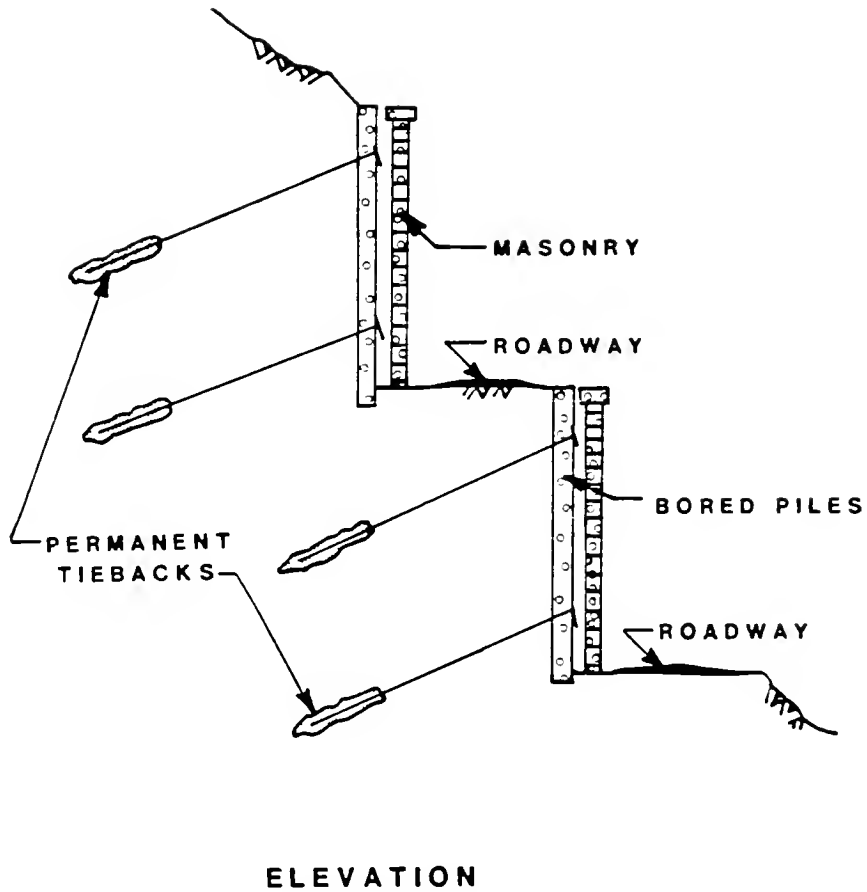


FIGURE 3. Tiered Permanently Tiedback Bored Pile Wall With Masonry Finish Near Innsbruck, Austria (After Weatherby, 1982)

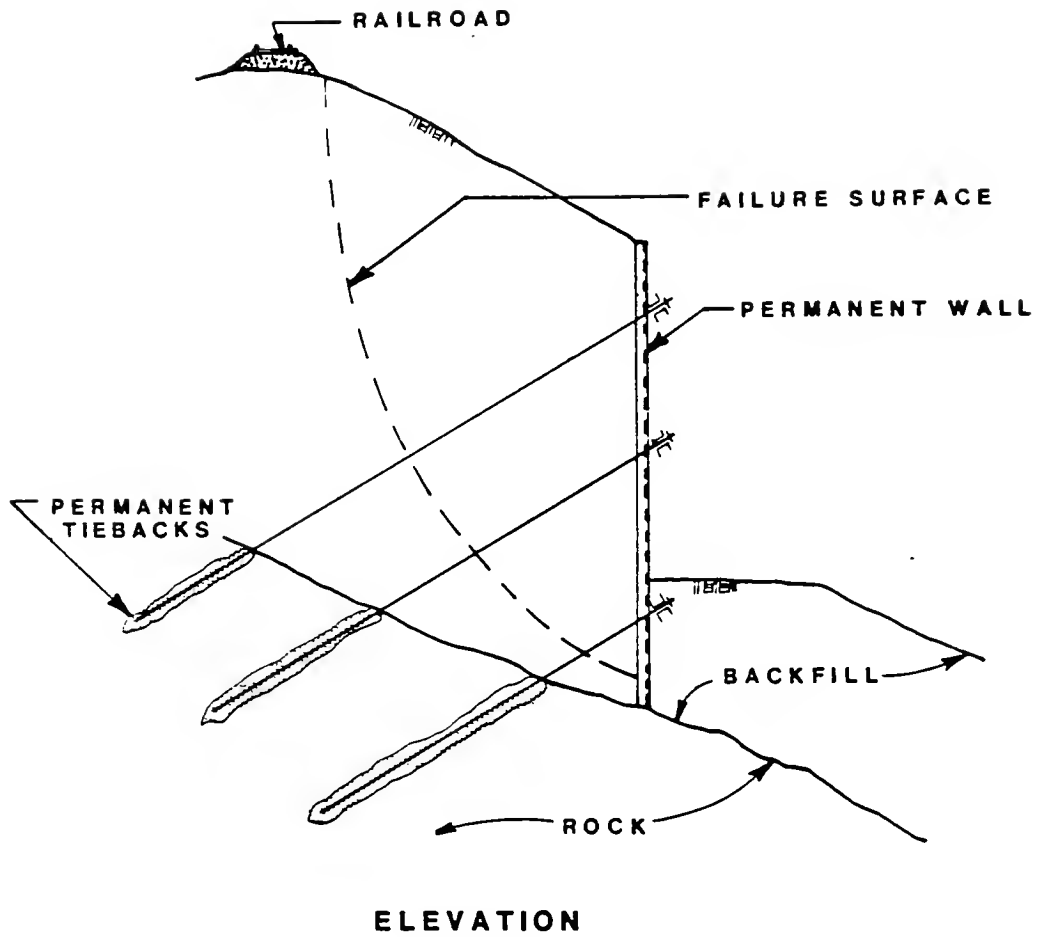


FIGURE 4. Permanently Tiedback Wall Used to Stabilize a Fill Slide Near Spruce Pine, NC (After Weatherby, 1982)

be continuous along the length of the slope as in soldier piles and wood lagging, or be discontinuous as in tiedback drilled piers (Figure 3), or concrete bearing pads or buttress elements placed on the face of the slope, (Figure 5). In addition, tie-downs can be used to increase the slope stability of dams, as shown in Figure 6.

Current methods for determining the internal and overall stability of multiple tiedback structures often involve errors in the statement of the problem, or require arbitrary assumptions to be made for performing the calculations. In addition, it is extremely difficult and tedious to take into consideration non-homogeneous soil conditions and multiple tiebacks with existing methods of stability analysis. Therefore, there exists a need for a convenient and logical method for determining the internal and external stability of multiple tiedback retaining structures considering non-homogeneous soil conditions.

#### Purpose of Study

The purpose of this study was to develop a rational and convenient method of assessing the internal and overall stability of tiedback and anchored retaining structures. Such a method has been developed by the author and is presented in Chapter III.

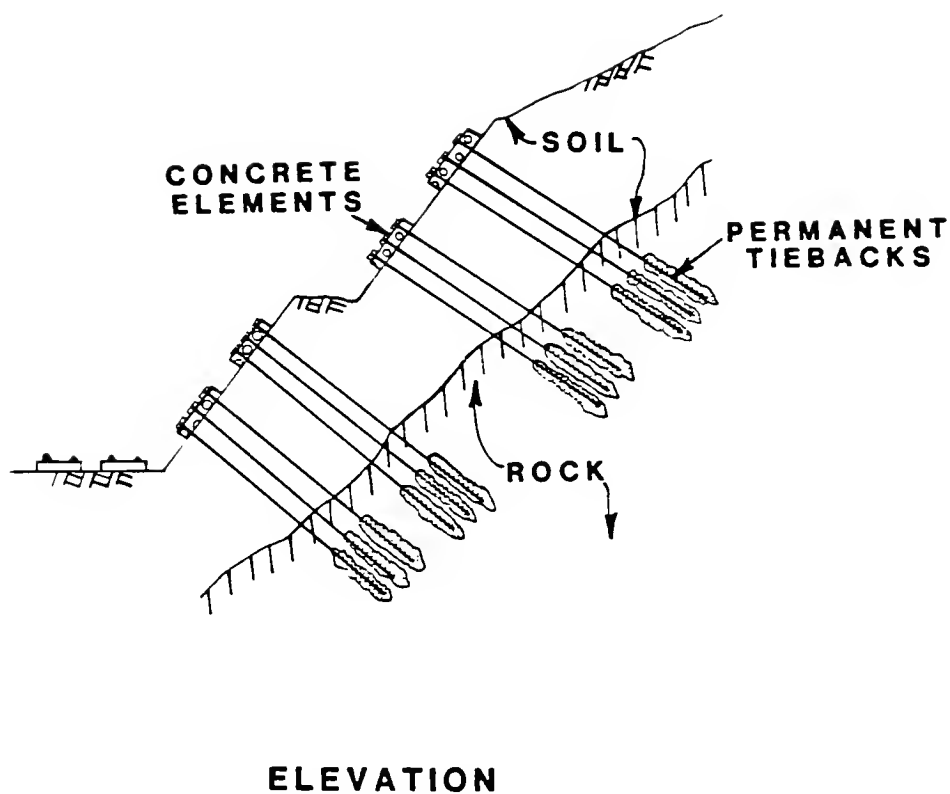


FIGURE 5. Permanently Tiedback Concrete Elements Used to Support a Rock Slope Near Alpnach-Stad, Switzerland (After Weatherby, 1982)

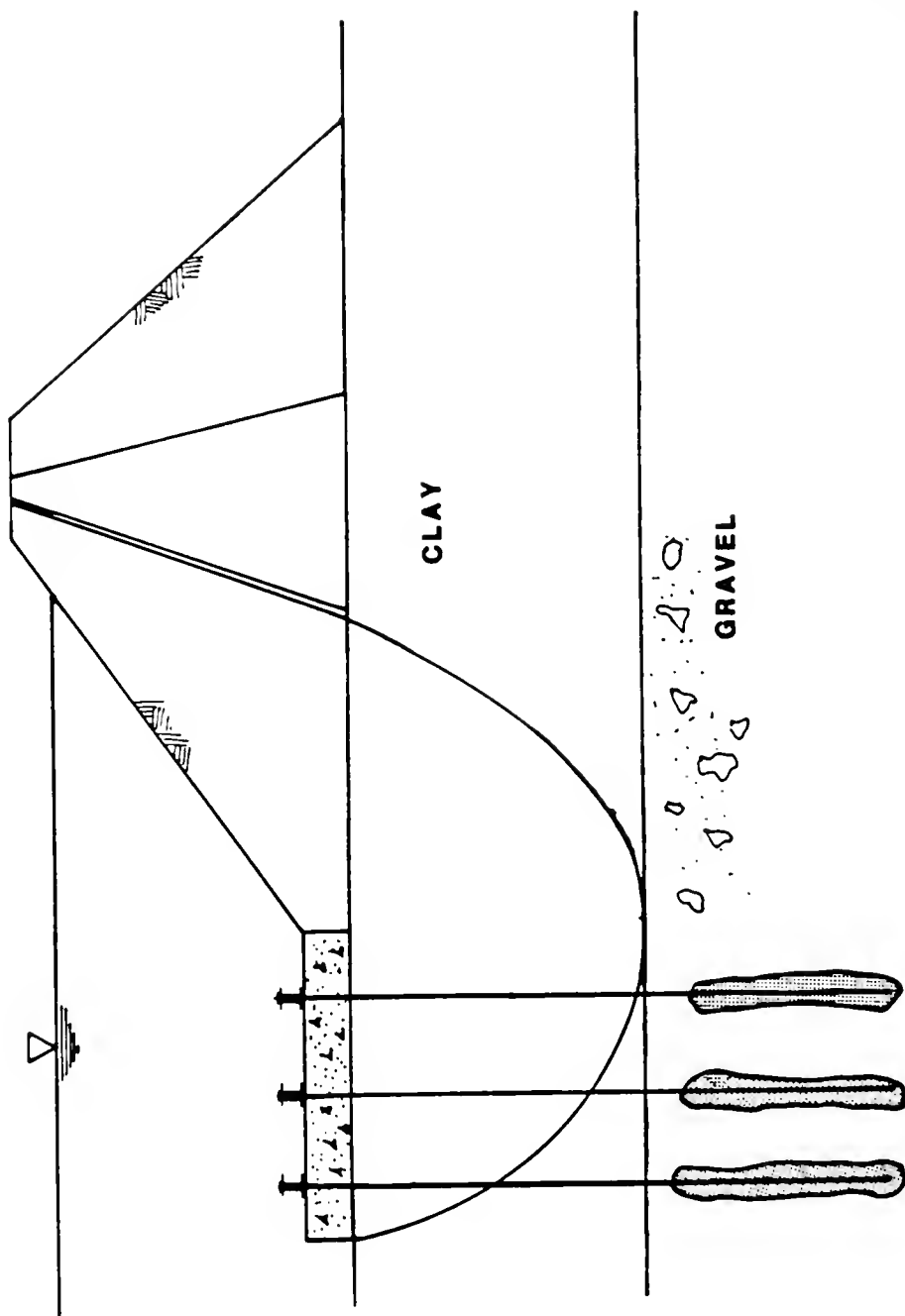


FIGURE 6. Tie-downs Used to Increase the Slope Stability of a Dam

## Organization of Report

Chapter II reviews the current methods used in practice for determining the internal and overall stability of tiedback and anchored structures. This chapter discusses the assumptions, strengths and weaknesses of each method.

Chapter III presents the author's development of the Load Distribution Method (LDM), contained in the slope stability program, STABL4. This method is capable of conveniently and rationally determining the internal and external stability of multiple tiedback and anchored retaining structures for support of temporary or permanent excavations, and for control of landslides. This chapter also presents several applications of STABL4's Load Distribution Method.

The results of several parametric studies using the Load Distribution Method are presented in Chapter IV. This chapter provides a study of the factors affecting the stability of tiedback retaining structures for both excavations and landslide control.

A brief discussion of the implementation of the mainframe computer program, STABL4, on the IBM microcomputer is presented in Chapter V. Chapter VI discusses the addition of Spencer's method of slices to the STABL program and the author's development of the Linear Approximation Method (LAM). The LAM is a new iterative procedure for

determining the factor of safety satisfying complete equilibrium.

The work performed and the results of this study are summarized in Chapter VII. Conclusions are drawn regarding extant stability analyses and the usefulness of the Load Distribution and Linear Approximation Methods. Recommendations for future work are also included in Chapter VII.

Finally, an appendix is included which presents the derivation of the Factor of Safety (FOS) by the Simplified Bishop method of slices as programmed in STABL considering tieback loads using the Load Distribution Method.

## CHAPTER II. EXISTING STABILITY ANALYSES FOR TIEBACK STRUCTURES

### Support of Excavations

Tiebacks tie a structure to a stable soil mass through an anchor secured in the earth. Figure 7 shows the components of a typical tiedback retaining structure. The anchor is attached to a steel tendon which is also connected to the retaining structure. After installation of the tendon and grouting of the anchor, the tendon is stressed (pulled) to the desired load using hydraulic jacks. This load is then locked off and permanently applied to the structure. The load in the steel tendon applies a stabilizing force to the structure which is developed by the anchor in the stable soil mass. Tiebacks are different from deadman anchors in that the tieback anchor is made through a hole drilled or driven into the soil for installation of the tendon.

Assumptions are made in the design of a tiedback retaining structure concerning the lateral earth pressure distribution behind the proposed wall. On the basis of the lateral earth pressure distribution, the location and magnitude of load applied to each tieback is determined for the internal, (local), stability of the wall. The

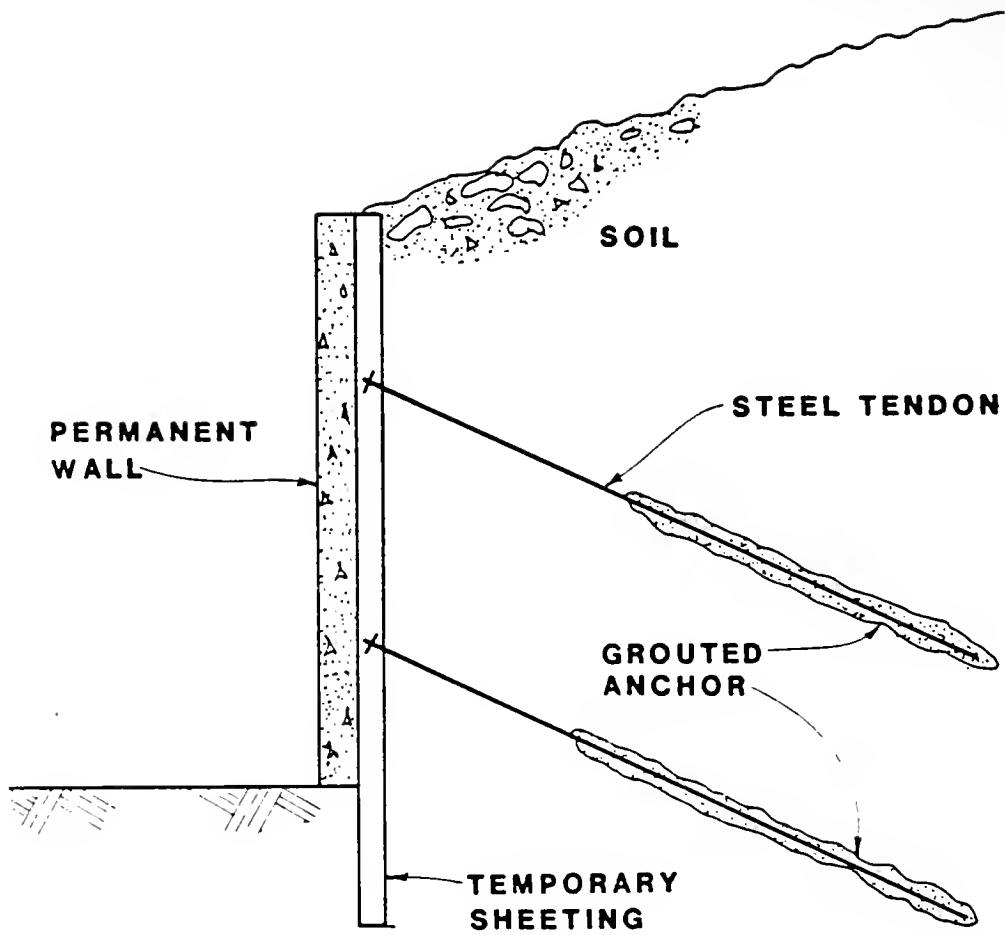


FIGURE 7. Components of a Tiedback Retaining Structure  
(After Cheney, 1984)

structure-anchor system must be designed to resist the lateral earth pressures with a suitable degree of safety, i.e. factor of safety (FOS). The tieback must then be designed to carry the computed load. The anchor of the tieback must be made long enough to be beyond the area which would be disturbed by wall movements and so that it will not pull out of the soil mass in which it is secured.

Tiebacks tie a structure to a mass of soil which must also be both internally and externally stable. The shape of the soil mass analyzed for overall stability, is often taken to be wedge shaped as shown in Figure 8. If a tiedback wall is properly designed and the tiebacks have the desired capacity, the pressure on the wall and the tieback will create stabilizing internal forces within this soil mass. The soil-structure-anchor system is then considered to be internally stable.

In addition to the internal stability of the soil-structure-anchor system, the overall stability of the system must also be checked and a suitable FOS determined. While the internal stability of the soil-structure-anchor system may be satisfactory, the overall stability of the system may not be suitable as shown in Figure 9. The determination of the FOS for any potential surface which passes behind the ends of the tiebacks is considered a FOS with respect to overall (external) stability, Figure 9a, while the FOS for any potential failure surface which passes between the ends

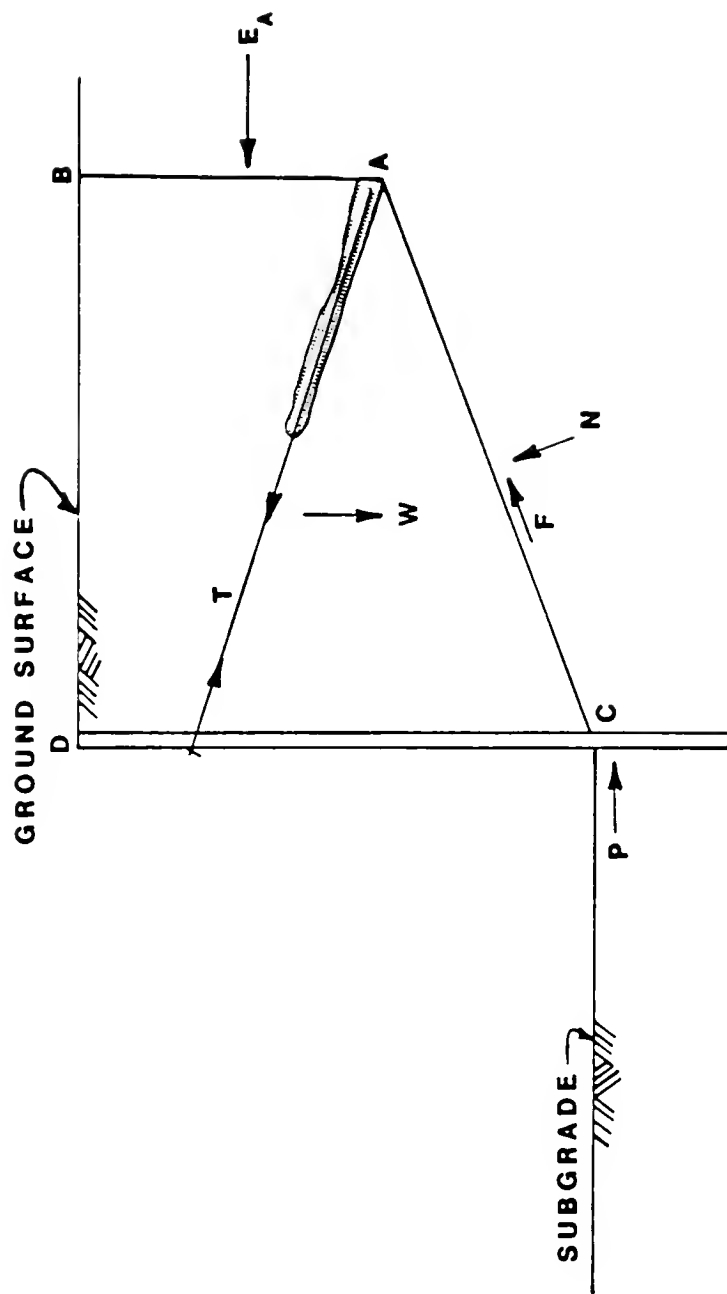
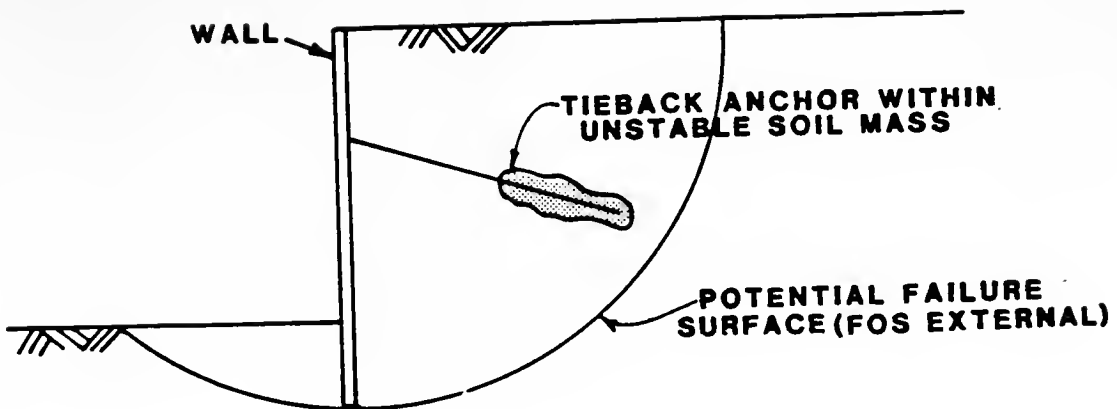
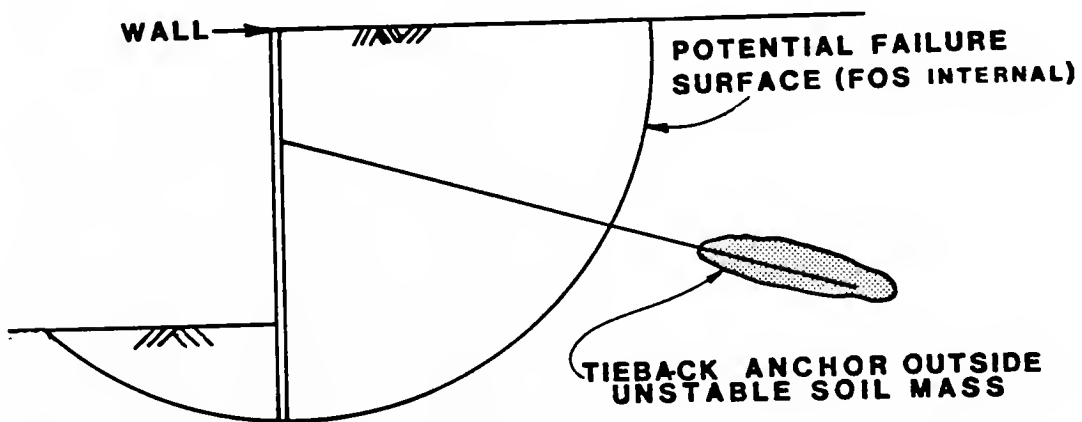


FIGURE 8. Soil Mass Analyzed for Overall Stability Analysis (After Schnabel, 1982)



**(A) INTERNALLY STABLE BUT EXTERNALLY UNSTABLE  
SOIL-STRUCTURE-ANCHOR SYSTEM**



**(B) INTERNALLY AND EXTERNALLY STABLE  
SOIL-STRUCTURE-ANCHOR SYSTEM**

FIGURE 9. Modes of Tiedback Wall Stability and Instability

of the tiebacks and the wall, is considered a FOS with respect to internal stability, Figure 9b.

For the overall stability of the soil-structure-anchor system, the soil mass of Figure 8 is often analyzed. The wedge shape of Figure 8 may be used to expedite hand calculations and is a simplification of the actual conditions. The forces tending to displace the soil mass are weight of the soil mass,  $W$ , and the earth pressure,  $E_a$ , on plane, AB. The earth pressure,  $E_a$ , on plane, AB, is usually taken as the active earth pressure, although the at-rest earth pressure condition is sometimes used (Schnabel, 1982). The external forces resisting displacement of the soil mass are the tangential and normal forces,  $F$  and  $N$ , on the failure plane, AC. The failure surface, AC, may not be straight as shown but may be curved depending upon the soil parameters. In addition, if the retaining structure penetrates some distance below the subgrade, passive resistance,  $P$ , will be mobilized at the base of the wall. The factor of safety with respect to overall stability is defined as the ratio of the sum of the resisting forces to the sum of the driving forces. A typical FOS for this type of analysis is 1.5 (Anderson, et al, 1983).

It is important to stress that the tieback force is an internal force within the wedge and does not affect the external stability of the soil mass. The tieback applies a load to the wall which pushes on the soil. The forces

between the wall and the anchor are equal and opposite, which tends to squeeze the soil together. Schnabel (1982), cites personal experience and tests performed in Germany on model walls which show that the failure surface caused by external instability is defined by the ends of the tiebacks. Failure of the model walls was caused by increasing the load on the tiebacks, and in all cases when failure occurred, the failure surface passed through the ends of the tiebacks.

If the external stability is insufficient, it is apparent from Figure 8 that the external stability may be increased by modifying the tieback geometry. This is usually accomplished by lengthening the tiebacks. Since the loads in the tiebacks are internal forces within the soil mass wedge, they do not increase the overall stability of the system. Increasing the load on the tiebacks or increasing the number of tiebacks will only serve to increase the internal stability of the wedge. These internal forces do not increase the external stability. The latter is improved only by modifying the tieback geometry, which usually means lengthening the tiebacks. Since the cost per tieback increases as the length increases, it is necessary to determine the shortest length of tiebacks that will provide a suitable FOS for external stability.

This type of simplified analysis is rather straight forward for a single row of tiebacks and homogeneous soil conditions, however, this method becomes somewhat cumbersome

and tedious for multiple tiebacks in layered or non-homogeneous soil conditions.

Several other methods of assessing the overall stability of single and multiple anchored structures have been proposed. Unfortunately, some of these methods sacrifice the basic laws of statics and make arbitrary assumptions concerning the forces internal and external to the soil mass. The remainder of this chapter will review the existing methods available for assessing the overall stability of anchored retaining structures and will discuss the merits and inadequacies associated with each method.

#### Krantz Method

Krantz (1953) was the first to propose a method for checking the overall stability of anchored walls. His method assumes a composite failure surface consisting of an active wedge behind the anchors and a passive wedge in front of the anchors, Figure 10. The Krantz method forms the basis for the 1980 German recommendations of the Committee for Waterfront Structures. The German method shown in Figure 10 considers the overall stability of free support sheet piling and anchored walls in uniform soils with a single row of tiebacks. The German method is merely a specific case of the Krantz method since the original work of Krantz considered multiple rows of anchors (Anderson, et. al., 1983).

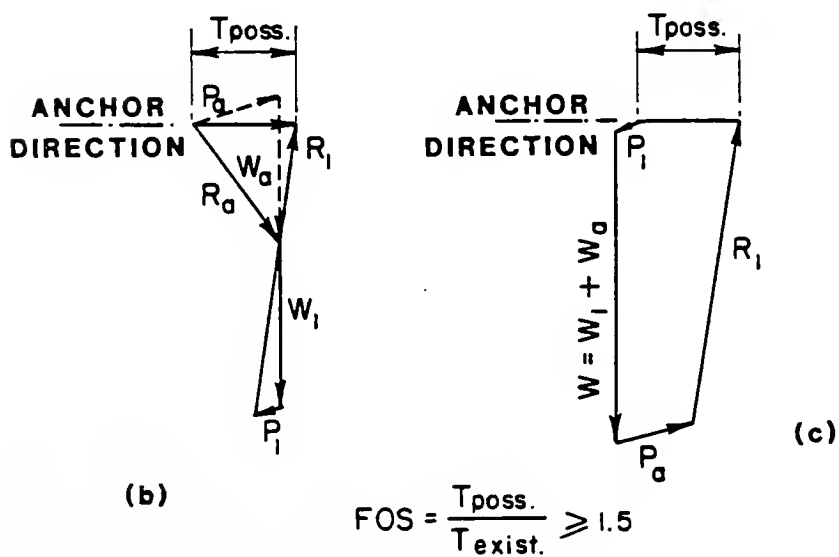
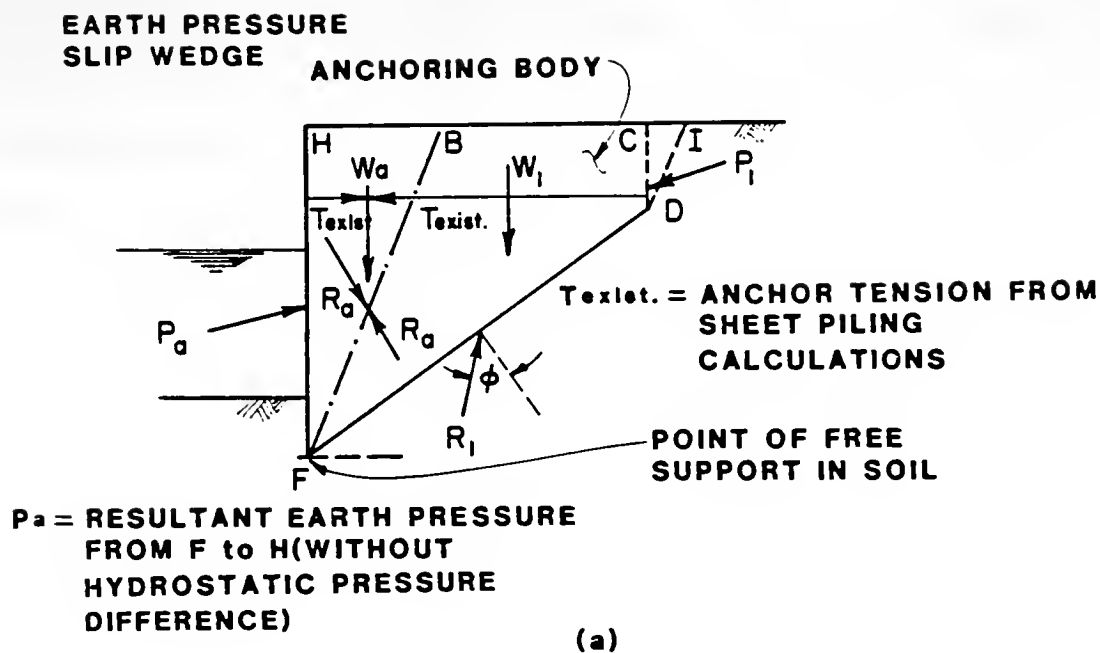


FIGURE 10. Determination of Overall Stability by Krantz Method (After Anderson, 1983)

The Krantz method is based on laboratory tests and analyses in which an external pull (force) is applied to the soil wedge. This method requires the calculation of an external force which would be required to displace the soil wedge in which the tiebacks are anchored. The external force is taken as the possible tieback load,  $T_{\text{poss}}$ .

The active earth pressure soil wedge, BFH, with slip surface BF and weight  $W_a$ , produces a load on the sheet piling and supports itself on the anchoring section, BCDF, with a resisting force,  $R_a$ . The active earth pressure wedge is determined by the dashed line between point F and B, and is inclined from the horizontal at an angle of  $45+\phi'/2$ . Note that no part of the fixed anchor may be located within this active earth pressure wedge where wall displacements are likely.

The anchoring section, BCDF, lies on the failure plane, DF, which is held by the resisting force,  $R_1$ . The force,  $R_1$ , is inclined from the normal of the failure plane by the angle of shearing resistance,  $\phi'$ . A resultant earth pressure force, (passive minus active),  $P_a$ , in front of the wall also resists movement of the soil mass, CDFH. According to Krantz, the driving forces on the anchoring section tending to cause instability are the anchor tension transmitted through the anchor plate, the weight of the soil wedge,  $W_1$ , and the active soil pressure,  $P_1$ , on the rear surface of the anchor plate produced by the slip wedge, CDI.

The system is theoretically stable when the potential force required to dislodge the anchoring section, BCDF, in the direction of the anchor, is greater than the actual force on the sheet piling due to the lateral earth pressure. The FOS is defined as the ratio of the potential (possible) force required to dislodge the anchoring section, BCDF, to the actual (existing) force on the sheet piling:

$$F = \frac{T_{\text{poss}}}{T_{\text{exist}}} \quad . . . . . (1)$$

and should be greater than or equal to 1.5.

The potential anchor force,  $T_{\text{poss}}$ , may be determined from the force polygon as shown in Figure 10b. The calculation is simplified if the force,  $R_a$ , is replaced by the two forces,  $W_a$  and  $P_a$ . The force  $R_a$  is therefore eliminated and the slip surface does not need to be determined. The simplified force polygon now considers the whole wedge, CDFH, as shown in Figure 10c.

However, this method involves serious errors in the statement of the problem which make it inappropriate for determining the overall stability of anchored structures (Schnabel, 1984). The errors result from the fact that the method assumes that the tiebacks pull on the soil without pushing on the wall. It is apparent from the force polygon in Figure 10c, that the method assumes that the anchor force is an external force acting on the soil wedge, BCDF, whereas, the anchor force is actually an internal force in

this wedge. As previously illustrated, a post-tensioned tieback anchor compresses the wedge of soil between the wall and its anchor, therefore, this force is an internal stabilizing force in the wedge. An equal and opposite force on wedge, BFH, is the tieback force, not  $P_a$ . The result of the force polygons shown in Figures 10b and 10c, is to mix internal and external forces acting on the wedge, CDFH. The tieback is in tension between the wall and its anchor and is not related to the force required to move the wedge, CDFH, but instead to the capacity of its tendon and anchor. It is therefore inaccurate to treat the tieback force as an external force acting to move the wedge, CDFH, (Schnabel, 1984).

Unfortunately, this method and others based on this method, are still used in practice today. In light of the inaccuracies of this method mentioned above, it is the opinion of the author and of Schnabel (1984) that this method should be discontinued in practice due to the errors in the model.

#### Ranke-Ostermayer Method

In 1968, Ranke and Ostermayer applied the same concept to overall stability analysis as Krantz. Figure 11 shows the model used by Ranke and Ostermayer. Again, as in the Krantz method, a value of tieback force is solved for and the FOS is defined as:

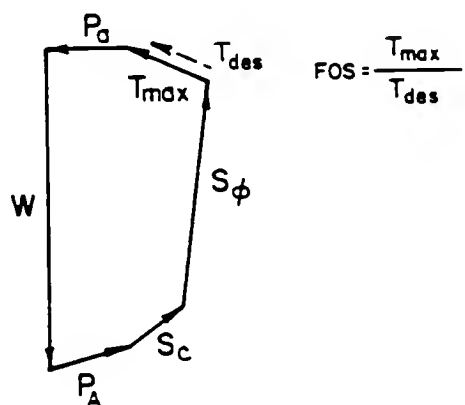
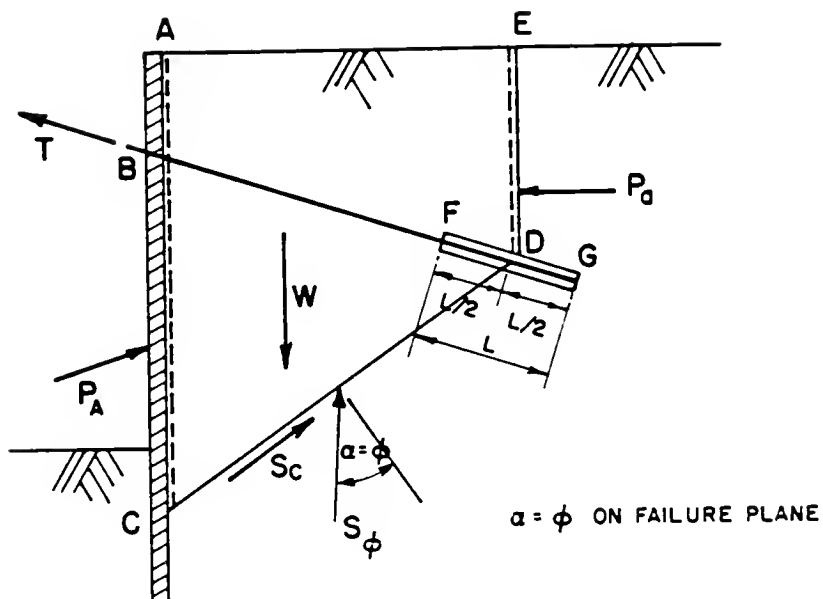


FIGURE 11. Determination of Overall Stability by Rankine-Ostermayer Method (After Cheney, 1984)

$$F = \frac{T_{\text{maximum}}}{T_{\text{design}}} \dots \dots \dots (2)$$

It is clear from Figure 11b that the tieback force is considered to be an external force acting on the soil wedge. Again, as in the Krantz method, it is inaccurate to treat the tieback force as an external force.

#### French Code of Practice Method

The French Code of Practice (1972) applies the Krantz method to multiple rows of anchors in layered soils. The Code recommends that an individual equilibrium analysis be performed for each row of tiebacks and that the influence of an anchor on the stability of another should also be considered. The following paragraphs and figures demonstrate both types of analyses.

Figure 12 considers the stability of two totally independent anchors. The Code assumes that the two equilibrium conditions are independent and that the stability analyses may be performed in any order. However, in practice, rarely are two anchors independent of one another, simply by the mere fact that they are connected to the same structure.

Figure 13 shows two different arrangements of anchors where only one anchor is completely independent. In Figure 13a, the upper anchor,  $C_1$ , is fixed in soil mass,  $M_2$ , while the lower anchor,  $C_2$ , is considered external to the mass,  $M_1$ . In Figure 13b, the upper anchor,  $C_1$ , is external to the

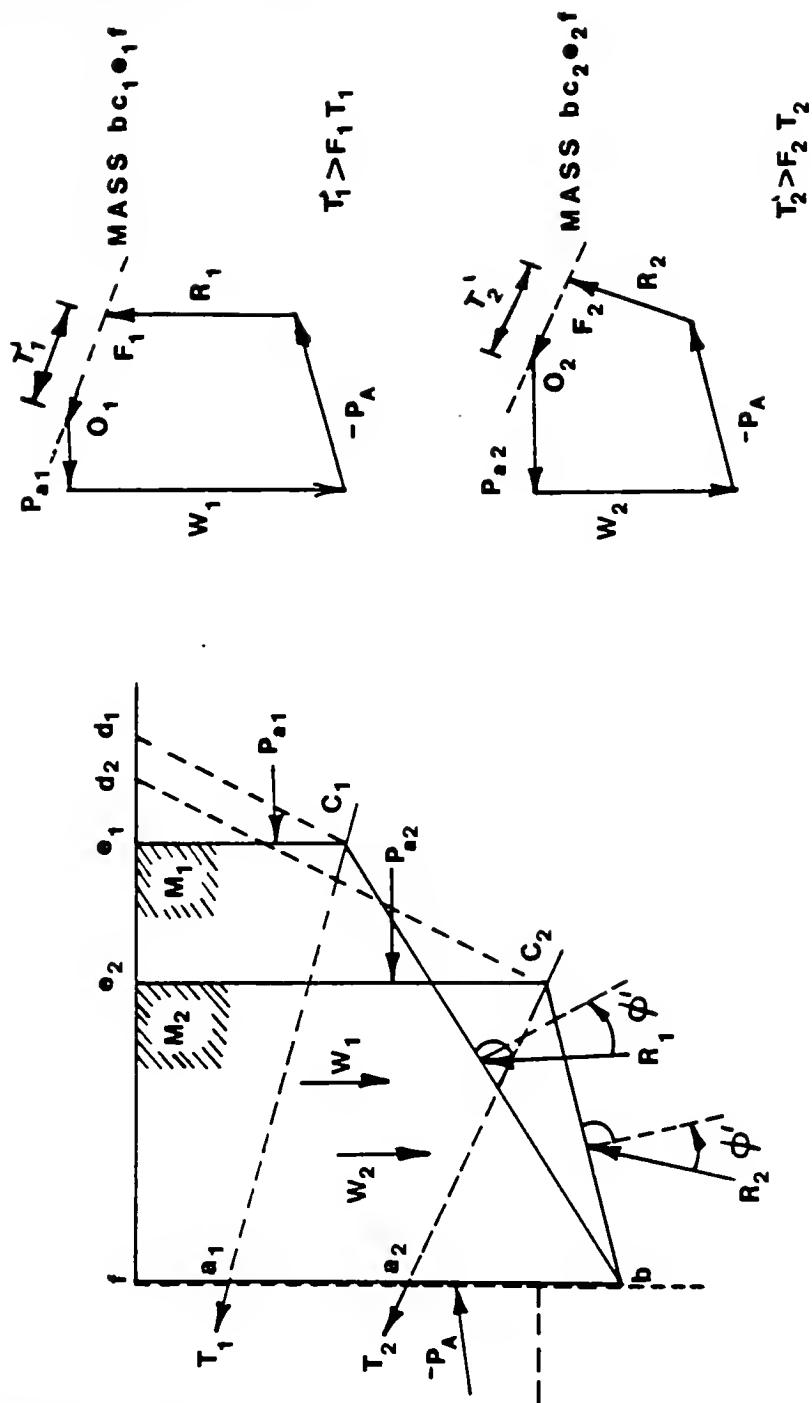
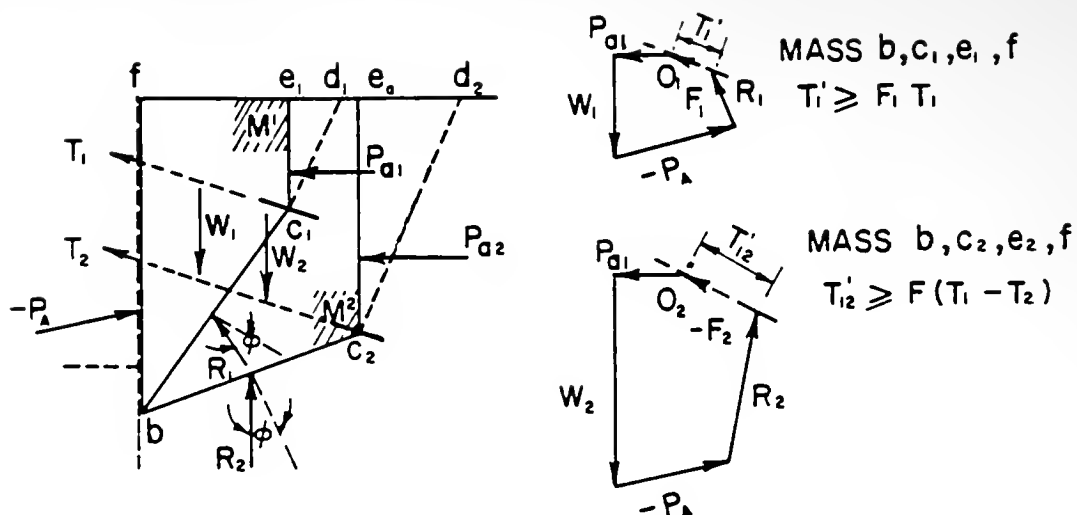
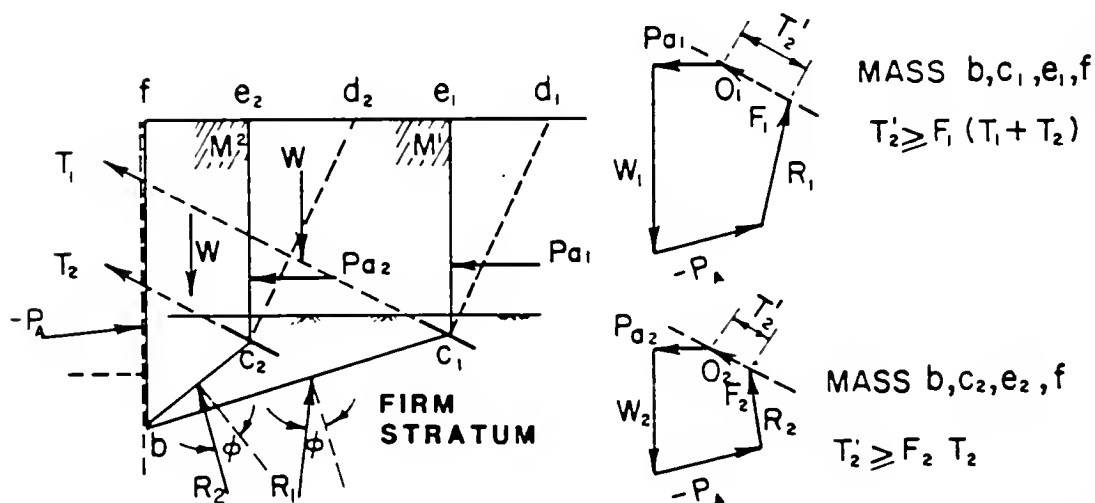


FIGURE 12. Overall Stability for Two Independent Anchors  
(After French Code of Practice, 1972)



(a) TOP ANCHOR INDEPENDENT



(b) BOTTOM ANCHOR INDEPENDENT

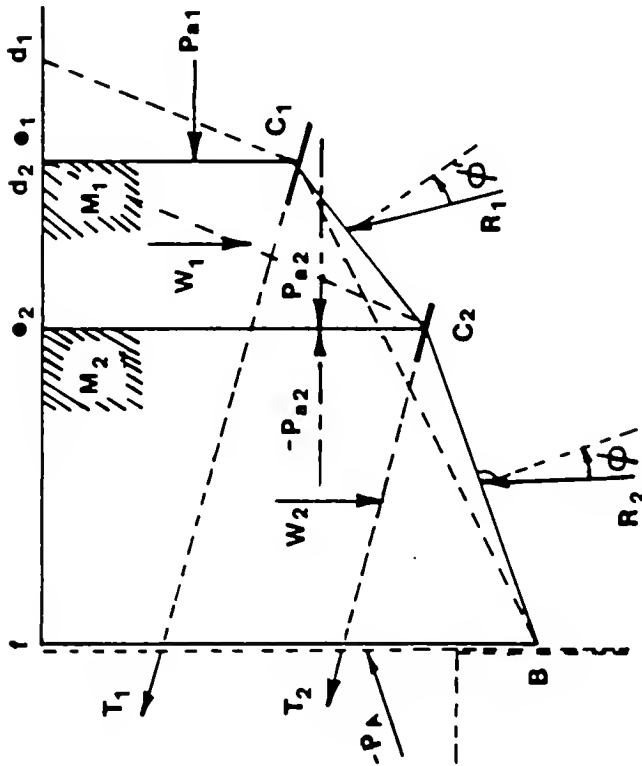
FIGURE 13. Overall Stability for Two Anchors  
(After French Code of Practice, 1972)

mass,  $M_2$ , while the lower anchor,  $C_2$ , is fixed in soil mass,  $M_1$ . In both cases, separate force polygons are drawn as shown in Figures 13a and 13b.

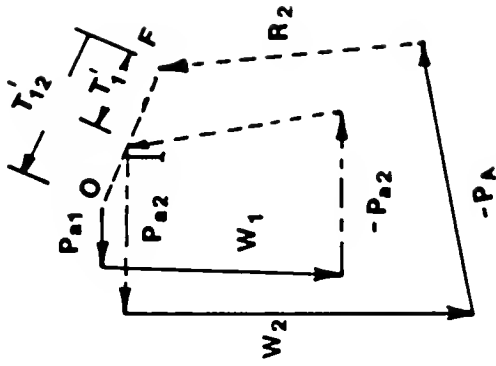
Figure 14 demonstrates the situation where the point of fixity of the lower anchor is close to the boundary of soil mass,  $M_1$ . A complex failure surface as shown is assumed. The first force polygon (equilibrium of  $C_2C_1e_1e_2$ ) is drawn from the origin and leads to intermediate point I, Figure 14b. From point I, the second force polygon (equilibrium of  $BCe_2f$ ) is drawn and leads to the final point, F. The two stability conditions are supposedly verified simultaneously.

However, since the French Code of Practice is based on the Krantz method, it too is invalid for assessing the overall stability of multiple anchored structures. The Code illustrates the difficulty of extending Krantz's technique to multiple tieback structures. The Code develops arbitrary rules to allow the mathematics to be performed; however the statement of the problem is again incorrect since the method assumes that the tiebacks pull on the soil without pushing on the wall. As stated previously, the tieback is in tension and applies a compressive force on the soil between the wall and the anchor. As Schnabel (1984) stated, "Sophisticated errors are still errors".

MASS  $C_2 C_1 \theta_1 \theta_2$   
 THEN MASS  $b c_2 \theta_2 f$



(A)



$$T'_1 \geq F T_2$$

$$T'_{12} \geq F (T_1 + T_2)$$

(B)

FIGURE 14. Overall Stability with Complex Failure Surface  
 (After French Code of Practice, 1972)

### Broms Method

In 1968, Broms modified the Krantz method to consider the axial force produced by the wall on the soil. The failure surface is shown in Figure 15 and is assumed to extend from point B located 2 m (6.2 ft) from the end of the anchor to point C on the sheet pile, which corresponds to the minimum penetration depth required to prevent failure.

The forces initiating failure are the earth pressure force,  $P_1$ , acting on the vertical section, AB, and the weight,  $W$ , of the sliding soil mass of wedge, ABCE. The forces resisting failure are the reaction force,  $R$ , the anchor force,  $T$ , the toe resistance,  $V$ , and the passive earth pressure thrust,  $P_p$ , above point C in front of the wall. The anchor force,  $T$ , although shown in the figure, is normally neglected in the calculations. The FOS is defined as:

$$F = \frac{(P_p)_{\text{available}}}{(P_p)_{\text{required}}} \dots \dots \dots (3)$$

and must be greater than 1.5.

By neglecting the anchor force,  $T$ , in the calculations, the Broms method properly considers the tieback force to be an internal force in the soil wedge. It is therefore similar to the method of analysis first described in this chapter, with the exception that the failure surface is assumed to pass through the tiebacks at a point 2 m (6.2 ft)

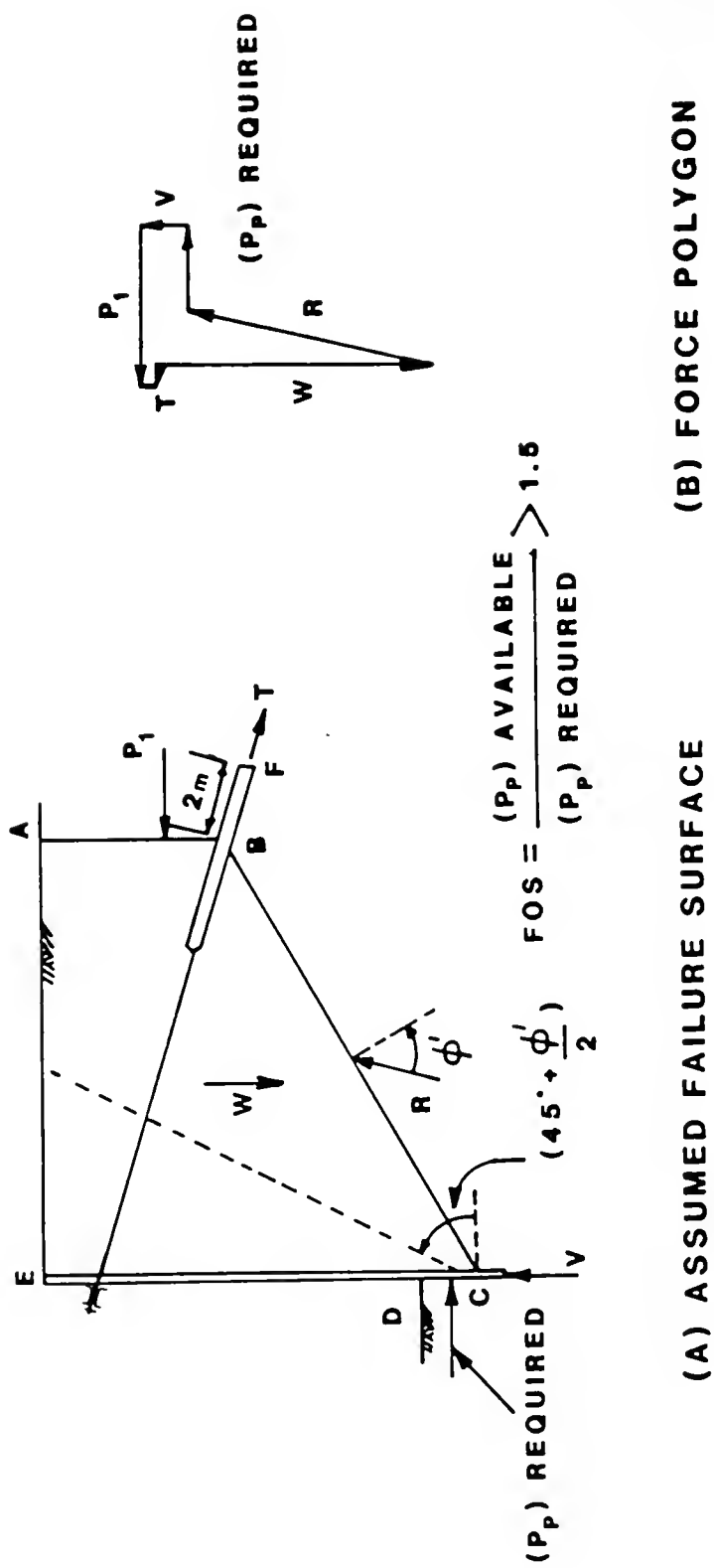


FIGURE 15. Determination of Overall Stability by Broms Method (After Broms, 1968)

from the ends of the tiebacks. The reason for, and validity of this assumption is not clear.

#### Littlejohn Method

In 1972, Littlejohn proposed a new definition of the FOS for a wedge analysis. The model used by Littlejohn is shown in Figure 16. The earth pressure force,  $P$ , acting on the vertical plane through the midpoint of the anchor is calculated assuming a nominal angle of shearing resistance,  $\phi_n'$ . The resultant force,  $R_n$ , on the inclined sliding plane must form the same angle,  $\phi_n'$ , with the normal to the sliding plane. The angle,  $\phi_n'$ , has been correctly assumed when the weight,  $W$ , and the forces,  $P$  and  $R_n$ , are in equilibrium. If the forces are not in equilibrium, then another value of  $\phi_n'$  is assumed and the calculation repeated.

The FOS is defined as:

$$F = \frac{\tan \phi'}{\tan \phi_n'} \quad . . . . . (4)$$

Note that this definition of the FOS breaks down for purely cohesive soils whose angle of shearing resistance is zero.

#### Ostermayer Method

Ostermayer (1977) and Schulz (1976) generalized the Littlejohn method for multiple tiedback structures and

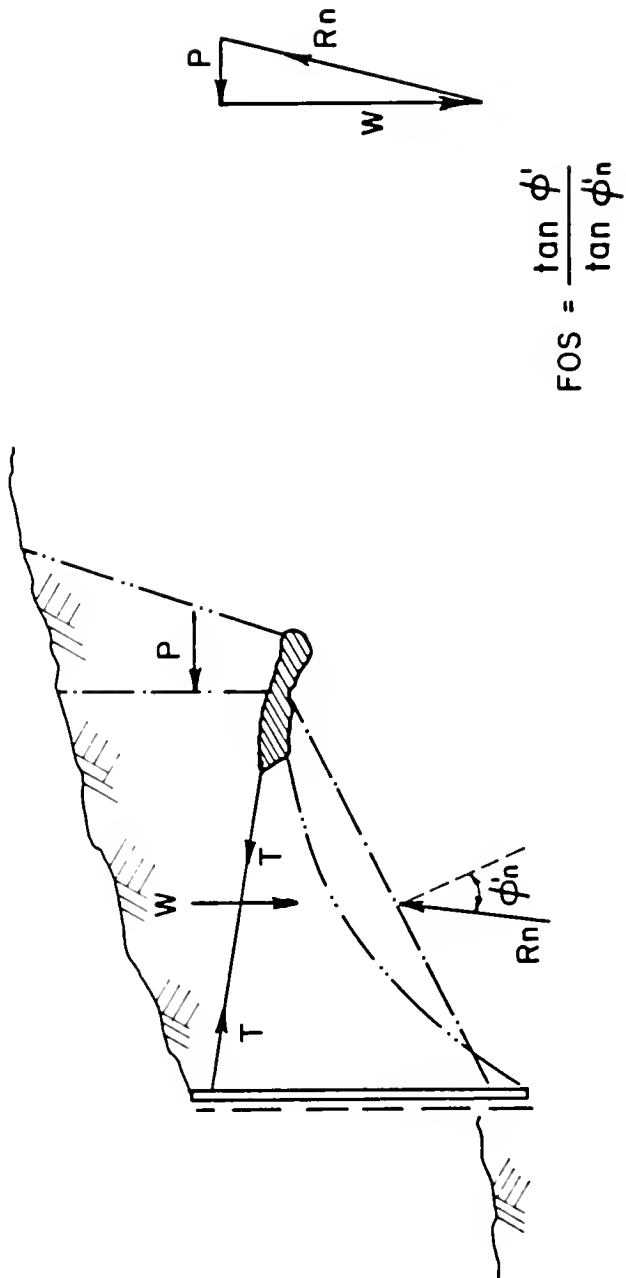


FIGURE 16. Determination of Overall Stability by Littlejohn Method  
(After Littlejohn, 1972)

suggested that the passive resistance in front of the wall be included in the equilibrium of the wedge as shown in Figure 17. The FOS is defined in the same manner as the Littlejohn method and is suggested to be equal to, or greater than, 1.2.

Ostermayer also suggested that an overall stability analysis be performed using a circular failure surface to ensure stability against rotational failure. Any limiting equilibrium slope stability computer program can be used to analyze potential failure surfaces located outside the zone of the tieback anchor since the tieback force is an internal force within the sliding mass. However, such a program does not properly consider the effect of the tiebacks on the stability of the sliding soil mass whose potential failure surface passes between the tieback anchor and the retaining structure. This point will be discussed in the Slope Stability Program Method section of this chapter.

#### Finite Element Method

Hanna (1978) suggested that a promising solution to the problem of assessing the overall stability of tiedback retaining structures is to model the wall construction excavation sequence using a finite element technique as shown in Figure 18. However, this type of analysis is relatively expensive and at this time there are a number of difficulties and uncertainties in: (1) modelling the behavior of the soil, (2) modelling the soil-structure

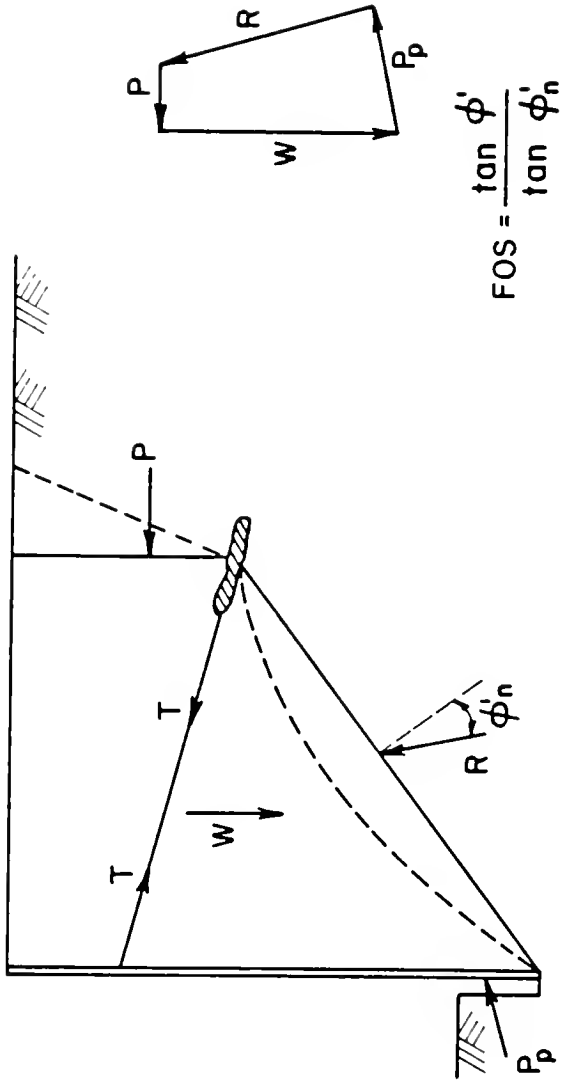
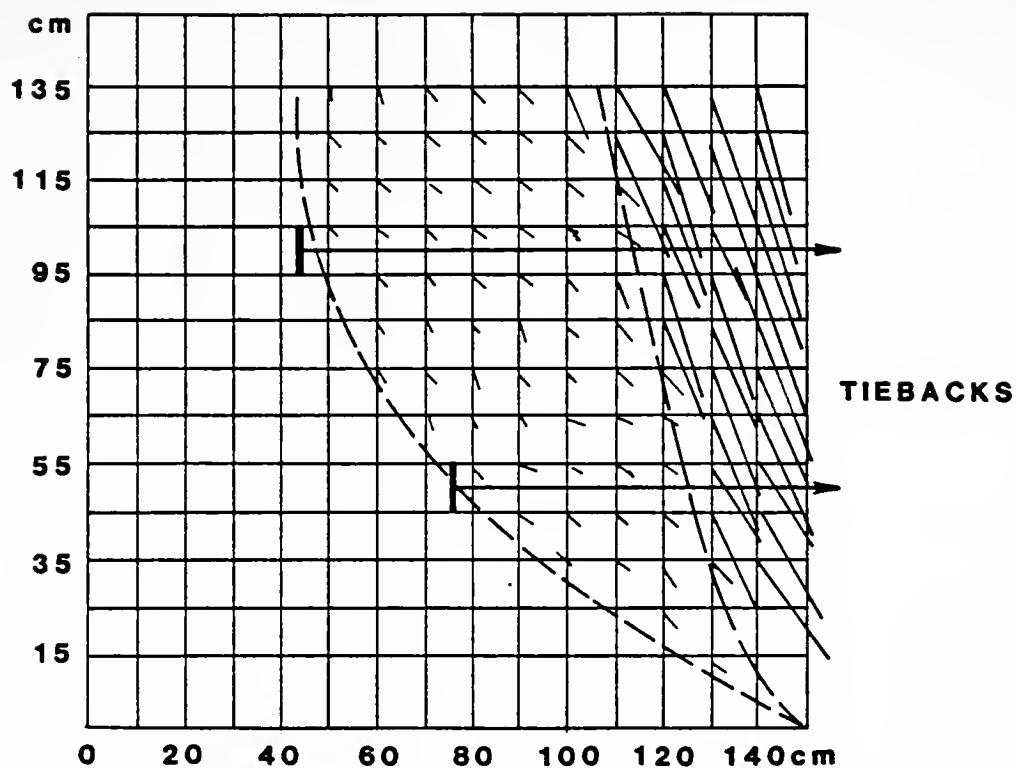


FIGURE 17. Determination of Overall Stability by Ostermayer Method  
(After Ostermayer, 1977)



**FAILURE OF A SAND BLOCK MODEL WITH  
DOUBLE ANCHORAGE SHOWING MOTION  
VECTORS**

FIGURE 18. Determination of Stability by Finite Element Method (After Hobst and Zajic, 1983; and, Bendel and Weber, 1966)

interface and interaction, (3) modelling the method of excavation, and (4) idealizing the anchors in the ground. In addition, most tiedback structures do not warrant analyses as sophisticated as a finite element technique.

### Summary

It is clear from the available methods presented for assessing the overall stability of tieback structures for support of excavations, that numerous simplifying assumptions are made regarding the shape of the failure surface and the loads involved. In addition, most methods cited are not applicable to multiple tiedback walls or non-homogeneous soil conditions, and those which are applicable, are extremely cumbersome. Also, the methods which define the FOS with respect to the angle of shearing resistance, break down for purely cohesive soils which have no frictional characteristics.

The most logical and practical type of analysis for assessing the stability of tiedback structures is a limit equilibrium method based on the method of slices where both sliding and rotational types of failures can be modelled. Such a method should allow the designer to specify and analyze logical potential failure surfaces within and outside the zone of the tiebacks, and which takes into account the compression of the soil mass between the structure and the anchor. In addition, such a technique should be capable of handling multiple tiebacks and non-

homogeneous soil conditions. Such a method has been developed by the author and implemented in the slope stability computer program, STABL. This new method will be described in Chapter III.

### Stabilization of Landslides

Tiedback retaining structures are frequently used for the control of landslides. These structures, in addition to supporting the soil mass directly behind the structure, must also apply a sufficient resisting force to the sliding mass which it is intended to stabilize. Not only must the tiedback retaining wall, shown in Figure 19, be able to resist the lateral earth pressure forces produced by the soil mass directly behind the wall, (shaded portion), but it must also apply a resisting force sufficient to stabilize the sliding soil mass above the landslide failure surface.

A sliding mass can be stabilized by increasing the resisting forces which act on it, or by decreasing the driving forces. Tiebacks stabilize a sliding soil mass by increasing the resisting forces. Tiebacks can penetrate the sliding surface and apply increased normal and tangential forces to the sliding body. Tiebacks are an excellent tool for stabilizing landslides because they provide a force which acts in nearly an ideal direction for resisting the driving forces, without seriously aggravating the stability of the slope.

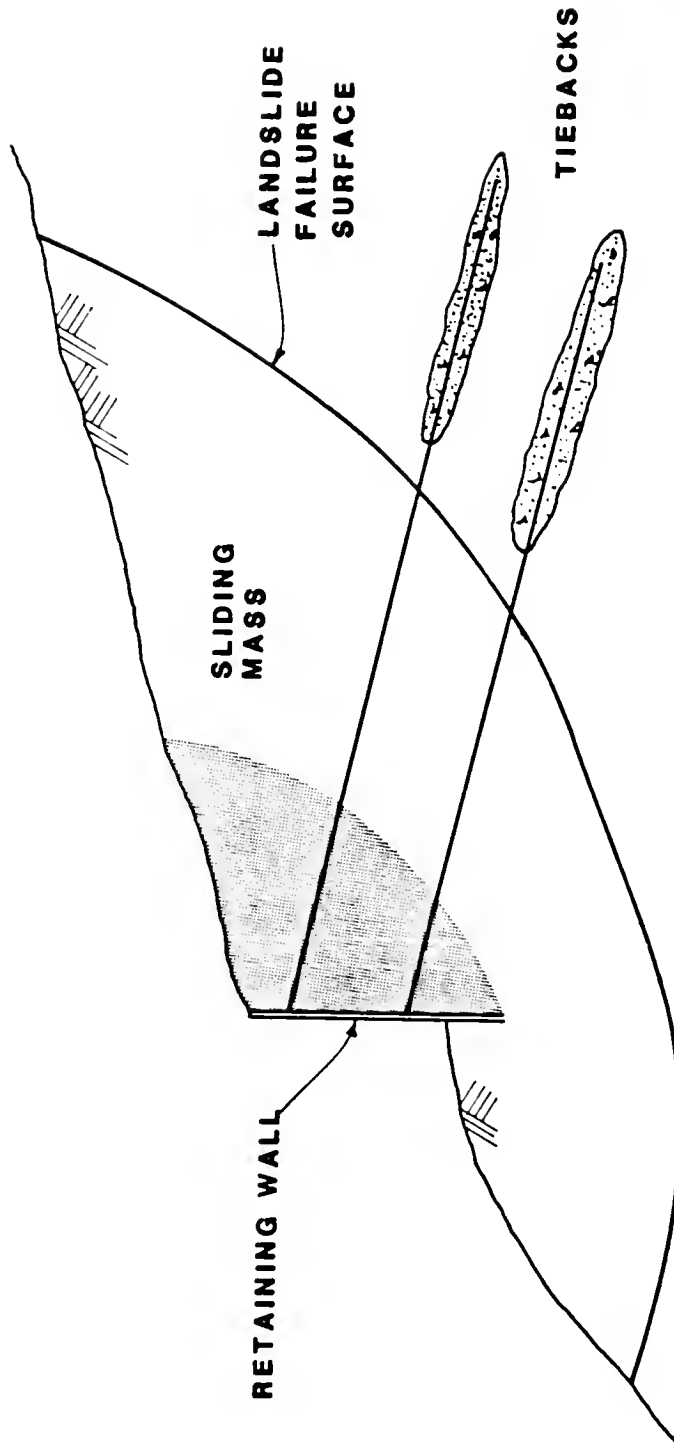


FIGURE 19. Landslide Stabilization Using Tiebacks

It can be seen from Figure 19, that the largest component of the tieback force acts in a horizontal direction. The tiebacks also provide a component of force to the soil mass which increases the normal force on the sliding surface. For soils with frictional characteristics, it can be seen from equation 5, that by increasing the normal force, and hence total normal stress,  $\sigma$ , on the sliding surface, the strength of the soil at the sliding surface will increase, hence providing increased resistance to sliding.

$$S_u = c' + (\sigma - u)\tan\phi' \quad . . . . . (5)$$

where:

$S_u$  = Undrained soil strength

$c'$  = Effective soil cohesion

$\sigma$  = Total normal stress

$u$  = Pore water pressure

$\phi'$  = Effective angle of shearing resistance

Both components of the tieback force on the failure surface tend to increase the resisting forces on the sliding mass.

Any type of stability analysis performed on slopes subjected to tieback loads should consider both components of resistance offered by a tiedback structure for landslide stabilization.

### Slope Stability Program Method

Slope stability computer programs based on a limiting equilibrium method of slices are routinely used for determining the stability of slopes and embankments. It is therefore logical to attempt to use such an analysis tool for the determination of the stability of tiedback structures used for landslide control.

However, existing limiting equilibrium slope stability computer programs, with the exception of the recent versions of STABL, do not properly account for the presence of tieback loads in the determination of the FOS. This is especially true for the simplified methods of slices, such as the Simplified Bishop method, and the Simplified Janbu method, which do not satisfy total equilibrium (Bishop, 1955; Janbu, 1954).

When tiedback retaining structures are used for control of landslides, large compressive stresses are produced within the soil mass between the retaining structure and the tieback anchors. This results in a significant change and increase in the state of stress along the failure surface. The change in state of stress along the failure surface due to the presence of tieback loads is illustrated in Figure 20 for a typical excavation. Figure 20 shows a typical distribution of stress along the potential failure surface for an unsupported excavation, and an excavation supported by a tiedback wall. It can be seen from this figure, that

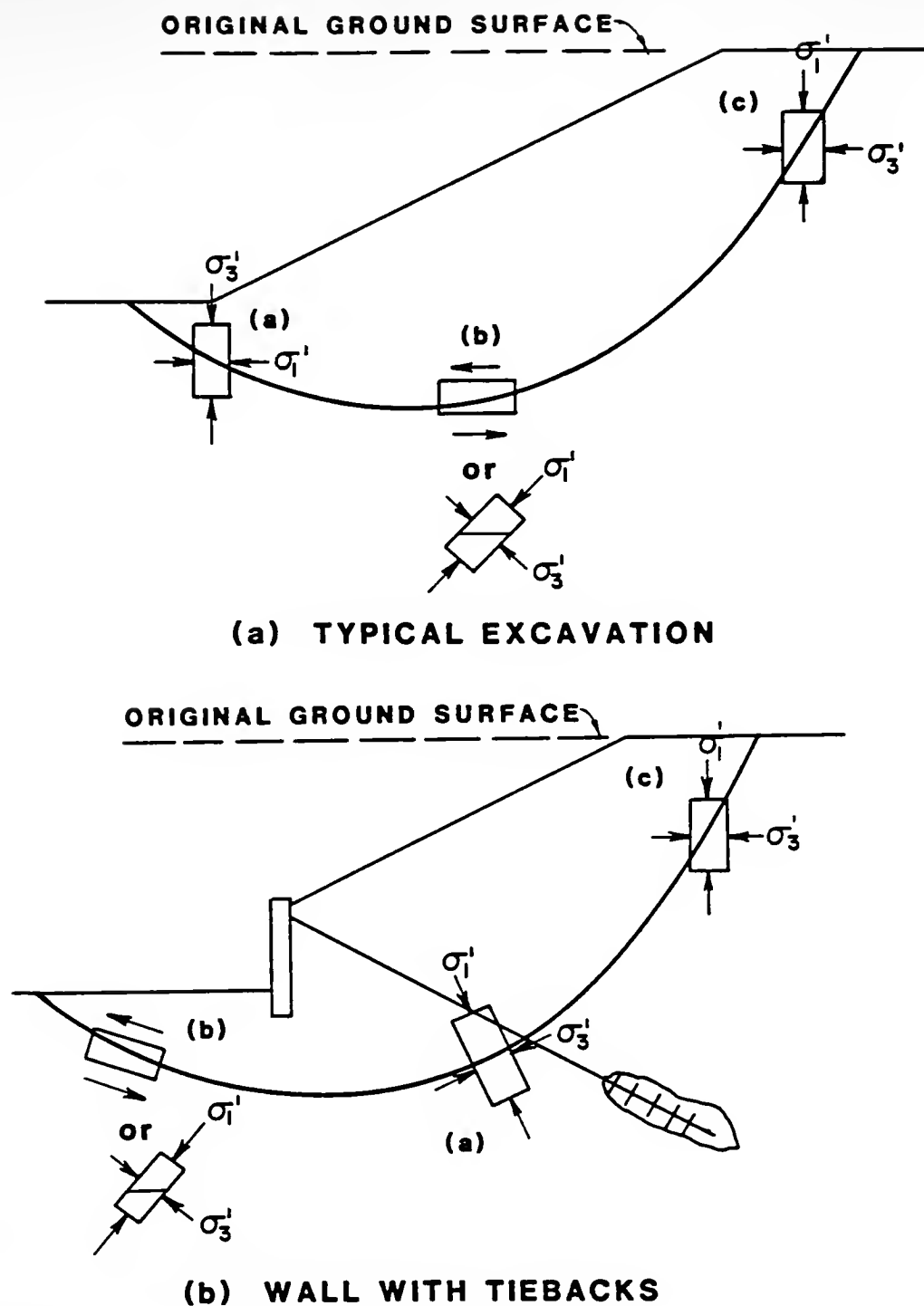
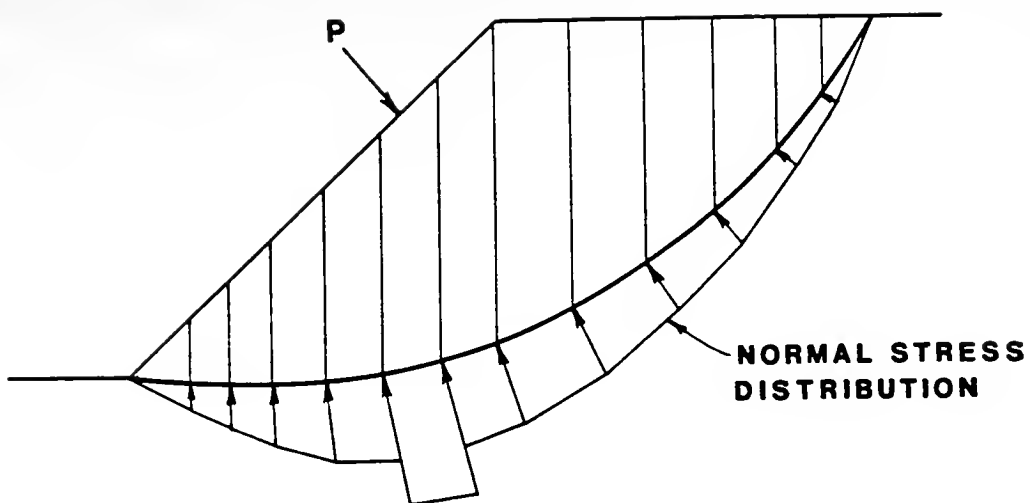


FIGURE 20. Distribution of Stress Along Potential Failure Surface (After Sangrey, 1982)

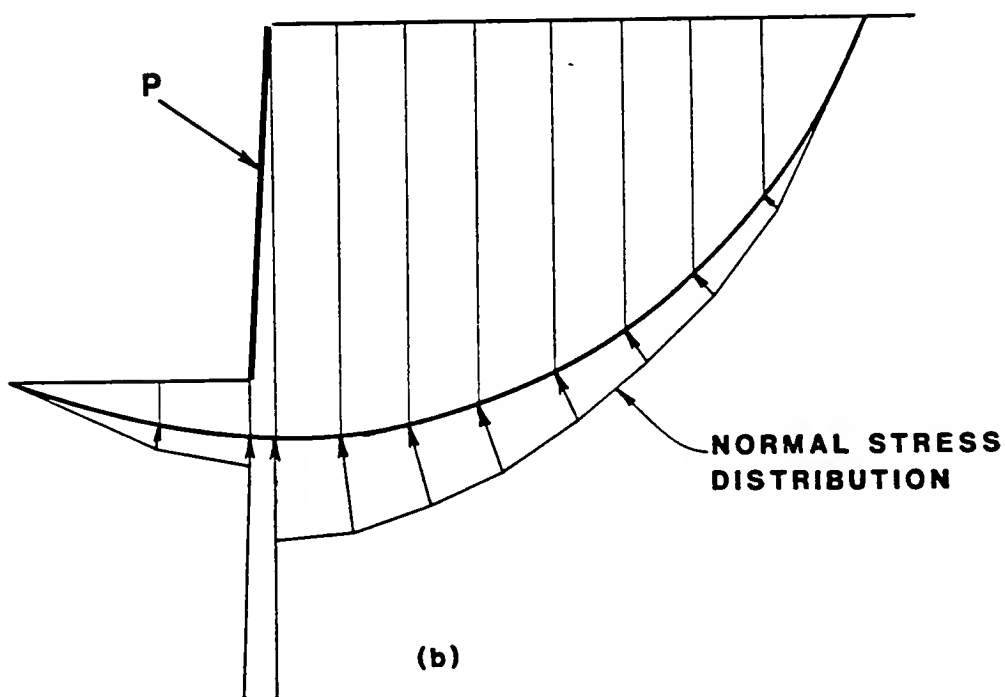
the stress distribution along the failure surface for the excavation supported by the tiedback wall is very different from that of the unsupported excavation. This is due to the large compressive stresses applied to the soil mass and failure surface by the tiedback retaining structure.

When vertical uniform distributed loads are present on the crest of the slope, there are no major drawbacks to using the Simplified Bishop or Janbu methods. However, using these methods for concentrated and inclined loads such as tieback loads, these methods are inappropriate for the following reasons:

1. The vertical component of an inclined tieback load is only taken into account in the numerator of the FOS for the slice on which it acts. This does not conform to the idea that stresses applied to the ground surface are diffused throughout the soil mass (Boussinesq, 1885; Flamant, 1886; Newmark, 1942; Baladi 1968), as previously discussed and shown in Figure 20. Figure 21a shows the distribution of normal stress on the failure surface, due to the presence of a concentrated load, such as an inclined tieback load,  $P$ , applied to the face of a slope. It is clear from this figure that the tieback load is only taken into account on the slice on which it acts. Since the normal stress on this slice is greatly increased



(a)



(b)

FIGURE 21. Normal Stress Distribution on Failure Surface Considering a Concentrated Load

while nearby slices remain unaffected, the soil resistance calculated for this slice, using equation 5, will be extremely high. The result is that the real FOS for this slice will be inappropriately high. This problem is especially critical when the width of the slice is small, as is typically true for near vertical tiedback retaining structures, shown in Figure 21b.

2. The horizontal component of a concentrated tiedback load is taken into account only in the denominator of the FOS. It will be seen in the following chapter, that the horizontal component of the tiedback load produces normal and tangential forces on the base of the slices, which contribute to the stability of the slope.
3. A concentrated horizontal load whose line of action passes through the center of rotation, will not be taken into account in the FOS determination with the Simplified Bishop method of slices since the moment arm of the load will be zero; hence the resisting moment from the load will be zero.

It is apparent that existing slope stability programs utilizing the simplified methods of slices are incapable of properly accounting for the presence of concentrated loads such as tiedback loads. In reality, large compressive stresses, due the presence of a tiedback load, are

distributed throughout the soil mass to the base of all the slices of the sliding mass. These stresses cause the normal and tangential stresses to be increased on the base of every slice of any failure surface which passes between the tieback anchor and the retaining structure. Any analysis for determining the stability of slopes subjected to tieback loads, should consider these increases in stresses at the base of each slice of the sliding mass.



### CHAPTER III. LOAD DISTRIBUTION METHOD - STABL4

As discussed in the previous chapter, limiting equilibrium slope stability programs do not consider the diffusion of stresses throughout a soil mass due to the presence of concentrated boundary loads. Instead, these programs take a concentrated boundary load, such as a tieback load, into account only on the slice on which it acts. Such programs therefore do not properly account for the diffusion of stresses throughout the soil mass.

In order to account for the diffusion of compressive stresses throughout a soil mass due to the presence of tieback loads, the author has developed the Load Distribution Method, (LDM), for use with the simplified methods of slices. The Load Distribution Method is programmed in the slope stability computer program, STABL4, and eliminates the drawbacks inherent to computerized slope stability analyses presented in the previous chapter. Unlike other slope stability programs, STABL4 distributes the force from a concentrated load throughout the soil mass to the whole failure surface and hence to all slices of the sliding mass. STABL4 is the only known limit equilibrium slope stability program that attempts to account for the

distribution of force to the failure surface caused by concentrated boundary loads, such as tieback loads. This distribution of load throughout the soil mass is a unique feature of STABL4.

The LDM routines in STABL4 are applicable to circular and non-circular failure surfaces and are specifically formulated to handle tieback loads, but as will be seen later, these routines are also capable of handling other types of loads applied to the ground surface. For simplicity and clarity, the following discussion will discuss the derivation of the LDM specifically for circular failure surfaces and tiebacks.

### Theory

A post-tensioned tieback applies a force to the structure which it supports. This force is developed by the tieback anchor within the soil mass. Since the forces between the wall and the tieback anchor are equal and opposite, they place the soil between the structure and the anchor in compression.

The Load Distribution Method (LDM) diffuses the stresses caused by the tieback load to the potential failure surface. This is accomplished by replacing the load applied to the ground surface with a statically equivalent distribution of forces applied to the midpoint of the base of the slices along the potential failure surface. By doing so, the load is distributed to the base of all, or nearly

all of the slices depending upon the slope geometry. The diffusion of stresses within the slope, and the increase in forces along the potential failure surface, is therefore considered in the determination of the FOS.

The distribution of stresses to the potential failure surface used in the Load Distribution Method is computed according to Flamant's (1886) distribution of stresses through an elastic half-space, as proposed by Tenier and Morlier (1982). The distribution of stresses is resolved into a distribution of discrete forces acting at the midpoint of the base of the slices. The resulting force distribution is modified so that the distribution of forces along the failure surface is in static equilibrium with the load applied to the ground surface.

Although soils do not generally behave as elastic materials, many solutions to the distribution of stresses throughout soils have shown that this approach is practical and reasonable for engineering purposes (Boussinesq, 1885; Newmark, 1942; Baladi, 1968). It will be seen later, that this distribution seems reasonable when compared to finite element studies by Tenier and Morlier (1982).

According to Flamant (1886), for a semi-infinite mass subjected to a concentrated load,  $P$ , the distribution of stresses is radial and is given by, (Figure 22):

$$\sigma_r = \frac{2(P) \cos \theta}{(\pi)(R)} \text{ (compression) . . . . . (6)}$$

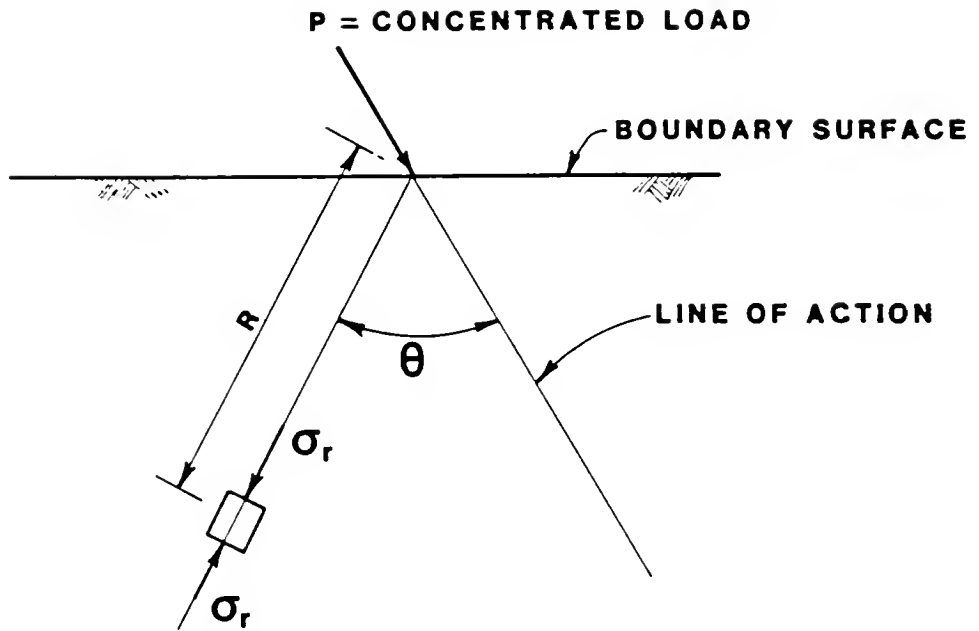


FIGURE 22. Flamant's Distribution of Stress

where:

- $\sigma_r$  = Radial stress at a point
- $P$  = Concentrated load applied to an elastic half space
- $R$  = Distance to the point in question
- $\theta$  = Angle formed by the line of action of the concentrated load, and the line connecting the point of application of the load on the boundary surface and the point in question

It is apparent from inspection of equation 6 that the radial stress,  $\sigma_r$ , is proportional to the applied load,  $P$ , inversely proportional to the distance,  $R$ , and dependent upon the angle between the point in question and the line of action of the applied load. For example, for a given distance,  $R$ , and applied load,  $P$ , the radial stress in the line of action of the load will be largest since  $\theta = 0$  (i.e.,  $\cos\theta = 1$ ), while for values of  $\theta$  approaching  $\pi/2$ , the value of  $\cos\theta$  will be small, and hence the radial stress at that point will also be small. In addition, for a given value of  $\theta$  and  $P$ , the radial stress will be smaller for a point far away from the point of application as compared to one which is closer to the point of application.

It is recognized that slopes or tiedback structures are not semi-infinite half spaces. Figure 23 illustrates the type of problem being modelled with Flamant's solution. The

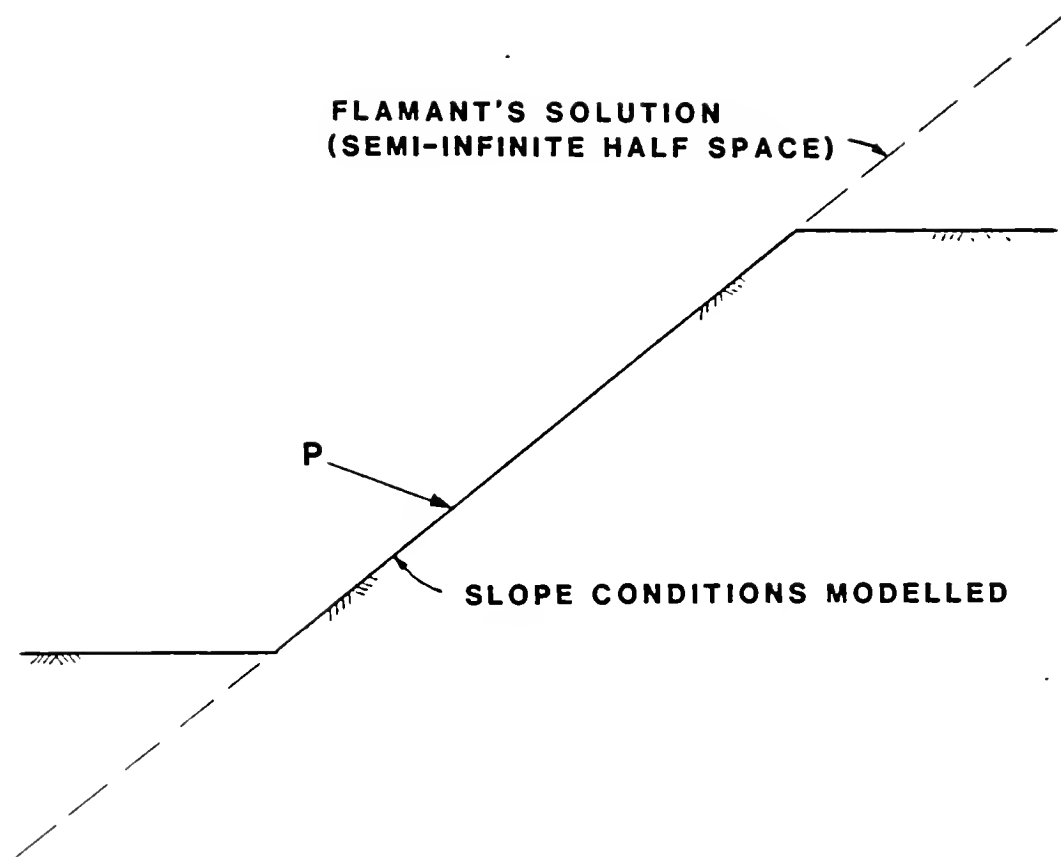


FIGURE 23. Application of Flamant's Solution to Tiedback Slopes

validity of using Flamant's semi-infinite half space solution to model slopes which are not semi-infinite will be investigated and the reasonableness of applying such a solution to tiedback slopes and retaining structures will be discussed later.

#### Implementation in STABL4

When tieback loads are specified using STABL4, the program first determines whether the grouted anchor is internal or external to the sliding mass. If the trial failure surface intersects the tendon portion of the tiebacks, (i.e., the anchor is external to the sliding mass; within the stable soil mass) as shown by Tieback Row #1 of Figure 24, the program replaces the tieback load with a statically equivalent distribution of load on the trial failure surface. However, if the trial failure surface intersects the grouted anchor portion of the row of tiebacks, (Tieback Row #2, Figure 24), or passes behind the anchors altogether, (Tieback Row #3, Figure 24), that row of tiebacks will not be considered in the determination of the FOS for the trial failure surface being analyzed.

It is clear that the upper row of tiebacks, Tieback Row #3, Figure 24, will have no effect on the stability of the trial failure surface shown, since the tiebacks are completely internal to the sliding mass. On the other hand, a portion of the grouted anchor of Tieback Row #2 lies within the sliding mass, while a portion of the anchor lies

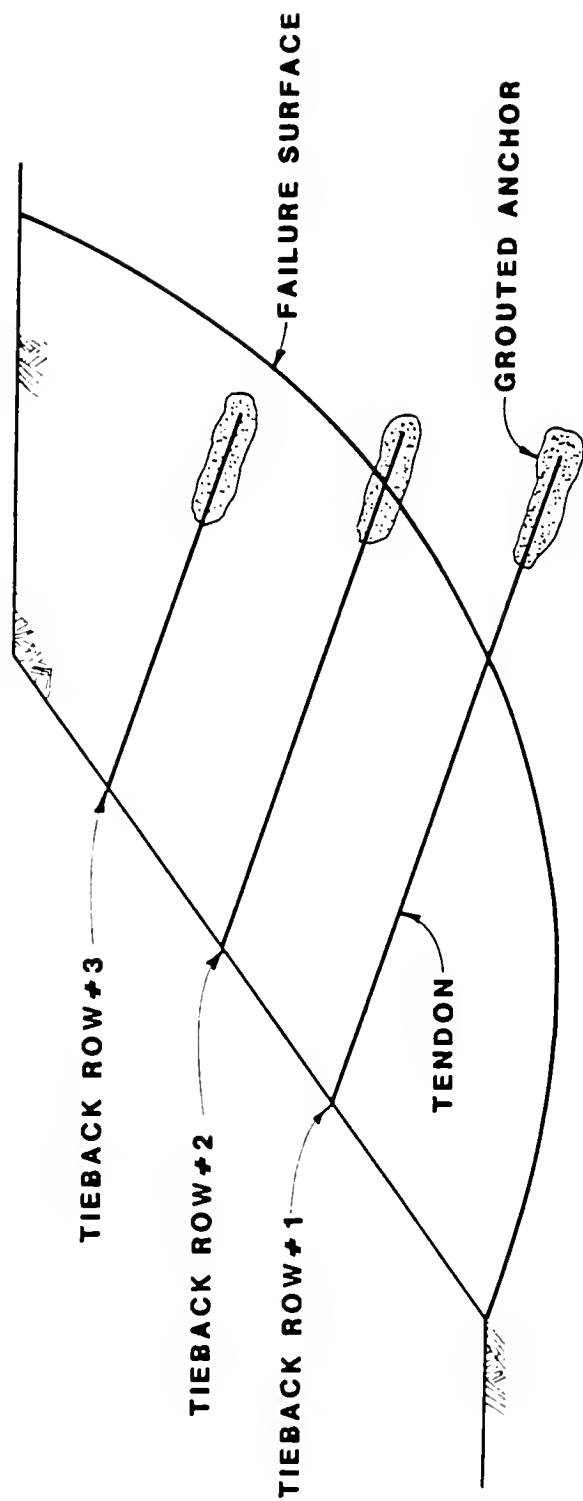
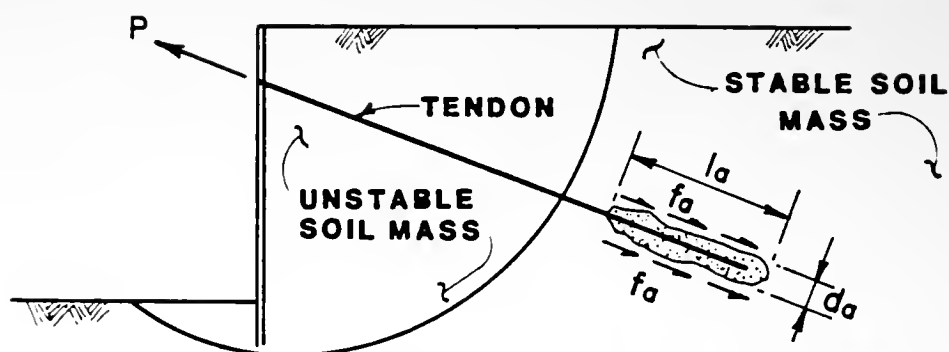


FIGURE 24. Intersection of Tieback Anchor with Trial Failure Surface

outside the sliding mass, i.e., within the stable soil mass. At first glance, it would seem that this tieback would be available to resist sliding of the unstable soil mass. However, upon inspection of the static equilibrium of Figure 25, it is apparent that only a portion of the tieback load is available to resist sliding. For example, if only half the tieback anchor is within the stable soil mass (Figure 25b), then only half of the tieback load can be mobilized to resist sliding.

In the Load Distribution Method, the load available to resist sliding from such a tieback is considered to be zero, rather than a fraction of the total load. This approach has been adopted since such refinements as considering only a fraction of the total available anchor load, are not justified considering the variable length of tiebacks constructed in the field. Either the full tieback load, or zero load, is used in the determination of the FOS. This approach is somewhat conservative, but deemed to be most realistic.

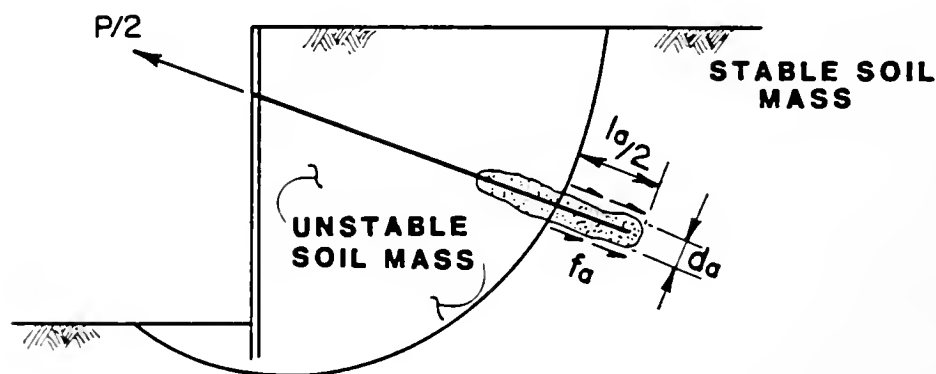
If the trial failure surface does intersect the tendon portion of a row of tiebacks, an equivalent line load is calculated for the row of tiebacks. The individual tieback load,  $P$ , for a given row of tiebacks, is divided by the corresponding horizontal spacing,  $H$ , between tiebacks, Figure 26. The resulting equivalent line load is designated



$$P = A_c \times f_a = \pi d_a l_a f_a$$

$P$	SHAFT-ANCHOR CAPACITY
$A_c$	CYLINDRICAL SURFACE AREA OF SOIL-ANCHOR BOND
$f_a$	AVAILABLE UNIT SOIL-ANCHOR BOND STRESS
$d_a$	DIAMETER OF ANCHOR
$l_a$	LENGTH OF ANCHOR

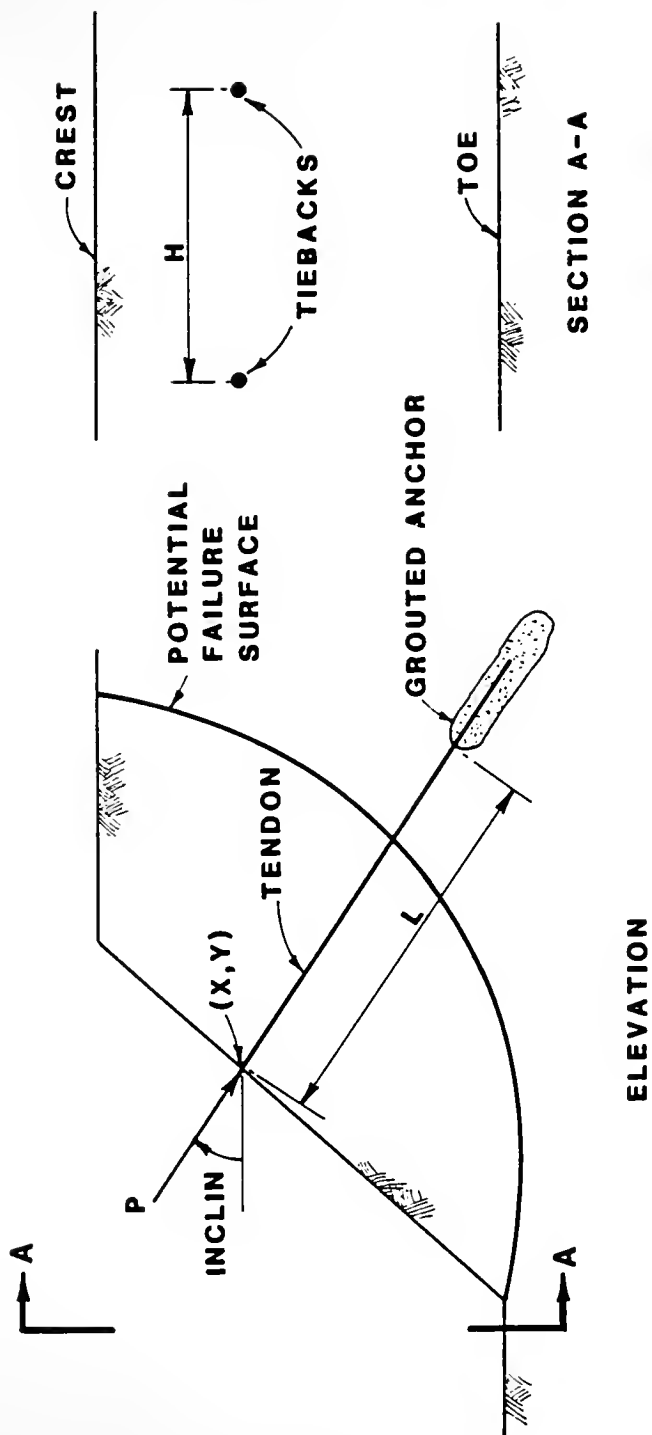
(a) FULL ANCHOR RESISTANCE DEVELOPED



$$P/2 = A_c/2 \times f_a = \pi d_a l_a/2 f_a$$

(b) ONE HALF ANCHOR RESISTANCE DEVELOPED

FIGURE 25. Development of Tieback Anchor Capacity



- Y Y COORDINATE OF POINT OF APPLICATION (ft) or (m)
- P MAGNITUDE OF LOAD PER TIEBACK (lbs) or (kg)
- H HORIZONTAL SPACING BETWEEN TIEBACKS (ft) or (m)
- I INCLINATION OF TIEBACK LOAD (deg)
- L FREE LENGTH OF TIEBACK (ft) or (m)

FIGURE 26. Tieback Input Parameters

as  $TLOAD_j$ , Figure 27, and is inclined from the horizontal by an angle,  $INCLIN$ .

The author considers the replacement of discrete tieback loads by an equivalent line load valid for tiedback structures since tiebacks are normally closely spaced (horizontally) and are anchored to horizontal load bearing elements, such as steel wales which transfer the tieback load to the retaining structure. The action of the wales causes a line load to be transferred to the structure. Based on the assumption of a uniform line load being formed between tiebacks, the TIES option in STABL neglects any three dimensional effects that may exist. If horizontal load bearing members are not present on a tiedback structure, or if the horizontal spacing between tiebacks is large, then this assumption is no longer valid. However, for structures with horizontal load bearing members and closely spaced tiebacks, it is the author's opinion that replacement of discrete tieback loads by an equivalent uniform line load is reasonable.

The radial stress on the midpoint of the base of a given slice is calculated using Flamant's Formula:

$$\sigma_{r_{ij}} = \frac{2(TLOAD_j) \cos(TTHETA_{ij})}{(\pi)(DIST_{ij})} \dots \dots \dots (7)$$

where:

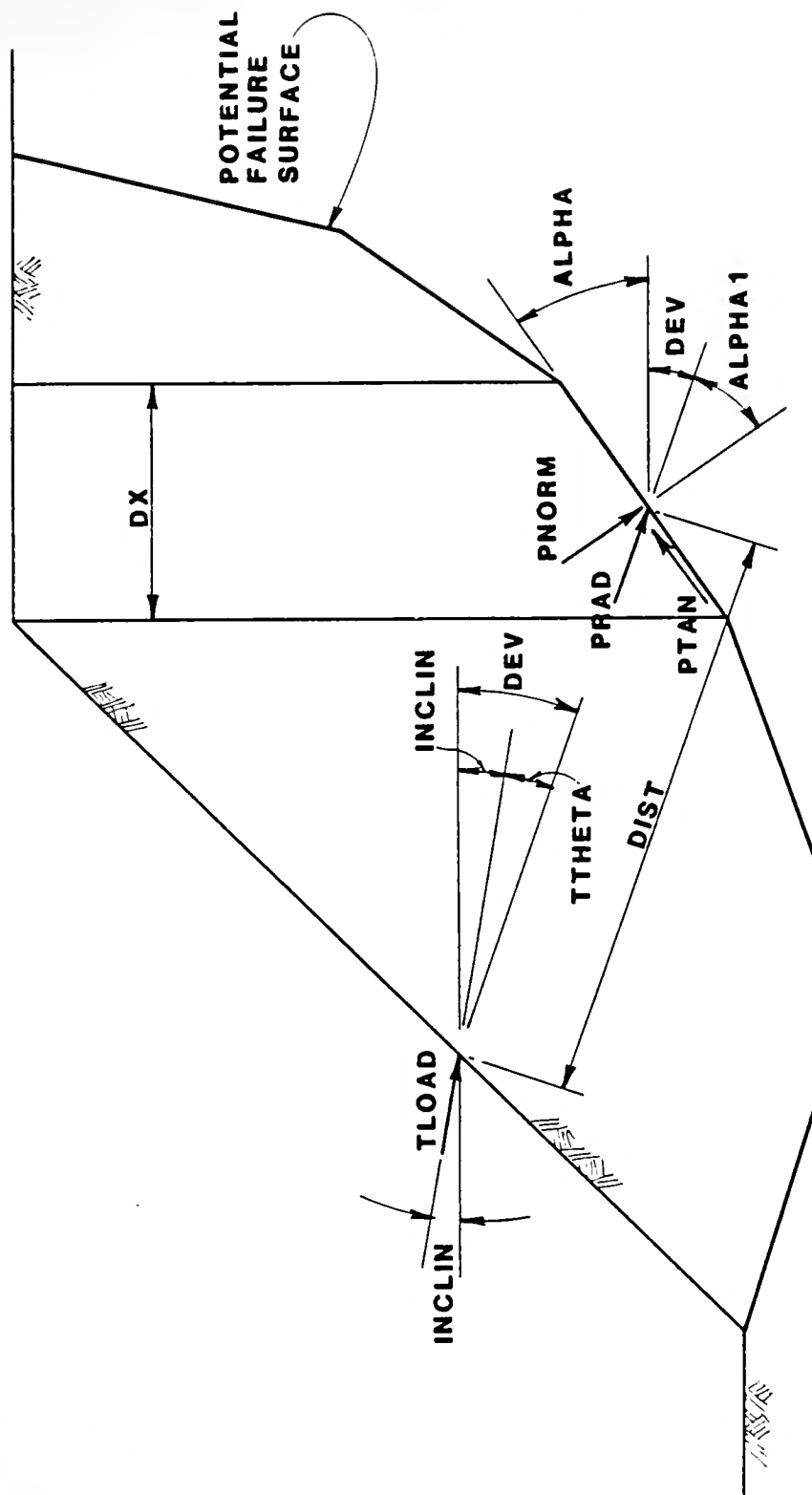


FIGURE 27. Transfer of Tieback Load to Potential Failure Surface

$\sigma_{rij}$  = Radial stress at the midpoint of the base of the  $i^{\text{th}}$  slice, produced by the  $j^{\text{th}}$  TLOAD

TLOAD<sub>j</sub> = Equivalent tieback line load for the  $j^{\text{th}}$  row of tiebacks

TTHETA<sub>ij</sub> = Angle formed by the line of action of the  $j^{\text{th}}$  TLOAD, and the line connecting the point of application of the tieback on the ground surface and the midpoint of the base of the  $i^{\text{th}}$  slice

$\pi$  = pi

DIST<sub>ij</sub> = Distance between the point of application of the  $j^{\text{th}}$  TLOAD on the ground surface, and the midpoint of the base of the  $i^{\text{th}}$  slice

The radial force, PRAD<sub>ij</sub>, at the midpoint of the base of a slice due to a given tieback load is calculated by multiplying the radial stress at that point in the soil mass by the length of the base of the slice:

$$\text{PRAD}_{ij} = \frac{2(\text{TLOAD}_j) \cos(\text{TTHETA}_{ij})}{(\pi)(\text{DIST}_{ij})} \cdot \frac{(\text{DX}_i)}{\cos(\text{ALPHA}_{ij})} \quad \dots (8)$$

where:

PRAD<sub>ij</sub> = Radial force acting on the midpoint of the base of the  $i^{\text{th}}$  slice due to the  $j^{\text{th}}$  TLOAD

$DX_i$  = Width of the  $i^{th}$  slice

$ALPHA_i$  = Inclination of the base of the  $i^{th}$  slice

The radial force,  $PRAD_{ij}$ , produced at the midpoint of the base of a given slice is proportional to the equivalent tieback line load applied,  $TLOAD_j$ , and the width of the slice,  $DX_i$ .  $PRAD_{ij}$  is inversely proportional to the distance,  $DIST_{ij}$ , between the point of application of the load, and the midpoint of the base of the slice.  $PRAD_{ij}$  is also dependent upon the angle,  $TTHETA_{ij}$ , which is the angle formed by the line of action of the load, and the line connecting the point of application of the load and the midpoint of the base of the slice. Therefore, slices whose bases intersect or nearly intersect the line of action of the tieback load will receive a larger portion of the total equivalent line load,  $TLOAD_j$ , than slices whose bases form a large angle,  $TTHETA_{ij}$ , with respect to the line of action of the tieback load.

The radial force acting at the midpoint of the base of a slice,  $PRAD_{ij}$ , is calculated in the same manner for all slices of the sliding mass.

Due to the slope geometry (i.e., slope is not a semi-infinite half space), location of the tiebacks, and shape of the failure surface, the sum of the radial forces acting at the midpoint of the base of the slices is normally not in static equilibrium with the applied load,  $TLOAD_j$ . The sum

of the radial forces in the direction of the line load is designated as  $PSUM_j$ , and is calculated by:

$$PSUM_j = \sum_{i=1}^n PRAD_{ij} \cos(TTHETA_{ij}) \dots \dots \dots (9)$$

where:

$PSUM_j$  = Sum of the radial forces acting at the midpoint of the base of the slices in the direction of the tieback load, for a given failure surface, due to the  $j^{th}$  TLOAD

$PRAD_{ij}$  = Radial force acting on the midpoint of the base of the  $i^{th}$  slice due to the  $j^{th}$  TLOAD

$TTHETA_{ij}$  = Angle formed by the line of action of the  $j^{th}$  TLOAD, and the line connecting the point of application of the tieback on the ground surface and the midpoint of the base of the  $i^{th}$  slice

As a result, a single multiplication factor is applied to the radial forces acting on the base of all the slices. The multiplication factor makes the sum of these forces in the direction of the applied load statically equal to the applied load. This multiplication factor, or correction factor, is designated as  $CORR_j$ , and is given by:

$$CORR_j = \frac{TLOAD_j}{PSUM_j} \dots \dots \dots (10)$$

where:

- $CORR_j$  = Correction factor for the  $j^{th}$  TLOAD for a given trial failure surface
- $TLOAD_j$  = Equivalent tieback line load for the  $j^{th}$  row of tiebacks
- $PSUM_j$  = Sum of the radial forces, at the midpoint of the base of the slices, in the direction of the  $j^{th}$  TLOAD for a given trial failure surface

The magnitude of  $CORR_j$  ranges from 0.56 to 1.31, with typical values being in the range of 0.89 to 1.11. These values were derived from circular, block and irregular shaped potential failure surfaces considering single and multiple tiebacks. The radial force applied to the base of each slice is modified as follows:

$$PRAD_{ij} = (PRAD_{ij})(CORR_j) \dots \dots \dots (11)$$

After equation 11 has been applied to the radial forces acting at the midpoint of the base of all the slices of the sliding mass, the sum of all the refined radial forces in the direction of the applied load will be in static equilibrium with the applied equivalent tieback line load,  $TLOAD_j$ .

The refined radial force for each slice,  $PRAD_{ij}$ , is broken into its components normal and tangential to the base

of each slice of the sliding mass for calculation of the FOS. The radial force on each slice is replaced by its normal and tangential components as calculated by:

$$PNORM_{ij} = (PRAD_{ij}) \cos(ALPHAL_{ij}) \dots \dots \dots (12)$$

$$PTAN_{ij} = (PRAD_{ij}) \sin(ALPHAL_{ij}) \dots \dots \dots (13)$$

where:

$PNORM_{ij}$  = Normal force on the midpoint of the base of the  $i^{th}$  slice produced by the  $j^{th}$  TLOAD

$PTAN_{ij}$  = Tangential force on the midpoint of the base of the  $i^{th}$  slice produced by the  $j^{th}$  TLOAD

$PRAD_{ij}$  = Refined radial force on the midpoint of the base of the  $i^{th}$  slice produced by the  $j^{th}$  TLOAD

$ALPHAL_{ij}$  = Angle formed by the line of action of the force  $PRAD_{ij}$  and the normal to the base of the  $i^{th}$  slice

The entire process outlined above is repeated for all additional rows of tiebacks. The normal components and the tangential components of the tieback loads due to all rows of tiebacks are summed separately and used in the slice equilibrium equations for calculating the FOS. The sum of the normal components of all the tieback loads acting on the midpoint of the base of a slice is designated as  $TNORM_i$ ,

while the sum of the tangential force components acting on the midpoint of the base of a slice is designated as  $TTAN_i$ .  $TNORM_i$  and  $TTAN_i$  are given by:

$$TNORM_i = \sum_{j=1}^m PNORM_{ij} \dots \dots \dots (14)$$

$$TTAN_i = \sum_{j=1}^m PTAN_{ij} \dots \dots \dots (15)$$

where:

$TNORM_i$  = Total normal force on the midpoint of the base of the  $i^{th}$  slice produced by all rows of tiebacks

$TTAN_i$  = Total tangential force on the midpoint of the base of the  $i^{th}$  slice produced by all rows of tiebacks

Figure 28 shows the forces acting on a slice considering tieback loads using the Load Distribution Method. The limiting equilibrium factor of safety equation for the Simplified Bishop method of slices considering tieback loads, as programmed in STABL4, is given as, (Notation after Siegel, 1975):

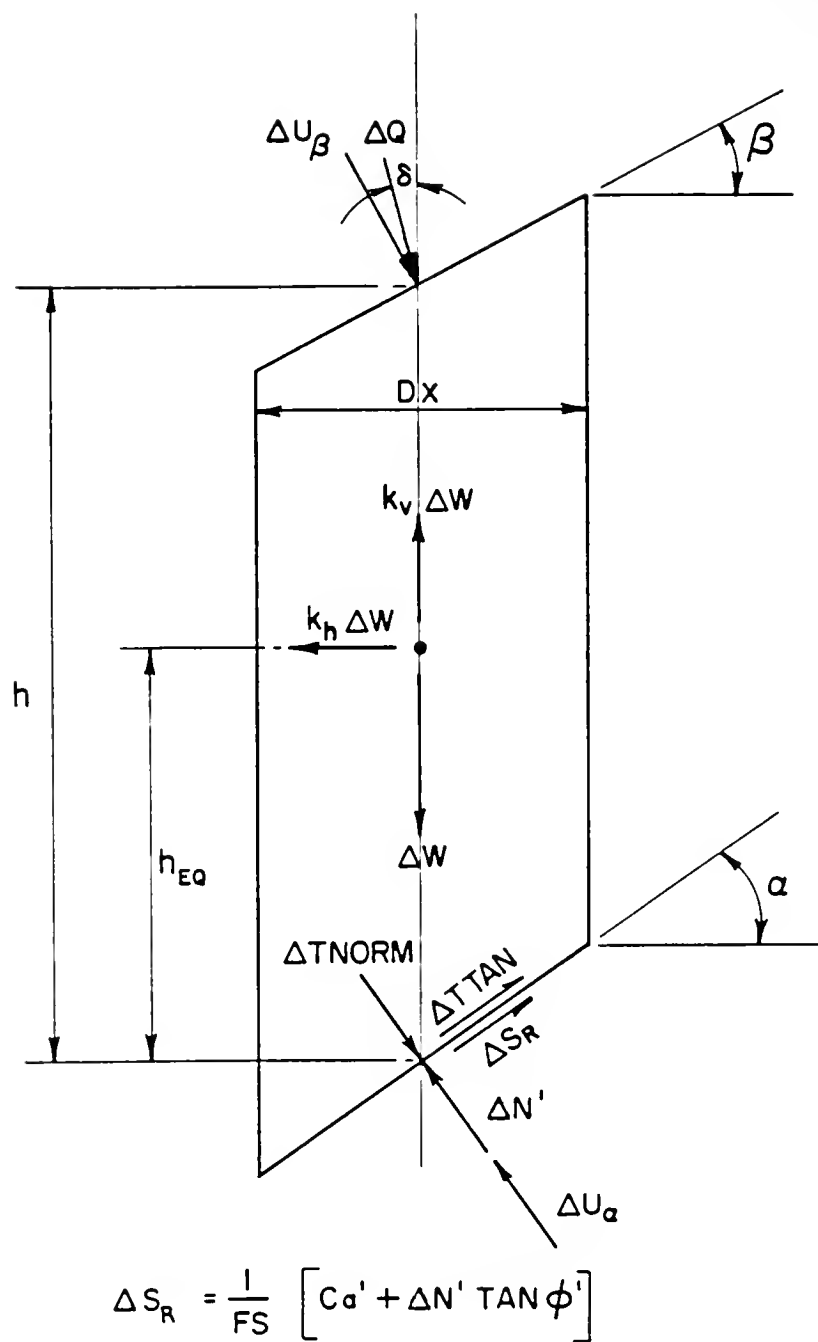


FIGURE 28. Slice forces Considered In STABL4 Using Load Distribution Method

$$FS = \frac{\sum_{i=1}^n \left[ \frac{A_1}{(1+A_2/FS)} \right]}{\sum_{i=1}^n [A_3] - \sum_{i=1}^n [A_4] + \sum_{i=1}^n [A_5] - \sum_{i=1}^n [A_6]} \dots \dots \dots (16)$$

where:

$$A_1 = C_a' + \tan\phi' \sec\alpha (\Delta W(1-k_v) + (\Delta TNORM - \Delta U_a) \cos\alpha + \Delta U_\beta \cos\beta + \Delta Q \cos\delta) - \Delta TTAN \sin\alpha$$

$$A_2 = \tan\alpha \tan\phi'$$

$$A_3 = (\Delta W(1-k_v) + \Delta U_\beta \cos\beta + \Delta Q \cos\delta) \sin\alpha$$

$$A_4 = (\Delta U_\beta + \Delta Q \sin\delta) (\cos\alpha - h/R)$$

$$A_5 = \Delta W k_h (\cos\alpha - h_{eq}/R)$$

$$A_6 = \Delta TTAN$$

$$C_a' = \text{Cohesion force} = c' \cdot (dx) / \cos\alpha$$

FS = Factor of safety: assumed equivalent on all slices

The complete derivation of equation 16 is found in the Appendix. The limiting equilibrium factor of safety equation for the Simplified Janbu method of slices considering tieback loads, as programmed in STABL4 using Carter's method (Siegel, 1975), is given below. Boutrup (1977) showed that the Janbu method should not be used for circular surfaces and that the Bishop method should be used only for circular failure surfaces. The derivation of equation 17 is similar to that of equation 16 with the exception that the center of rotation is taken at infinity.

$$FS = \frac{\sum_{i=1}^n \left[ \frac{A_1}{(1+A_3/FS)} \right]}{\sum_{i=1}^n [A_2]} \dots \dots \dots (17)$$

where:

$$A_1 = [C_a' + \tan\phi' \sec\alpha (\Delta W(1-k_v) + (\Delta TNORM - \Delta U_\alpha) \cos\alpha + \Delta U_\beta \cos\beta + \Delta Q \cos\delta)] / \cos\alpha$$

$$A_2 = \Delta W(\tan\alpha + k_h + k_v \tan\alpha) + \Delta U_\beta (\cos\beta \tan\alpha - \sin\beta) + \Delta Q(\cos\delta \tan\alpha - \sin\delta) - \Delta TTAN / \cos\alpha$$

$$A_3 = \tan\alpha \tan\phi'$$

$$C_a' = \text{Cohesion force} = c' \cdot (dx) / \cos\alpha$$

FS = Factor of safety: assumed equivalent on all slices

Note that both equations 16 and 17 assume that the factor of safety on each slice is the same. This assumption requires that each slice of the sliding mass must fail simultaneously. The result is that the FOS calculated by equations 16 and 17 is an average FOS for all the slices. However, in reality the factor of safety on each slice is not the same and it is possible to have slices which have failed while others remain stable. The assumption that the FOS is the same on all slices is required for the solution of limiting equilibrium stability equations and is used extensively (Janbu, 1954; Bishop, 1955; Morgenstern and Price, 1965; Spencer, 1967).

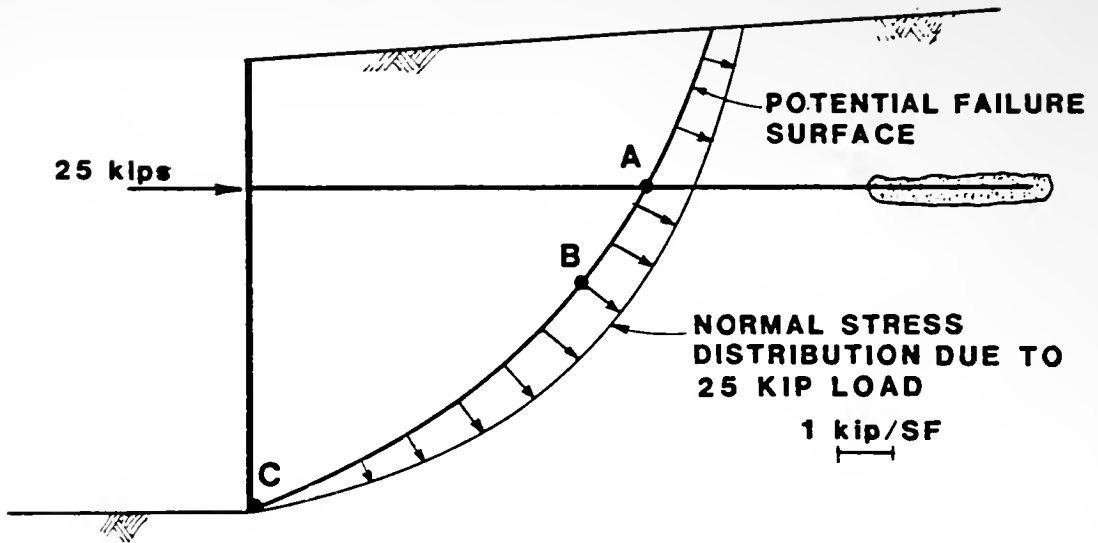
### Distribution of Load to Failure Surface

The distribution of stress (and hence force) to the base of the slices of the sliding mass has been studied in detail to verify the reasonableness of the distributions generated. The following sections examine the distribution of stresses to the potential failure surface produced by the Load Distribution Method. Restrictions on the distribution of stress to the failure surface will also be discussed.

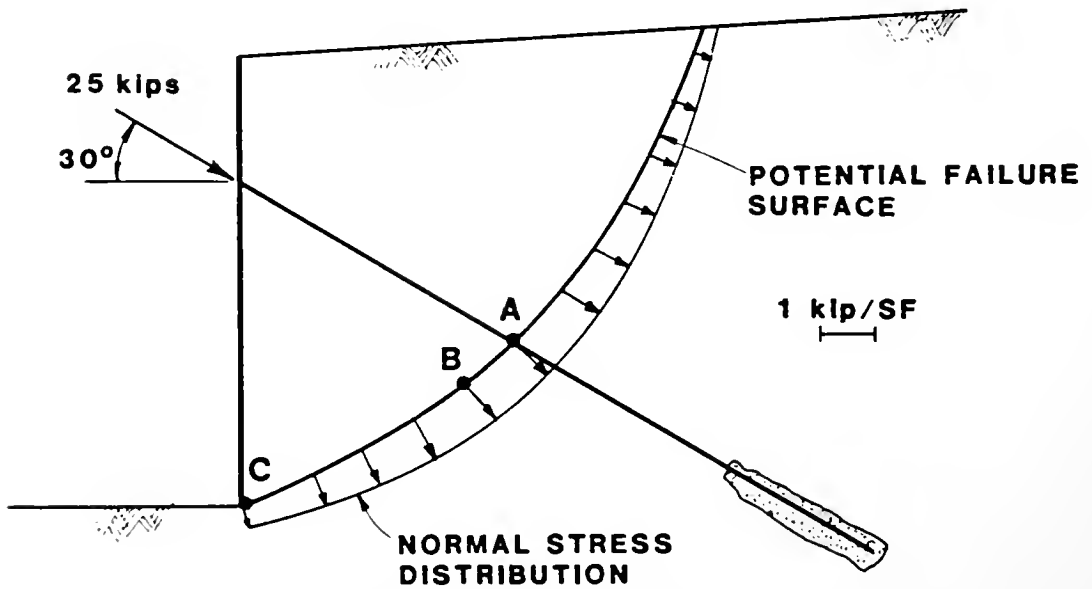
#### Distribution of Normal and Tangential Stresses

To clearly demonstrate the distribution of normal and tangential stresses (and hence forces) to a failure surface produced by the Load Distribution Method, a simple tiedback wall has been chosen as an example. The wall shown in Figure 29, is 15 feet (4.57 m) high and has a circular potential failure surface. Two different configurations of tiebacks are considered to demonstrate the change in distribution of stress produced along the potential failure surface with variation in tieback/failure surface geometry.

Figure 29a shows the wall subjected to a horizontal tieback load of 25 kips. The 25 kip tieback load is replaced by an equivalent distribution of normal and tangential stresses on the failure surface as computed using the LDM. The distribution of normal stress along the failure surface is smooth and is largest at approximately the midpoint of the failure surface (point B). Note that the normal stress is not largest in the direction of the



(a) TIEBACK HORIZONTAL



(b) TIEBACK INCLINED AT 30°

FIGURE 29. Distribution of Normal Stress to Potential Failure Surface

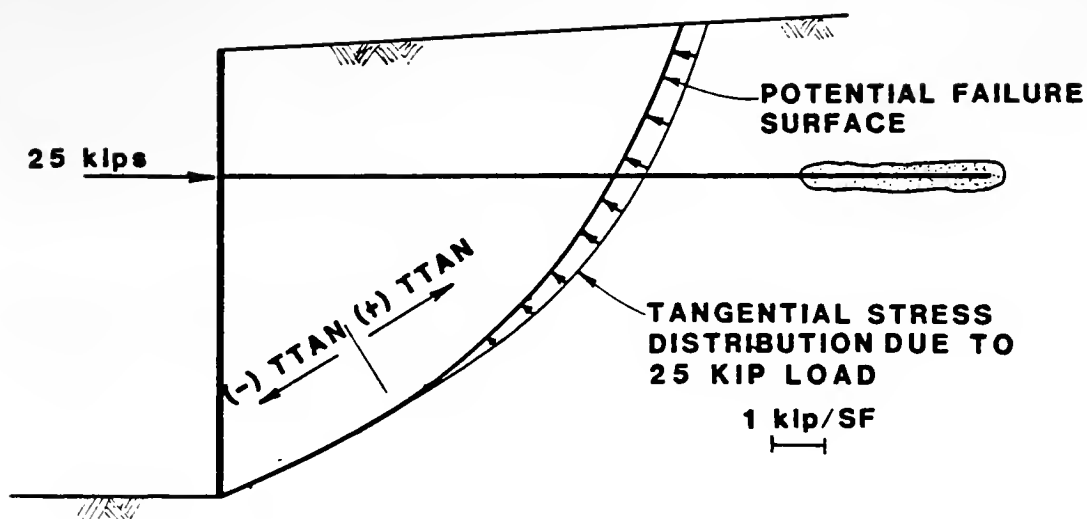
tieback ( $T\theta_{ij}=0$ , point A), but at point B. This is due to the fact that point B on the failure surface is slightly closer to the point of application of the tieback load on the wall than point A, even though  $T\theta_{ij}$  at point B is not zero (Eqn. 8). The result is that point B has a higher normal stress than point A even though the value of  $\cos(T\theta_{ij})$  is largest at point A. In addition, note that point C on the failure surface has no normal stress caused by the tieback load since this point is normal to the direction of the tieback load (i.e.,  $T\theta_{ij}=90^\circ$ ;  $\cos 90^\circ=0$ ;  $P\theta_{ij}=P\theta_{ij}=P\theta_{ij}=0$ : Figure 27; Eqns. 7,8,12,13). It is apparent that both the distance from the point of application of the tieback load, and the deviation from the line of action of the tieback load have an effect on the stress produced at the midpoint of the base of a slice.

Figure 29b shows the same wall subjected to a tieback load of 25 kips inclined at  $30^\circ$  from the horizontal. The normal stress distribution is similar to that of Figure 29a, except that the stress distribution is shifted lower on the failure surface. Again the normal stress at point B is greater than in the direction of the tieback load (point A). Note that the normal stress at point C is no longer zero since  $T\theta_{ij}$  has some value less than  $90^\circ$ . In addition, the the normal stress at the upper portion of the potential failure surface is smaller for Figure 29b, as compared to that of Figure 29a.

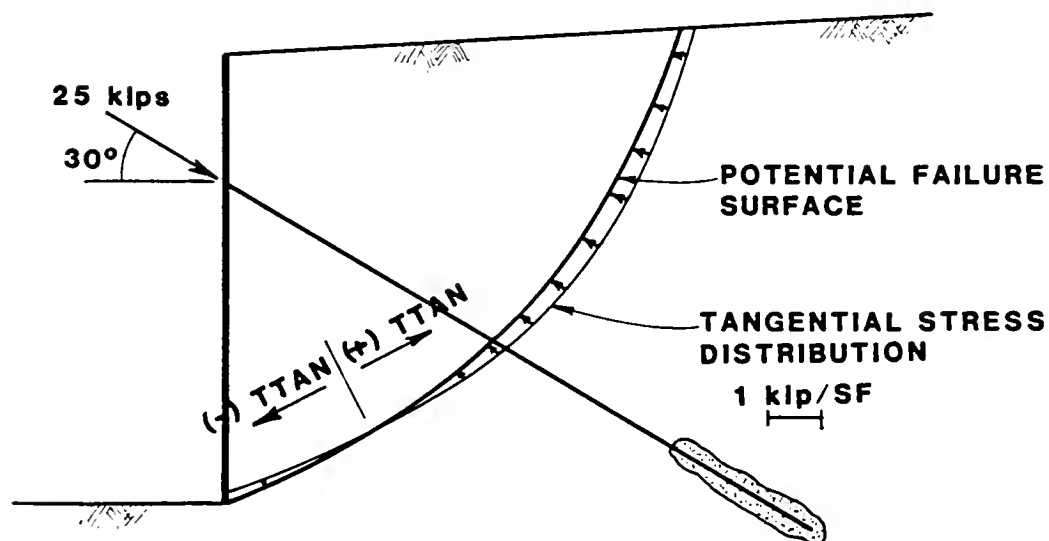
Figures 30a and 30b show the tangential stress distributions to the potential failure surface produced by the Load Distribution Method for the tiedback wall of Figure 29. A positive value of the tangential stress indicates that the stress acts to resist rotation (upward direction), while a negative value indicates that the stress actually tends to promote rotation (downward direction). The negative stress values result from the interaction of the direction of the tieback load and the inclination of the base of the slice, (i.e.,  $\text{ALPHA}_{ij} < 0$ ;  $\sin(\text{ALPHA}_{ij}) < 0$ ; Figure 27; Eqn. 13).

Figure 31a shows the normal stress distribution on the potential failure surface of a wall subjected to two tiebacks. The normal stress distributions of Figure 29a and 29b are superimposed to form the distribution shown in Figure 31a. Likewise, the tangential stress distributions of Figures 30a and 30b are superimposed to form the distribution shown in Figure 31b.

Similar distributions of normal and tangential stresses were obtained by Tenier and Morlier (1982). They compared the results of finite element analyses with those obtained using Flamant's distribution of stresses corrected for static equilibrium. The results verified that the distributions of normal and tangential stresses obtained using Flamant's distribution of stresses, corrected for

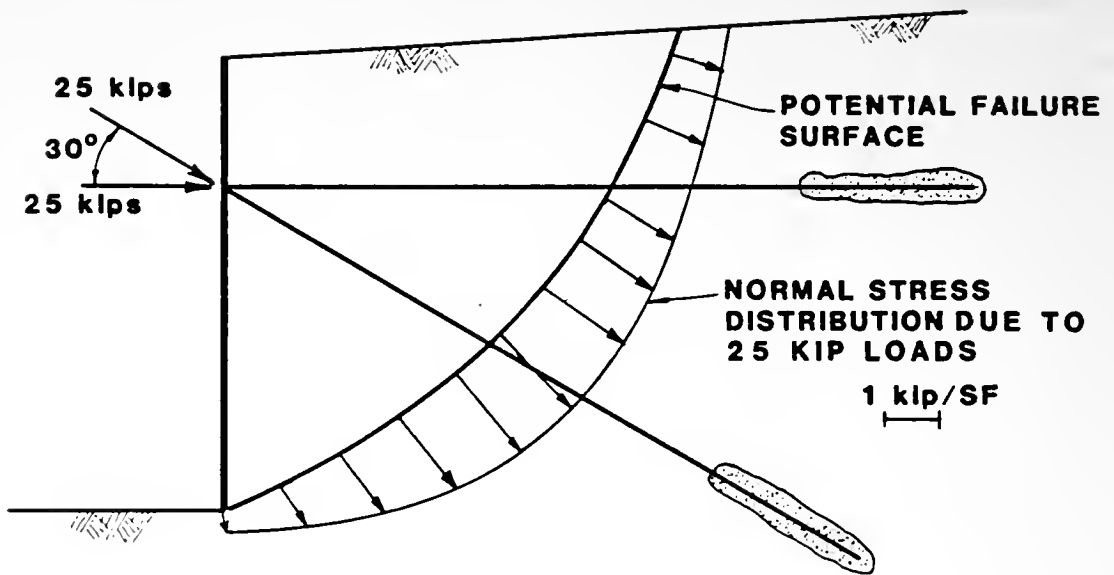


(a) TIEBACK HORIZONTAL

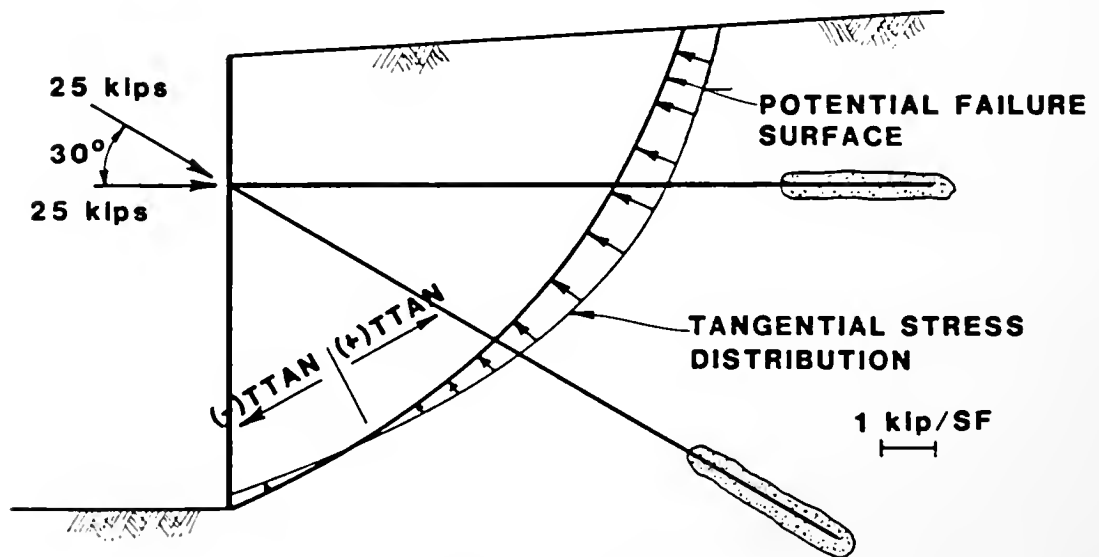


(b) TIEBACK INCLINED AT 30°

FIGURE 30. Distribution of Tangential Stress to Potential Failure Surface



(a) DISTRIBUTION OF NORMAL STRESS TO POTENTIAL FAILURE SURFACE



(b) DISTRIBUTION OF TANGENTIAL STRESS TO POTENTIAL FAILURE SURFACE

FIGURE 31. Distribution of Tieback Stress to Potential Failure Surface for Two Tiebacks

static equilibrium, were in good agreement with those obtained using a finite element model.

Tenier and Morlier's analyses were performed on simple slopes subjected to tieback loads with homogeneous soil parameters. The analyses did not consider nonhomogeneous soil conditions, ground water tables, pore pressures or earthquake loading. STABL4, on the other hand, is capable of handling all the conditions mentioned above.

#### Restrictions on Distribution

There are two situations when the load from a tieback is not distributed to all the slices of the sliding mass. The first situation occurs when the line between the point of application of the tieback load on the ground surface and the midpoint of the base of a given slice intersects the ground surface. Figure 32 shows the limit of stress distribution to the failure surface, as restricted in the LDM, for a benched slope subjected to a tieback load. The tieback load is not distributed to the extreme upper and lower portions of the failure surface, since this requires the transfer of load outside the soil mass.

The second restriction ensures that negative (upward/tensile) radial stresses are not transferred to the potential failure surface using the Load Distribution Method. Negative radial stresses could potentially be produced when a point on the failure surface is behind the normal to the tieback load line of action (Point A), Figure

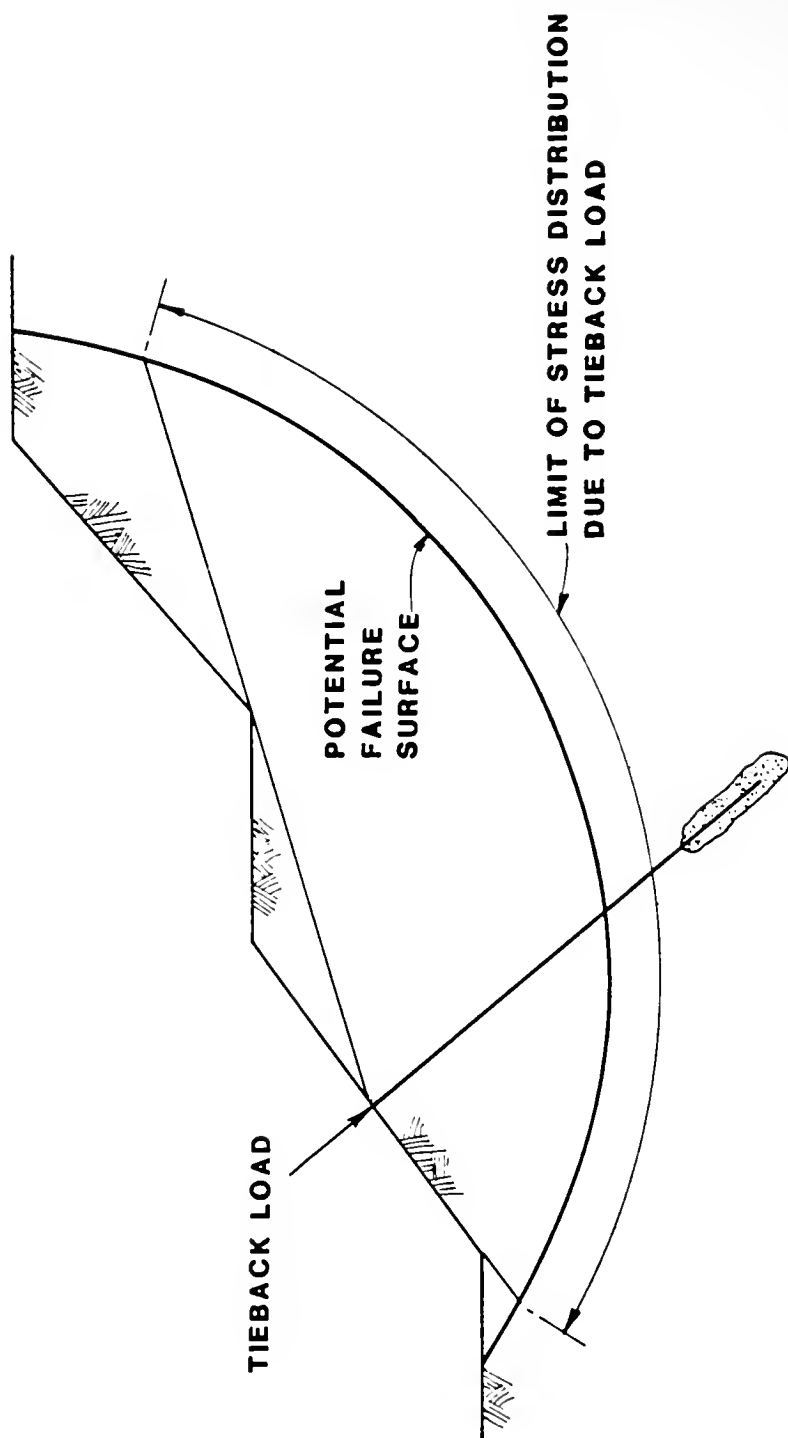


FIGURE 32. Limit of Stress Distribution to Potential Failure Surface Due to Tieback Load

33. Since soils are capable of sustaining little or no tensile loads, it is not realistic to allow tensile stresses to be transferred to the failure surface. Therefore, the Load Distribution Method sets the radial stress on such a slice to zero.

### Applications

The Load Distribution Method programmed in STABL4 is extremely versatile and is capable of modelling not only tieback loads, but also uniform line loads, surcharge loads, strut loads from braced excavations, tiedback structures below the ground surface and reinforced earth and fabric reinforced walls. These applications are discussed below.

#### Uniform Line Loads

Horizontal, inclined, or vertical uniform line loads may be modelled using the LDM by specifying that the horizontal spacing between "tieback loads" is unity (one) and that the length of the "tieback" is zero. Specifying a horizontal spacing of unity indicates that a uniform line load is specified. When a tieback length of zero is specified, STABL4 distributes the load to all potential failure surfaces generated.

#### Distributed Loads

Inclined or vertical distributed loads may be modelled with the LDM by replacing the distributed load with a series of statically equivalent line loads (Figure 34). As with

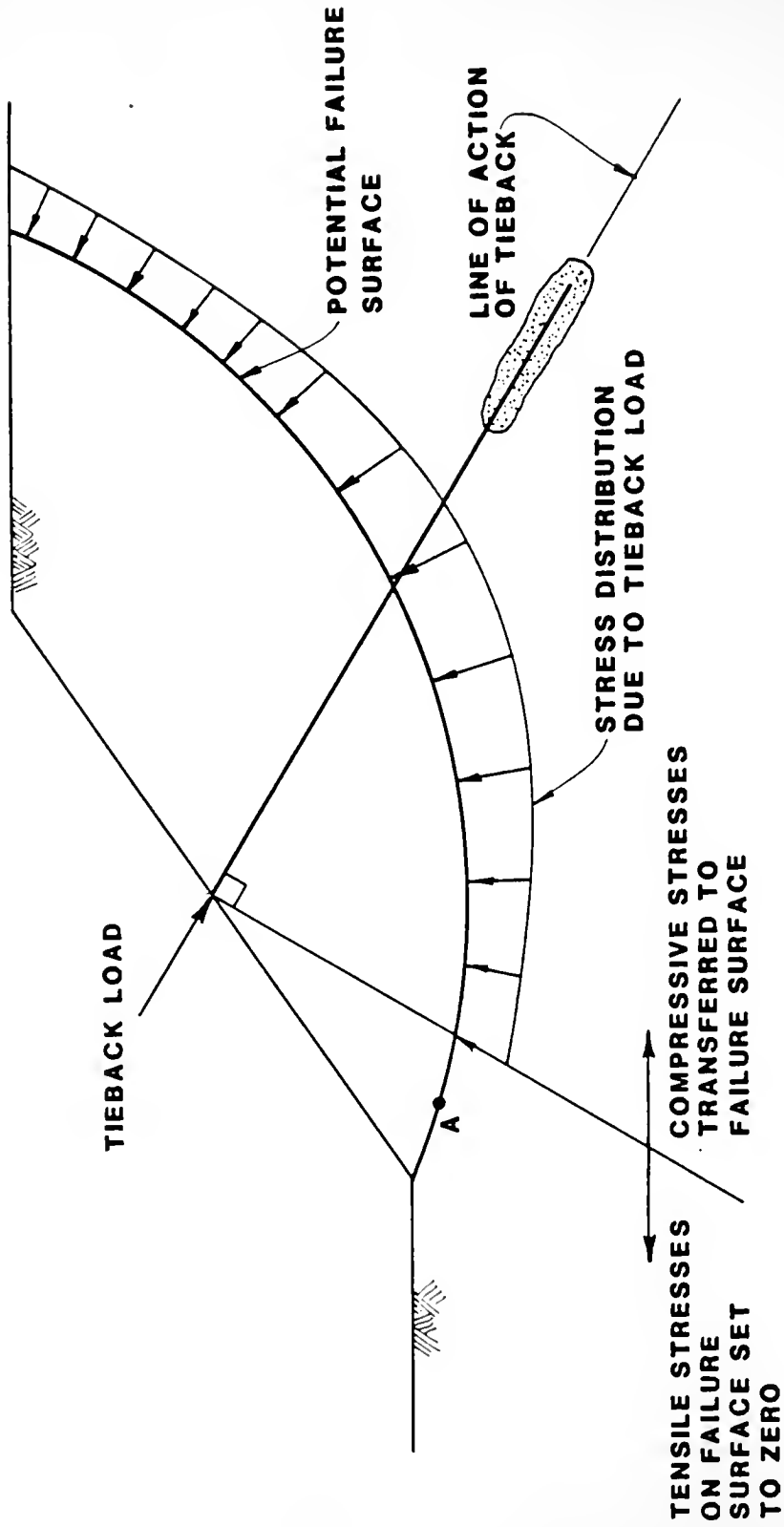


FIGURE 33. Restriction of Stress Distribution to Potential Failure Surface Due to Tieback Load

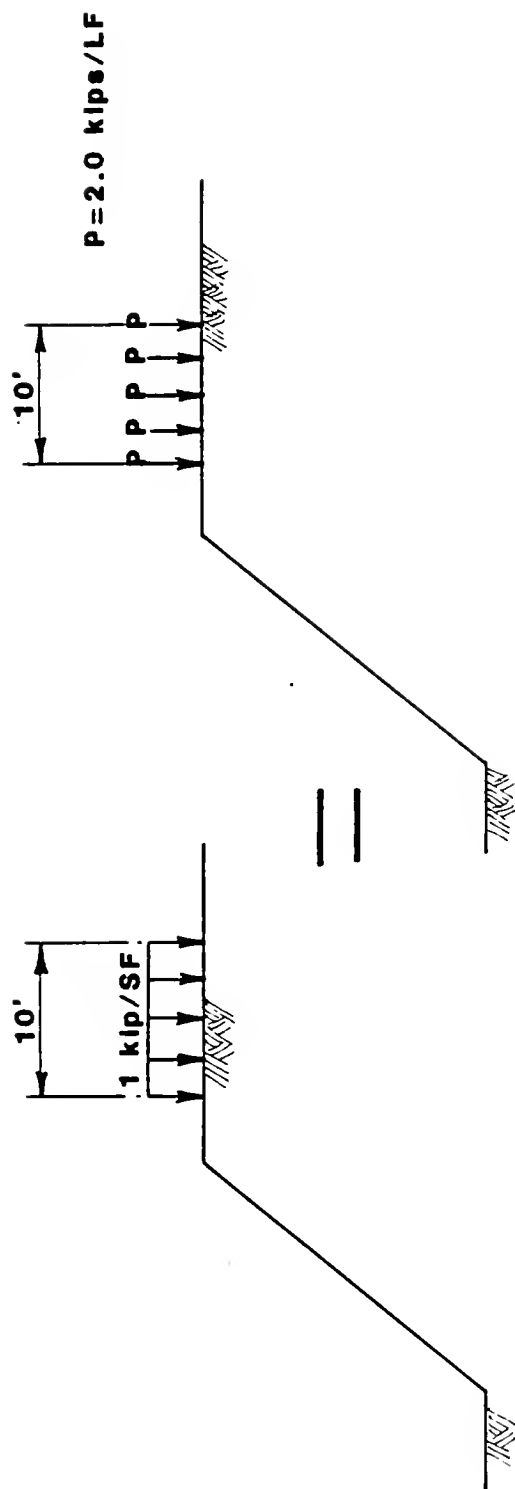


FIGURE 34. Modelling Distributed Loads with Concentrated Loads Using Load Distribution Method

uniform line loads, the horizontal spacing is specified as unity and the length of the "tieback" is specified as zero. The load from the series of line loads will be distributed to all potential failure surface. Replacing the distributed with a series of line loads shouldn't produce concern since the load from a line load is considered not only on the slice on which it acts, but is distributed to the entire failure surface.

The LOADS option in STABL4 handles distributed loads by replacing the total distributed load acting on a slice with a statically equivalent concentrated load applied to the top of the slice. Therefore with the LOADS option, the load from a distributed load is taken into account only on the slices on which it acts. Conversely, if a distributed load is modelled with the LDM, the load will be taken into account on all slices of the sliding mass. However, it is the author's opinion that the LOADS option should continue to be used rather than the TIES options for distributed loads since results obtained using the LDM have not been reasonable. Further study into this application is required.

#### Braced Excavations

Strut loads against the side of a braced excavation may be modelled with the LDM. The estimated or measured loads in the struts are specified along with the horizontal spacing between struts. As with line loads, the length of

the "tieback" is specified as zero. Since the struts bear against horizontal wales, the action of the wales will cause an equivalent uniform line load to be produced against the retaining structure.

#### Buried Tiedback Structures

Modelling a tiedback structure which is buried below the ground surface may seem to present a problem since the TIES option requires that the tieback load be applied to a ground surface boundary. However this situation may be easily modelled. Figure 35 shows how this problem may be handled. The boundary on which the tieback load acts is specified as a ground surface boundary. Since STABL does not permit vertical ground surface boundaries, the buried wall is modelled as slightly inclined to the right and the soil in front of the wall is modelled as a ground surface boundary slightly inclined to the left.

Modelling the buried tiedback wall in this manner will satisfy the input requirements for STABL4, yet it will not improperly model the actual conditions of the slope.

#### Reinforced Earth Walls/Fabric Reinforced Walls

The forces supporting a reinforced earth or fabric reinforced wall can theoretically be modelled using the LDM. The forces within the strips or layers of fabric may be modelled as a line load applied to the face of the wall. The real challenge in such an analysis is estimating or

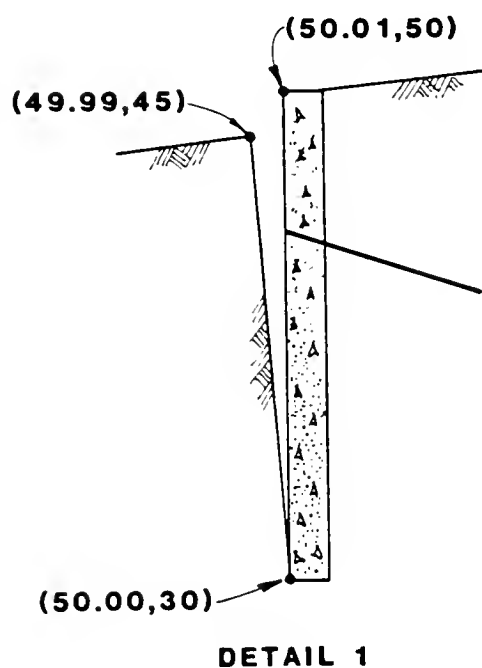
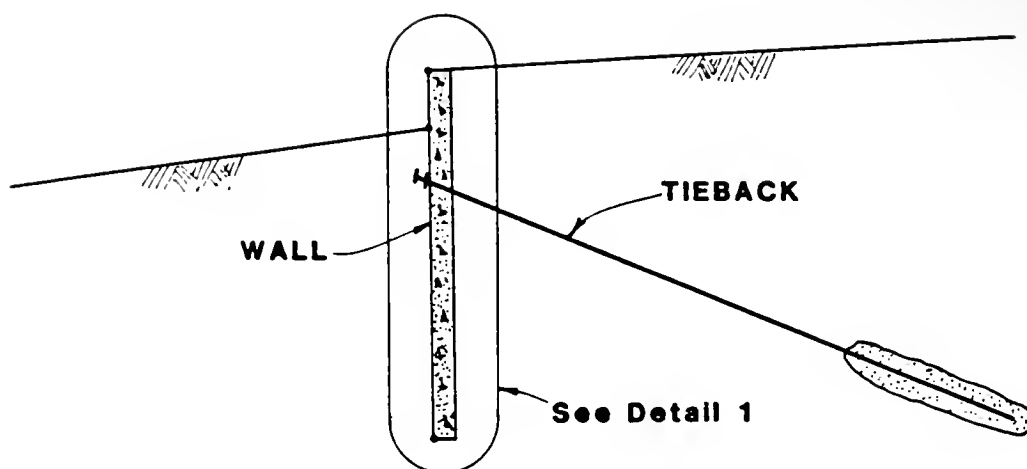


FIGURE 35. Modelling Buried Tiedback Structures

determining the loads within the strips or layers of fabric available to resist sliding or rotation for input into a stability analysis. The determination of such loads is beyond the scope of this study.

### Limitations

Since the LDM is based on a solution of stress distribution through a homogeneous elastic half-space, the LDM does not take into account the relative stiffness of individual soil layers. Hence, the stresses distributed to the potential failure surface are independent of the deformation characteristics of the soil profile. The load from a tieback will be distributed to a potential failure surface in the same manner for both a homogeneous soil profile and a layered soil profile.

This limitation is not significant for most layered soil profiles whose individual soil layers do not have grossly different stiffness characteristics. However this limitation may be more significant for soil profiles which have grossly different soil layer stiffness characteristics. This topic is worthy of further investigation.

Of greater importance is the fact that most slopes and retaining walls do not conform to the assumption of a semi-infinite half space. Harr (1977) shows that Flamant's distribution of stresses is affected by the boundary conditions imposed (i.e., semi-infinite elastic half space versus some other type of elastic space). Therefore, the

validity of using Flamant's solution for the distribution of stresses in a semi-infinite elastic half space for problems which do not conform to a semi-infinite half space must be investigated. This point will be discussed further in the following chapter.

It is important to note that the Load Distribution Method or any type of limiting equilibrium slope stability analysis does not consider displacements of the soil mass or the tiebacks. Displacements may result in increased loads on the tiebacks and reduced soil resistance.

When analyzing the stability of a tiedback slope or retaining wall, the pullout resistance of the anchor must be designed separately. In addition, local failure of the soil directly behind the structure due to excess loads must be investigated. Analysis of the stability of a tiedback structure is just one of many design considerations in the design of a tiedback retaining structure. STABL is only one tool for performing the stability calculations. The reasonableness of any solution provided by STABL or any other computer generated solution must be judged by the engineer.

#### CHAPTER IV. PARAMETRIC STUDIES USING THE LDM

Parametric studies were performed on slopes and walls subjected to tieback (or concentrated) loads using the Load Distribution Method. The studies were performed to determine the effect of several variables on the FOS such as point of application of load, load inclination, load magnitude, soil strength characteristics, and multiple tiedback structures. The results of these studies are presented below. The slope models used in this chapter have been chosen for their simple geometry and soil conditions so that the results obtained may be clearly evident to the reader. Similar results are obtained for more complex soil and geometry conditions, as well as for noncircular surfaces analyzed using the Simplified Janbu method of slices.

##### Effect of Point of Application on Factor of Safety

The point of application, or vertical location, of a tieback load is an important factor to consider when designing a support system for a retaining wall or slope. The vertical location of tieback loads on a retaining wall is determined by the lateral earth pressure distribution behind the wall. Therefore, the point of application of the tiebacks is relatively fixed and is not a variable in the

design of the overall stability of the wall. However, for landslide stabilization, the point of application is not fixed and may be varied to ensure the required stability.

Figure 36 shows the effect of the point of application of a load (on the ground surface) on the FOS for a specific potential failure surface. The FOS for this slope without any tiebacks is 1.087. It is apparent that the FOS increases as the load is placed lower on the slope. This observation should be expected since the moment arm of the load, with respect to the center of rotation, increases as the load is placed lower on the slope. Since the Load Distribution Method does not consider the moment arm of the load, it is important to understand how the LDM produces a higher FOS for the lower loads.

The FOS is largest for the bottom load since the distance from the point of application of the load on the ground surface to the potential failure surface is the smallest. Therefore, the normal and tangential forces produced by the load on the potential failure surface, in the direction of this load, will be greater than for any of the upper loads (Eqns. 8,12,13). In addition, since the bottom load is so low on the slope, it will produce only positive (upward/resisting) tangential forces on the potential failure surface whereas the upper loads will produce some negative (downward/driving) forces.

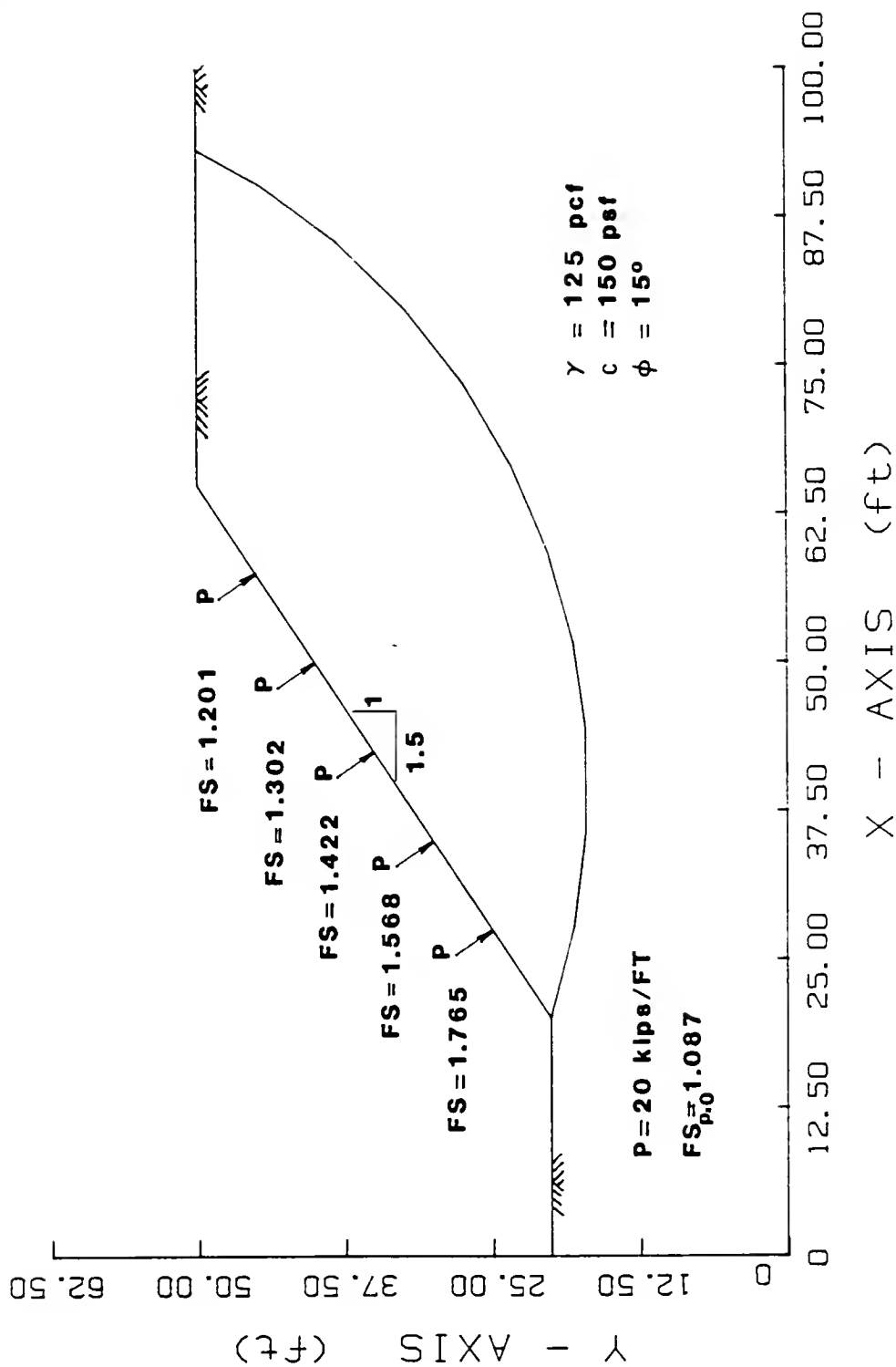


FIGURE 36. Effect of Point of Application on Factor of Safety

One important feature and advantage of the LDM is that it accounts for the presence of concentrated loads acting through the center of rotation. Figure 37 shows a slope subjected to a load whose line of action passes through the center of rotation of the sliding mass and bisects the length of the potential failure surface.

If this slope has purely cohesive soil characteristics, the load should have no effect on the FOS. It is apparent from Figure 37 that a load acting through the center of rotation does not alter the FOS of the slope. The FOS is unaltered since the tangential forces produced on the potential failure surface are balanced above and below the intersection of the line of action of the load and the potential failure surface (Point A, Figure 37). The tangential forces above Point A are positive and equal in magnitude to the negative tangential forces along the potential failure surface below Point A. The sum of the tangential forces is therefore zero. In addition, since the soil has no frictional component, the increase in normal force along the potential failure surface (produced by the presence of the load) has no effect on the mobilized soil resistance.

In contrast, if the slope has a frictional component of soil resistance, a load whose line of action passes through the center of rotation should increase the FOS since the normal force on the potential failure surface is increased,

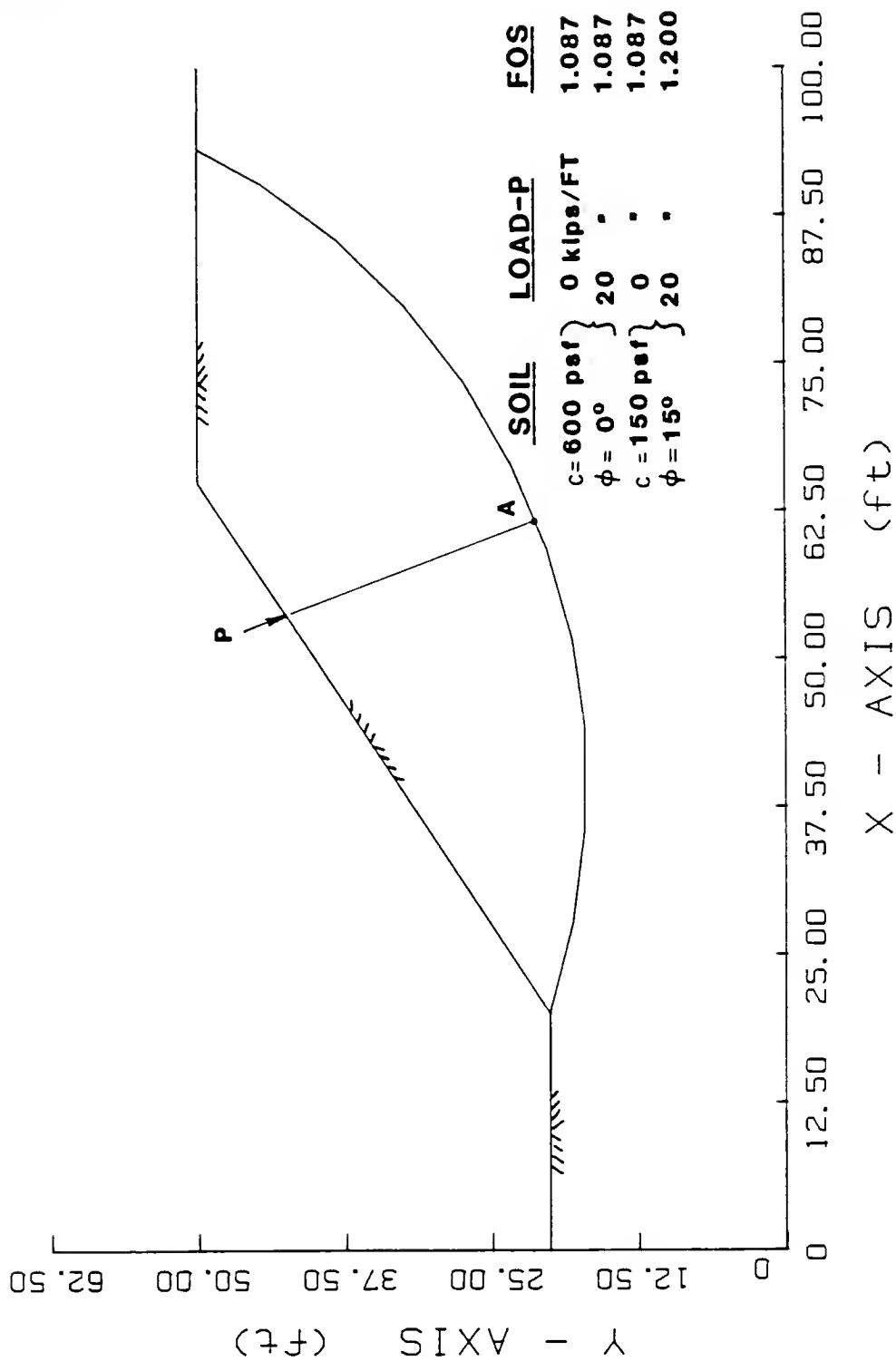


FIGURE 37. Load Line of Action Through Center of Rotation

thereby increasing the mobilized soil resistance (Eqn. 5). Figure 37 shows that the FOS is indeed increased using the LDM for a slope with frictional soil characteristics subjected to a load whose line of action passes through the center of rotation. Again the sum of the tangential forces on the potential failure surface is zero and does not affect the FOS. The increase in the FOS is due solely to the addition of the distribution of normal force on the potential failure surface produced by the load using the LDM. The increase in normal force along the potential failure surface increases the mobilized soil resistance.

#### Load Inclination versus Factor of Safety

Figure 38 shows the slope model used to study the effect of load inclination on the FOS. Loads A and B were applied to the slope independently and the angle of the applied load was varied between  $0^{\circ}$  and  $90^{\circ}$ , with respect to the horizontal. The results of the study are shown in Figure 39.

Figure 39 shows that the FOS is highest when the load acts in the horizontal direction, and decreases as the inclination of the load is increased. It is apparent that the FOS is only mildly affected for a moderate variation in load inclination. For example, for a typical range of tieback inclination limits, between  $5^{\circ}$  and  $30^{\circ}$ , the variation in the FOS is only approximately 0.1.

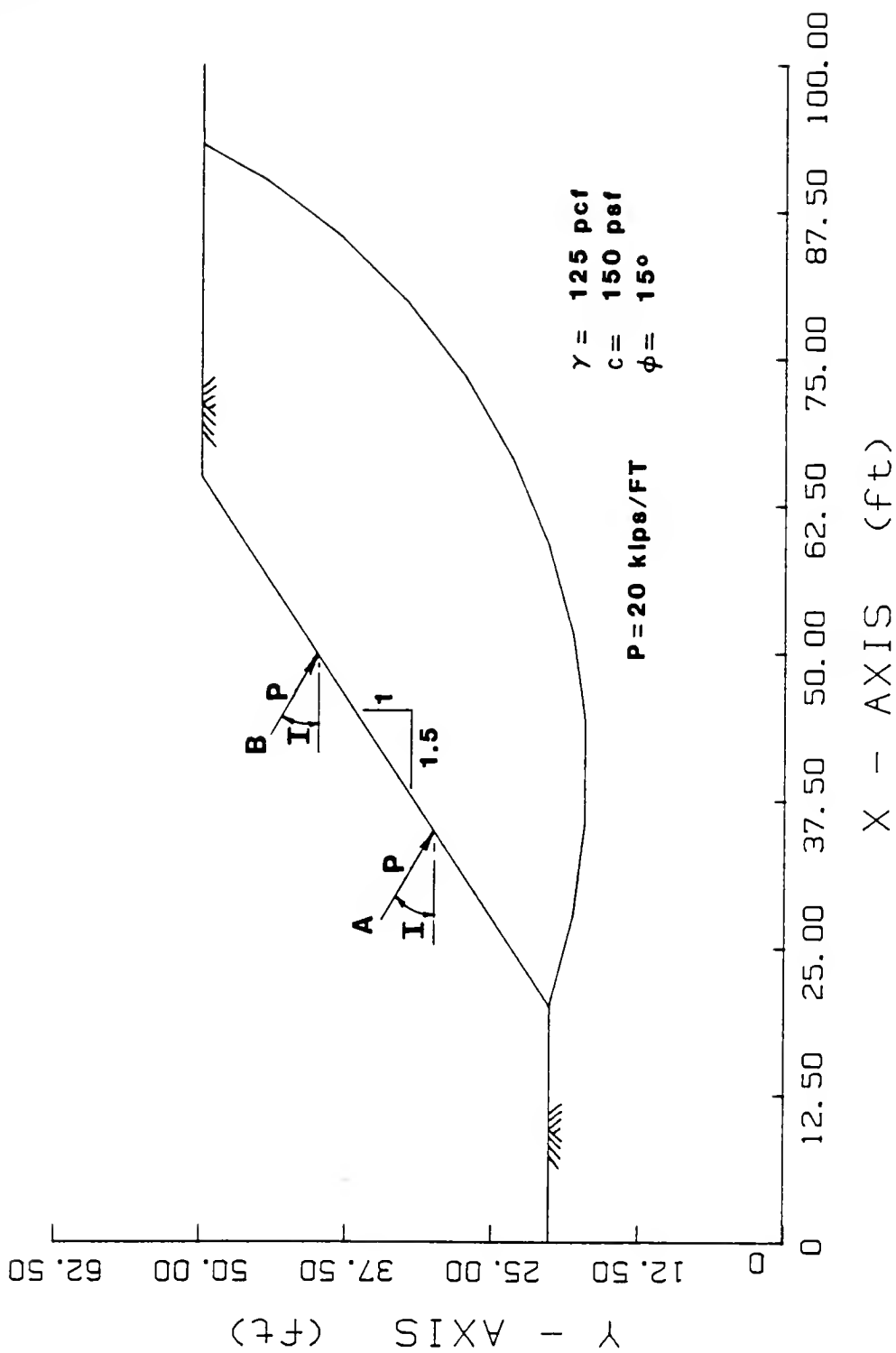


FIGURE 38. Slope Model for Load Inclination versus Factor of Safety Study

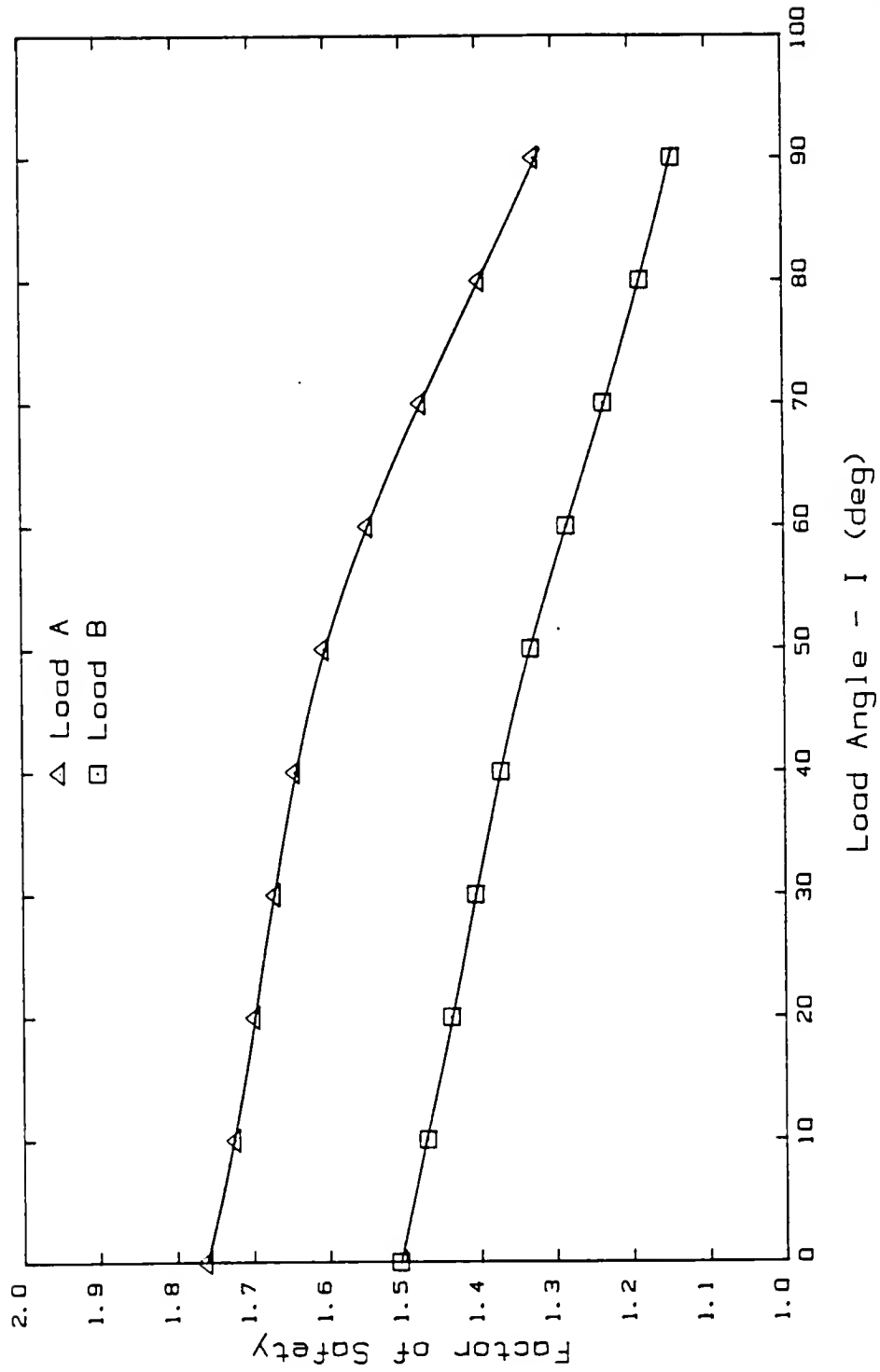


FIGURE 39. Load Inclination versus Factor of Safety

Note that the distribution of the load to the failure surface is restricted for this load/slope combination for load angles less than  $57^{\circ}$  or greater than  $72^{\circ}$ . These restrictions are discussed in Chapter 3 and are responsible for the change in curvature of the lines shown in Figure 39 for load angles less than  $57^{\circ}$  or greater than  $72^{\circ}$ .

Figure 39 also shows that the vertical location of the load on the ground surface has a more significant effect on the FOS than a moderate variation in the angle of load inclination.

#### Load versus Factor of Safety

One of the prime factors considered in the design of tiedback structures is the determination of the magnitude of the applied load required to ensure stability. The effect of the magnitude of the applied load was investigated for various soil conditions for the slope shown in Figure 40.

#### Purely Cohesive Soils

The effect of increasing the normal force on the failure surface, through the use of an applied load such as a tieback load, will not increase the mobilized soil resistance for slopes with purely cohesive soil characteristics (Eqn. 8). Therefore, the distribution of the component of an applied load normal to the failure surface will have no effect on the overall stability of the slope. However, the tieback does offer resistance to

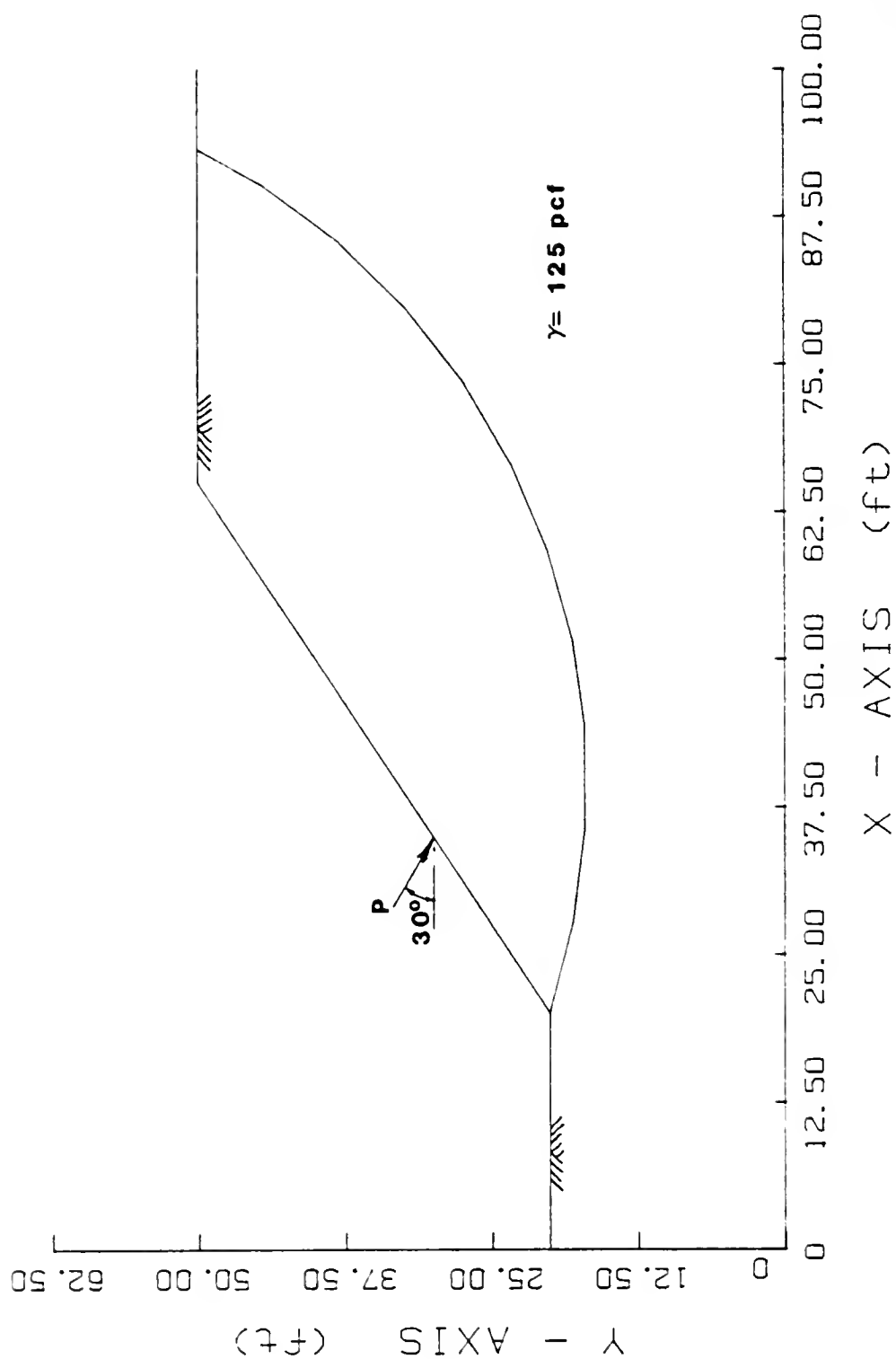


FIGURE 40. Slope Model for Load versus Factor of Safety Studies

sliding through the distribution of the component of the tieback load tangential to the potential failure surface.

Figure 41 demonstrates the effect of increasing load on the FOS for three purely cohesive soil strengths. The FOS is observed to increase nearly linearly with an increase in applied load. Note that the increase in FOS is due only to the presence of the components of the load tangential to the potential failure surface.

Theoretically, the lines shown in Figure 41 should be linear since the only variable being changed is the load applied to the slope and since the normal force on the base of a slice has no effect on the soil resistance for purely cohesive soils. Therefore, the FOS should vary linearly with a linear increase in the load applied to the slope. The curvature of the lines shown in Figure 41 is attributed to the fact that a solution for stress distribution in a semi-infinite half space (Flamant's equation; Eqn. 6) is being used for a problem which does not conform to a semi-infinite half space. It is apparent from this figure that more research should be performed to modify the stress distribution used to account for problems which do not conform to a semi-infinite half space.

#### c - $\phi$ Soils

For slopes with both cohesive and frictional soil strength characteristics, the resistance to sliding will be increased by the distribution of both the normal and

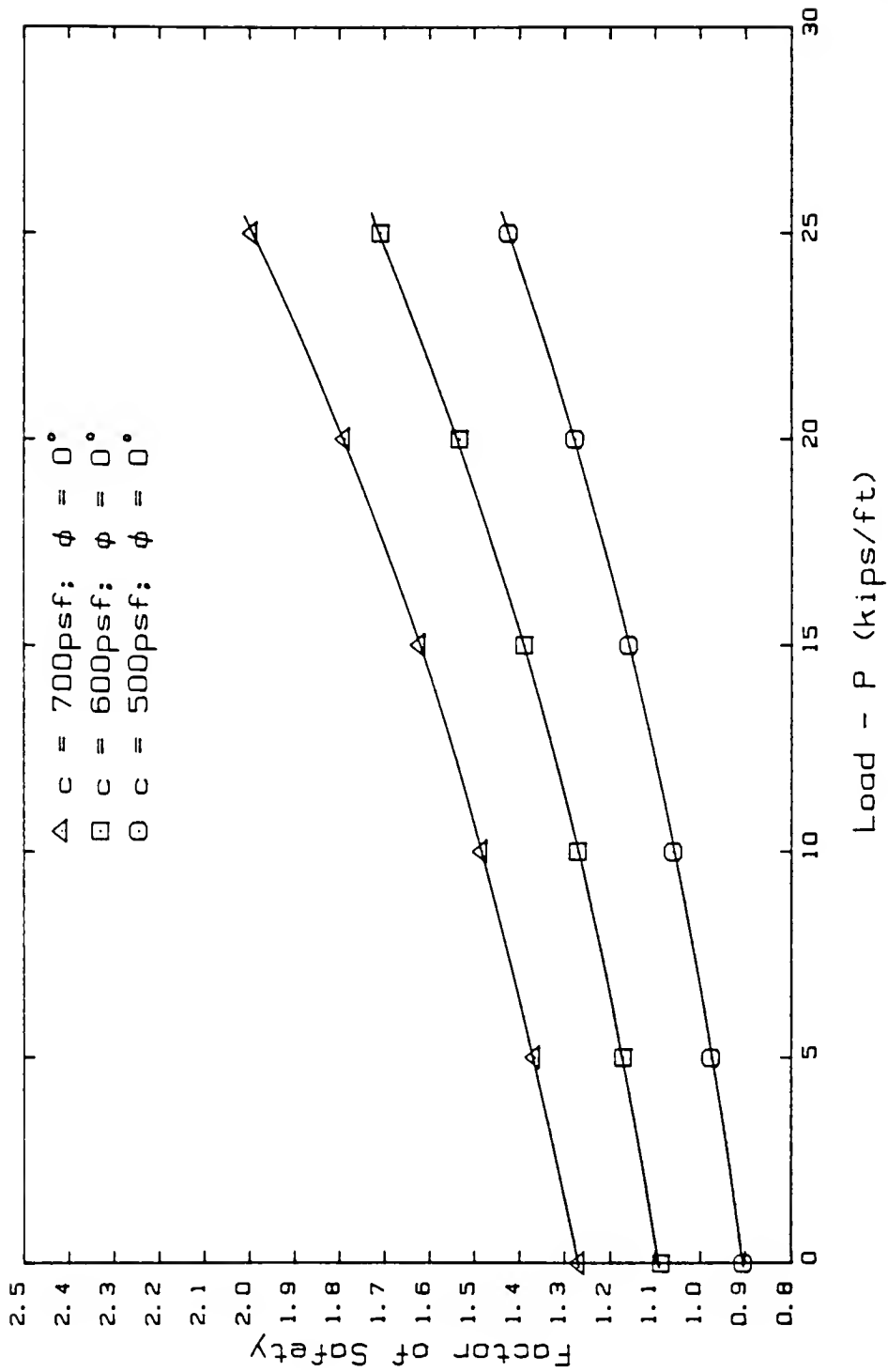


FIGURE 41. Load versus Factor of Safety for Purely Cohesive Soil Slopes

tangential components of the applied load acting on the potential failure surface. Figure 42 shows the results obtained when the slope of Figure 40 was analyzed with three different  $c - \phi$  soil strength characteristics.

As with purely cohesive soils, the FOS increases with increasing load. However the rate of increase (slope of the lines) in FOS with increasing load is greater than that of Figure 41 for purely cohesive soil conditions. For  $c - \phi$  soils, both components of the applied load distributed onto the failure surface act to increase stability. The FOS increases at a faster rate for the slope with  $c - \phi$  soil characteristics, since the distribution of the normal component of the load on the failure surface acts to increase the mobilized soil resistance. This resistance is in addition to the resistance offered by the distribution of the tangential component of the load along the failure surface.

Note that for a given increase in load, the FOS increases at a faster rate for higher values of  $\phi$ . The effect of the distribution of the normal component of the applied load on the FOS is demonstrated in Figure 43.

Note that at large loads, a rather significant increase in FOS is obtained for relatively small values of  $\phi$ . In addition, inspection of Figures 41 through 43 indicates that the soil strength parameters chosen for stability analysis have a profound effect on the FOS. As in any stability

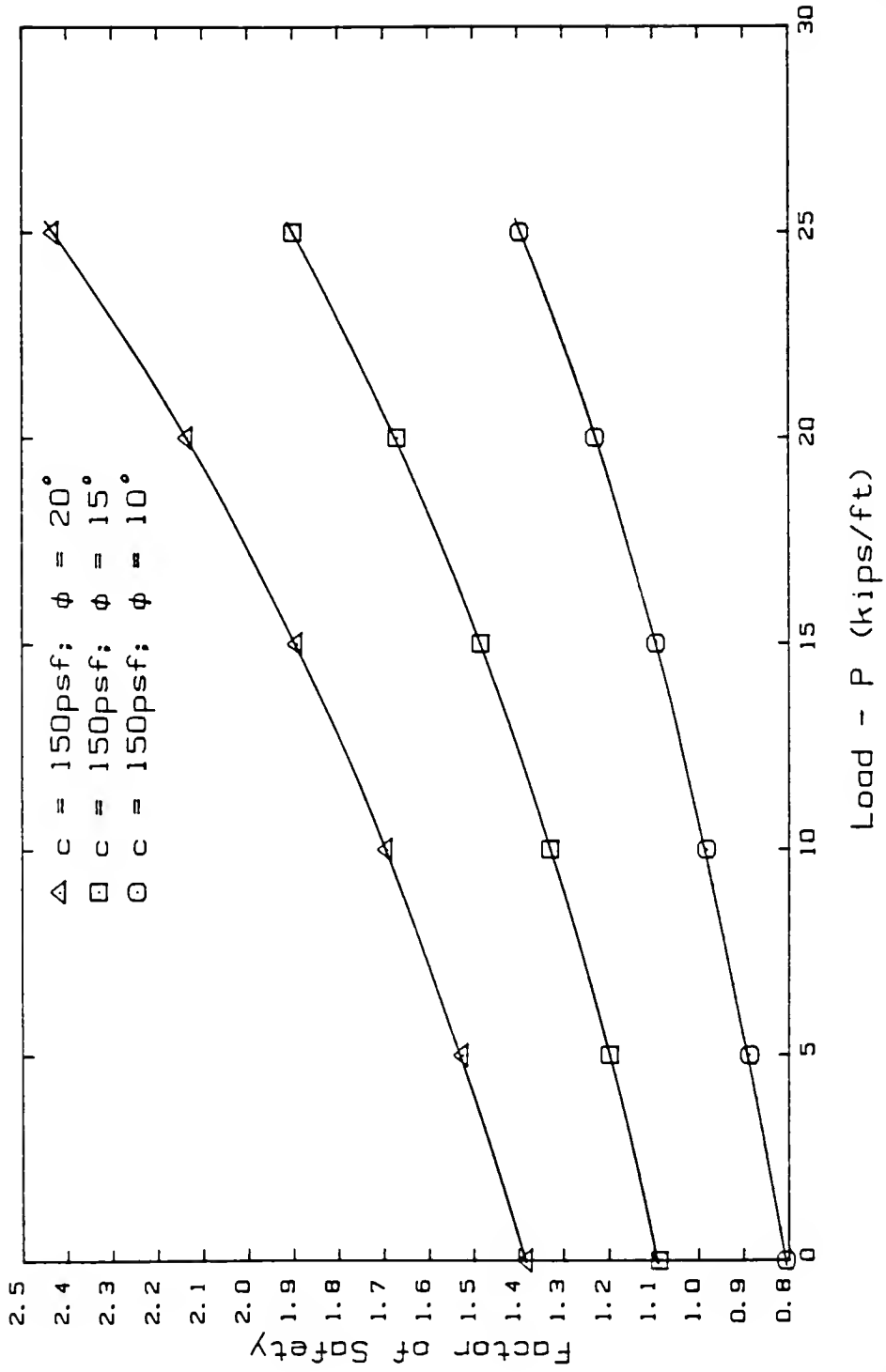


FIGURE 42. Load versus Factor of Safety for  $c - \phi$  Soil Slopes

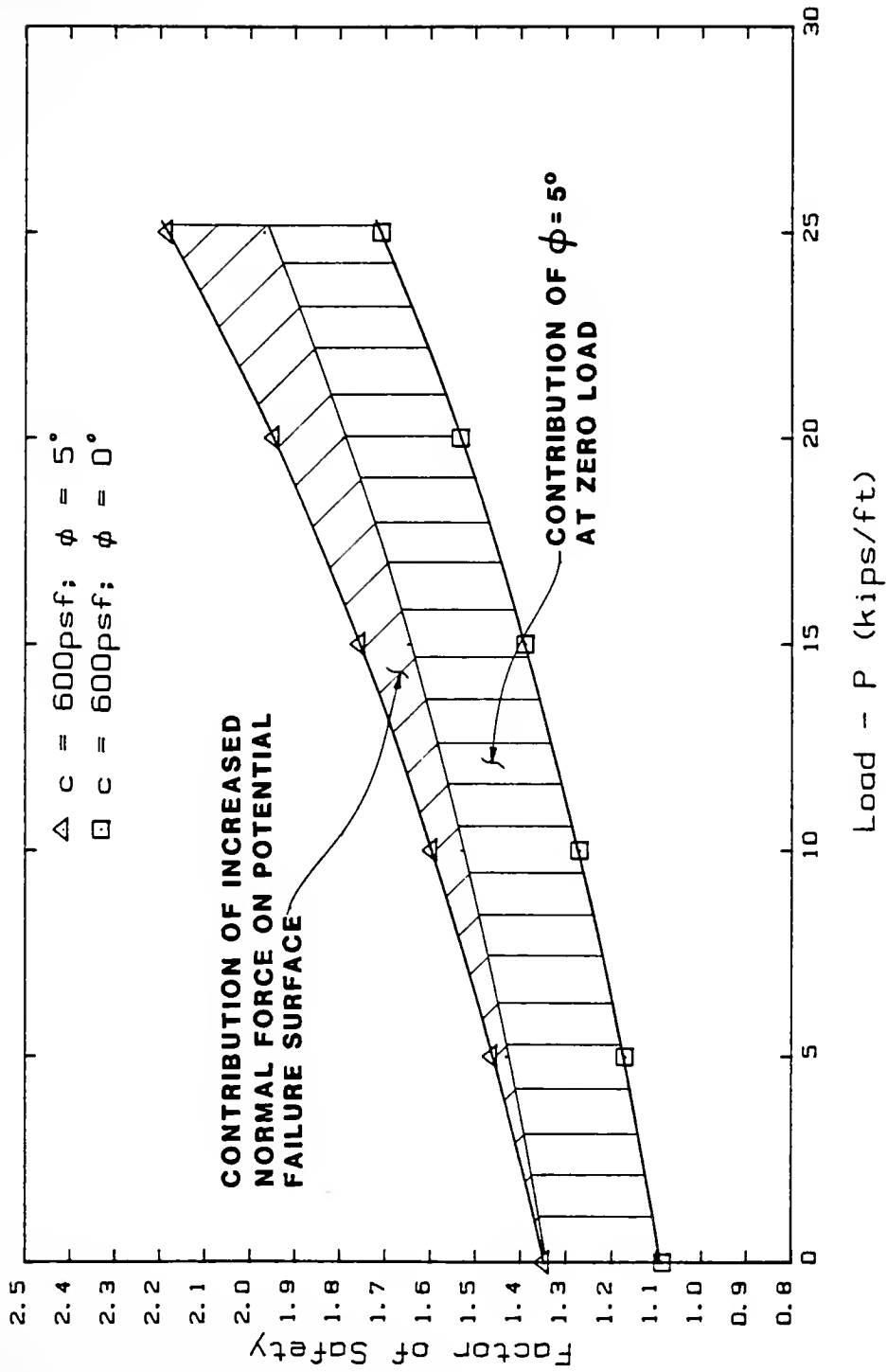


FIGURE 43. Effect of Increased Normal Component on Factor of Safety for  $c - \phi$  Soil Slopes

analysis, the choice of soil strength parameters is one of the most critical factors affecting the FOS obtained (Boutrup, 1977).

As mentioned previously in reference to Figure 41, the curves for Figures 41 through 43 should theoretically be linear. The nonlinearity is due to the fact that a stress distribution solution for a semi-infinite elastic half space has been used to model a slope which does not completely conform to a semi-infinite half space. Therefore, care should be exercised when interpreting the results of load versus FOS using the LDM.

As shown by Figures 41, 42 and especially Figure 43, the selection of the soil strength parameters is also critical when considering slopes subjected to tiedback loads. For example, if the slope of Figure 40 had soil strength characteristics interpreted to be  $c = 600$  psf and  $\phi = 5^\circ$ , and was subjected to a total applied load of 15 kips/ft, the FOS would have been found to be 1.75 (Figure 43). However, if the frictional component of the soil strength for the same slope and applied load was actually zero, then the FOS would be 1.38 rather than 1.75 (26.8% difference). Note that if the same misinterpretation in  $\phi$  of only  $5^\circ$  was made for the same slope at zero load, the difference in the factors of safety would have been 23.8% (1.35-1.09). Greater errors in the determination of the FOS would be obtained for larger misinterpretations of the soil

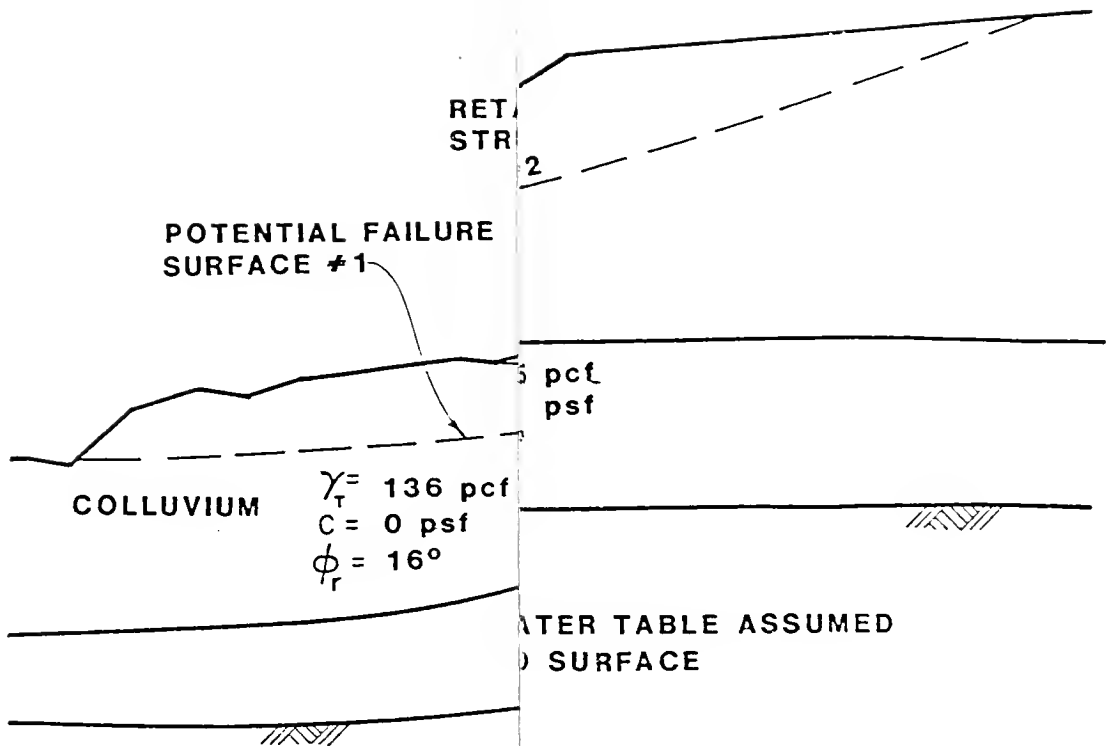
strength characteristics. If a similar analysis was performed for the plots of Load versus FOS found in Figure 41 for purely cohesive soil slopes, it would be found that the error in the FOS induced through the misinterpretation of soil characteristics remains approximately constant with increasing applied load.

#### Effect of Multiple Tieback Structures on Factor of Safety

Figure 44 shows the slope model used for this study. The slope shown in Figure 44 is a hypothetical slope which has been slowly moving for several years. The slope is long and consists of colluvium over alluvium which is underlain by bedrock. Two long and relatively shallow potential failure surfaces have been identified from boring information within the colluvium stratum. The majority of the slope movement occurs in the spring when the ground water table is near the ground surface. The factors of safety on the two potential failure surfaces under these conditions have been found to be approximately equal to 1.0 when analyzed using STABL4 and the Simplified Bishop method of slices.

One or more tiedback structures have been proposed to stabilize the slope. Two retaining structures have been considered as shown in Figure 44. Each structure is 12 ft (3.66 m) deep and will be supported by two tiebacks inclined at an angle of  $30^{\circ}$  with respect to the horizontal.

is now of  
the year  
1921





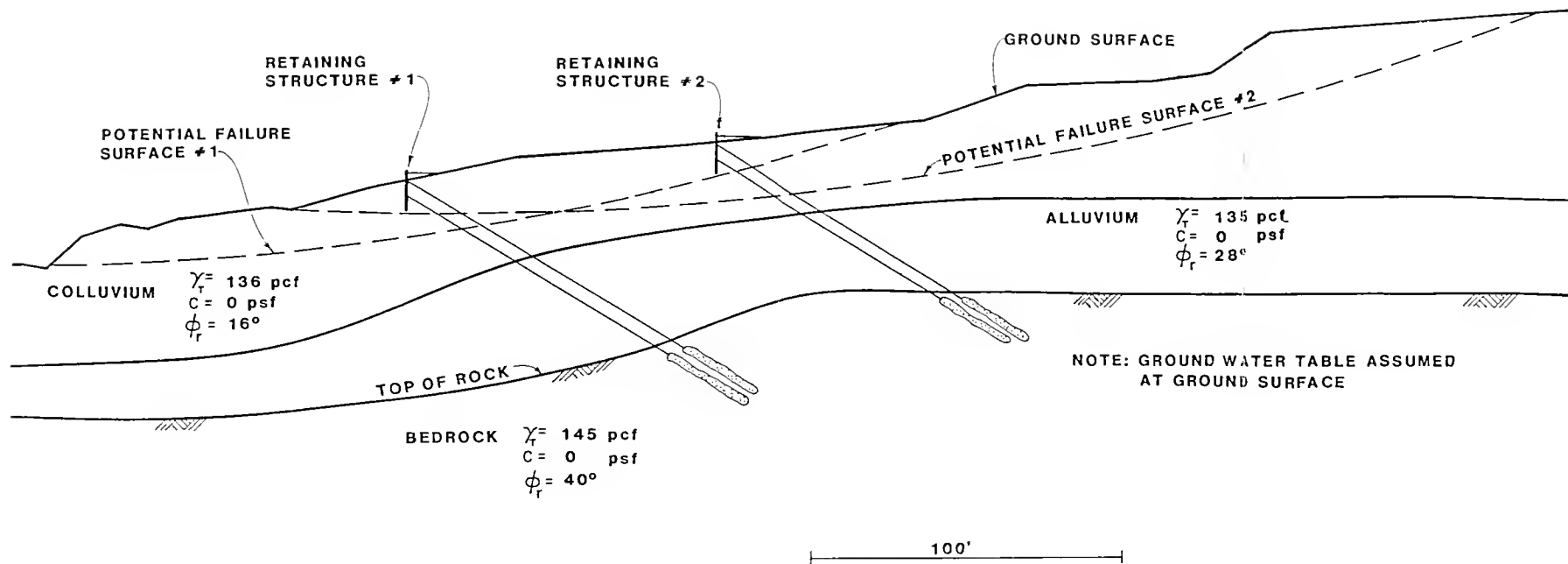


FIGURE 44. Slope Model for Multiple Tiedback Structures Study



It is desired to know the magnitude of the tieback load required on each retaining structure to stabilize the two potential failure surfaces identified. In addition, it is desired to know which retaining structure location is more efficient than the other for stabilizing the slope and whether or not only one structure is sufficient.

The stability of each of the two potential failure surfaces was analyzed when subjected to a tieback load from only one tieback structure at a time. The results of this analysis are shown in Figure 45. Figure 45 shows that either retaining structure is equally efficient in stabilizing either potential failure surface. For example, at a total tieback load of 30 kips/ft on either retaining structure, the FOS for potential failure surface #2 is apparently equal to 1.3. However, the apparent stability produced by retaining structure #2 on potential failure surface #1 is misleading. The FOS obtained is misleading because the retaining structure supports only a small portion of the sliding mass at the upper end of the failure surface. The FOS calculated by the program represents an average FOS for the entire failure surface. In reality the FOS for of the sliding mass above the structure will be very high, while the FOS of the sliding mass below the structure will be very low. It may even be possible that the sliding mass below the structure will be unstable. The FOS obtained from STABL will therefore only be valid if the retaining

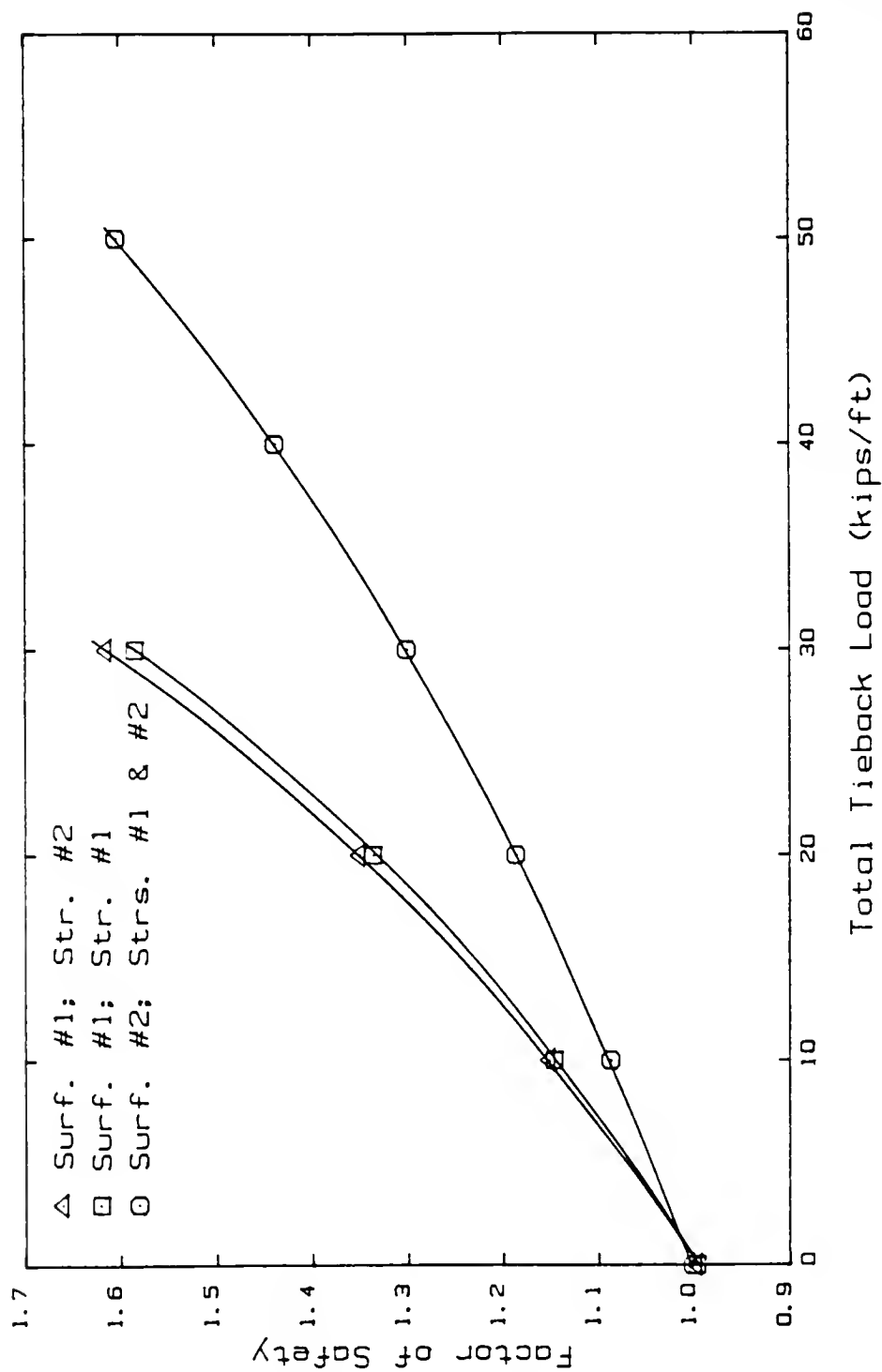


FIGURE 45. Total Tieback Load versus Factor of Safety

structure is present at the lower end of the failure surface and supports most of the sliding mass. This example demonstrates the importance of engineering judgement when using the results from any computerized solution.

It is also apparent from Figure 45 that a greater total tieback load is required to obtain the same FOS for potential failure surface #2 than for potential failure surface #1. The reason that more load is required to stabilize potential failure surface #2 is that the size of the sliding mass is greater than that of potential failure surface #1. Therefore, the ratio of a given applied load to the weight of the sliding mass is smaller for potential failure surface #2 than for potential failure surface #1.

Potential failure surface #1 was analyzed for stability considering various tieback loads from both retaining structures simultaneously. The results are shown in Figure 46 in the form of a design chart. Figure 46 is extremely useful to the designer since it allows the him or her to choose several combinations of retaining structure tieback loads to provide a given FOS for potential failure surface #1. For example, a FOS of 1.5 may be obtained for potential failure surface #1 using a load on structure #1 ( $T_1$ ) of  $T_1 = 8.8$  kips/ft and a load on structure #2 ( $T_2$ ) of  $T_2 = 12$  kips/ft, or  $T_1 = 11.5$  kips/ft and  $T_2 = 8$  kips/ft, or  $T_1 = 13.7$  kips/ft and  $T_2 = 4$  kips/ft. In addition, interpolation

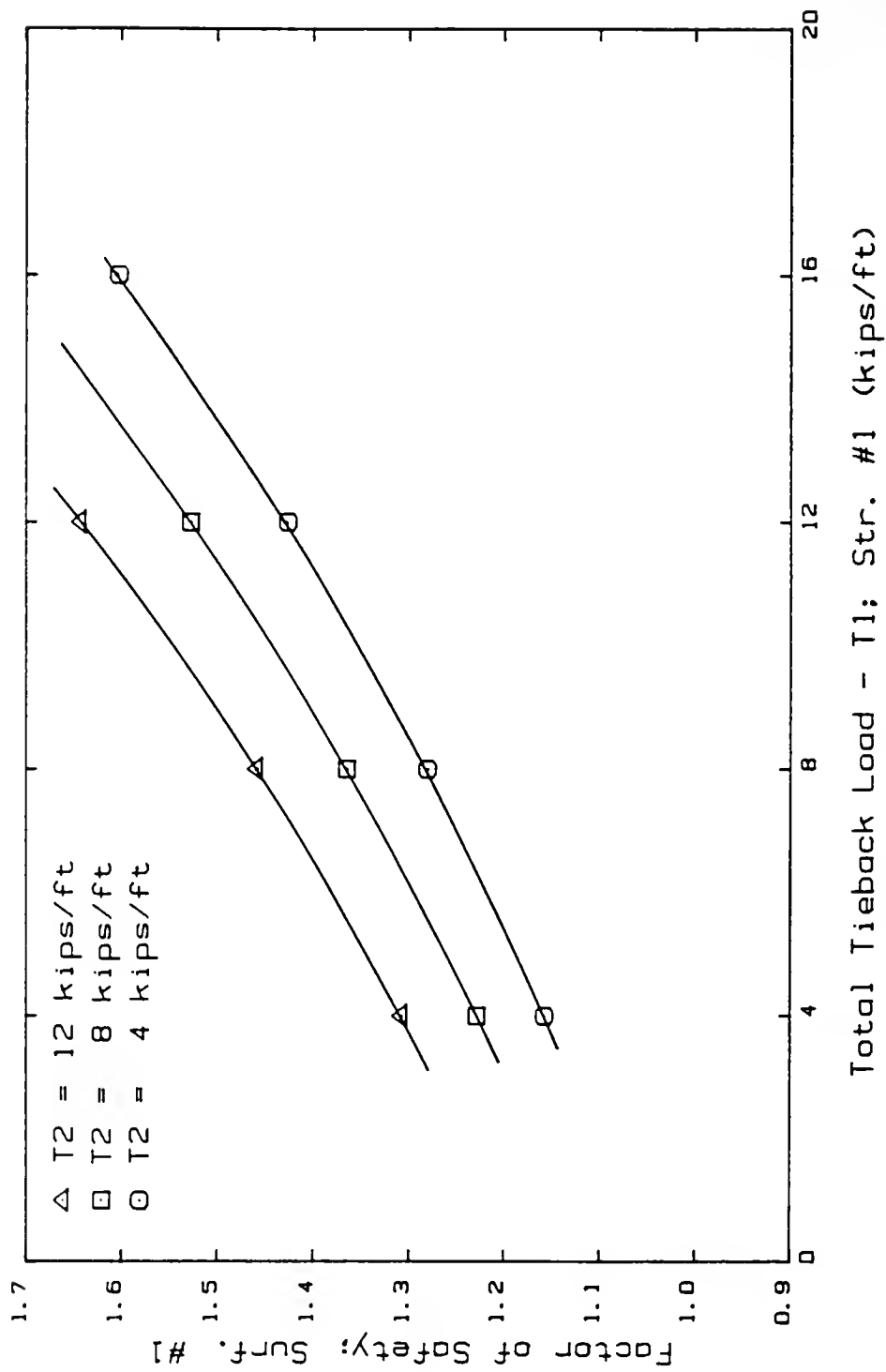


FIGURE 46. Total Tieback Load versus Factor of Safety - Potential Failure Surface #1

between the lines shown in Figure 46 permits several other combinations of load to be analyzed.

Potential failure surface #2 was also analyzed for stability considering various tieback loads from both retaining structures simultaneously. The results are shown in Figure 47 in the form of a design chart. The results obtained in Figure 47 are similar to those shown in Figure 46. By comparing Figures 46 and 47, it is again apparent that a greater total tieback load is required to stabilize potential failure surface #2 since it is a larger sliding mass.

Design charts similar to those of Figures 46 and 47 could be formulated if more than two retaining structures were being considered. The ability to analyze slopes subjected to multiple tiedback structures is a unique feature of STABL4.

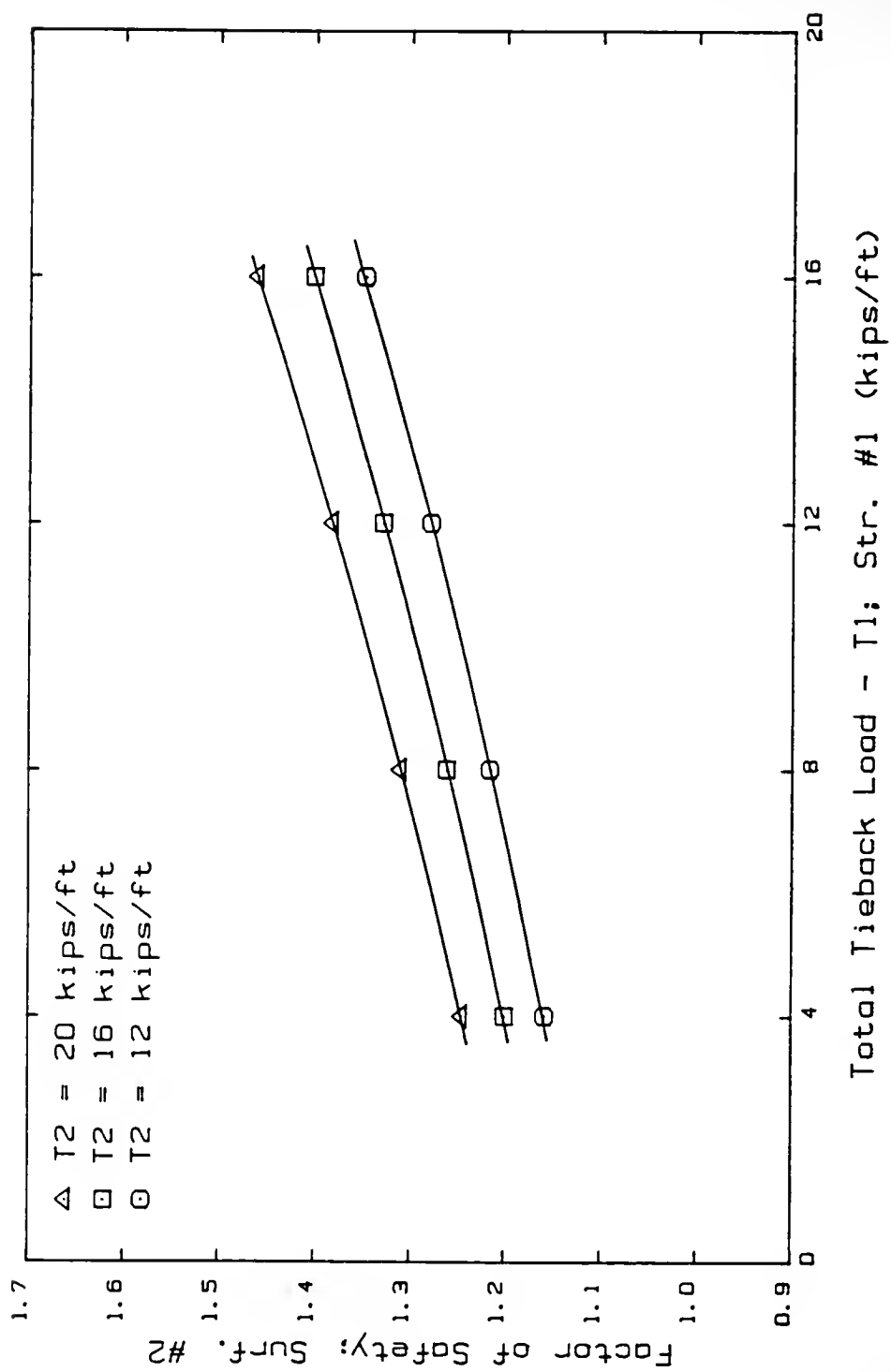


FIGURE 47. Total Tieback Load versus Factor of Safety - Potential Failure Surface #2

## CHAPTER V. MICROCOMPUTER IMPLEMENTATION OF STABL4 - PCSTABL4

In order to maintain the versatility of STABL, and to keep pace with today's trend towards the use of microcomputers for engineering, STABL4 has been implemented on an IBM microcomputer. The microcomputer version of STABL4 is named PCSTABL4. PCSTABL4 will run on IBM and IBM compatible microcomputers.

The capacity and speed of microcomputers today has increased to a degree that permits the implementation and efficient operation of large programs such as STABL4 on a microcomputer. The trend towards microcomputers stems from the fact that microcomputers are relatively inexpensive and can be obtained by even small engineering firms. In addition, significant cost savings can be realized using a microcomputer versus using mainframe computer systems. Mainframe computer systems are often very costly to utilize and many engineering firms who do not have their own systems must conduct their analyses on a time sharing basis. With a microcomputer, the engineer can perform analyses at his or her desk and obtain the results immediately, without incurring computer time costs.

### Implementation Process

The Microsoft FORTRAN compiler, version 3.2, was used to create an executable version of the program on the microcomputer. This compiler is both a subset and a superset of the ANSI FORTRAN 77 standard. The compiler is a rather complete implementation of FORTRAN 77. In addition, the compiler provides non-FORTRAN commands which provide increased program operation efficiency on the microcomputer. The Microsoft compiler is not required to run PCSTABL4, but is only required if the user makes changes in the program.

STABL4 was transferred from the Purdue University computer system to an IBM PC/XT via a direct link between the Purdue system and the microcomputer. Before STABL4 was transferred to the microcomputer, the program was broken into separate files consisting of individual subroutines for ease in editing and compiling.

Once STABL4 was transferred to the microcomputer, the subroutine and variable definitions included at the beginning of each subroutine listing were removed from the program listing. Removal of the definitions from the listing reduced the overall size of the program by approximately one third, which resulted in a considerable savings in disk storage space required. These definitions are compiled in an alphabetical definition list found in Appendix A of the PCSTABL4 User Manual (Carpenter, 1985a). This master definition list eliminates duplicate definitions

and is much easier to use than having to search through the program listing to find variable definitions.

Each subroutine was compiled separately using the Microsoft compiler. When compilation errors were detected, appropriate measures were taken to correct the errors. Conceptually, this process is rather simple and straight forward; however, the process was extremely time consuming. Several significant and numerous miscellaneous minor changes were made to the program for implementation on the microcomputer. Only the more notable changes will be highlighted here.

STABL uses many alphanumeric variables to control execution of the program and to display error messages. These variables were previously declared as REAL variables. Compilation errors were produced when such variables were encountered. As a result, all variables used to store alphanumeric data had to be declared and dimensioned as CHARACTER variables.

STABL was originally written with ENTRY points within several subroutines. These entry points were incompatible with the compiler and were thus eliminated. Subroutines containing ENTRY points were either broken into several separate subroutines, or flags (control codes) were inserted in the program and subroutines to control execution of the program.

Routines were created within the main program to prompt the user for input and output information. These routines prompt the user for the date, time, user's name, input filename, output filename, and plotted output filename. In addition, the output format was modified to fit on a standard 8.5 inch wide page. All output written to the disk file is also echoed to the screen so that the user may view the results while the program is running.

Once the individual subroutines were compiled successfully, the subroutines were grouped into eight files for ease in linking the compiled sections of the program together with the Microsoft linker. The eight files containing the compiled portions of the program were linked together to form an executable program. The program was then run and tested for accuracy and errors.

One of the problems encountered upon execution of the program was that the pseudo-random number generator produced only one random number with the remainder of the numbers generated being zero. The problem stemmed from the fact that the random number generator included in STABL4 produces integer numbers larger than can be represented by the IBM microcomputer. Therefore, when an integer was generated which was outside the capacity of the computer, the number was set to zero. An alternative random number generator was sought which was compatible with the IBM microcomputer. The STABL3 random number generator was found to be compatible,

and when tested, it produced a good distribution of random numbers with the sequence of pseudo-random numbers being repeated only after generation of approximately 1500 pseudo-random numbers. As a result, when comparing results obtained using PCSTABL4 and STABL4, small differences in the potential failure surfaces generated and corresponding factors of safety will be noted.

To avoid an error in the Microsoft linker, all labelled common blocks used in the subroutines and main program had to be included in the main program. Subroutines in the previous versions of STABL included only those common blocks necessary for the transfer of information and data in and out of a particular subroutine.

It was found that when PCSTABL4 was rerun immediately using the same input data, the program did not return the same results as the previous run. This condition existed because the IBM microcomputer does not zero its memory registers upon execution or termination of a program. Therefore it was necessary to zero all labelled common block memory registers before execution of the program through the use of a BLOCK DATA subprogram. The BLOCK DATA subprogram included in PCSTABL4 allocates memory space for all arrays and matrices in the common blocks and sets the arrays and matrices to zero upon execution of the program.

Plotting routines were developed for the microcomputer which emulate the Calcomp and Versatec plotting routines

included in STABL4. The new plotting routines provide report quality line plots using a Hewlett-Packard HP-7470A two-pen plotter. These new plotting routines are described in the next section.

Finally, since STABL has undergone revisions and modifications over the past 10 years, including those made to implement the program on the microcomputer, the program listing line numbers have become discontinuous. The program listing has therefore been renumbered.

#### Plotting Routines - PLOTSTBL

The mainframe version of STABL utilized Calcomp or Versatec plotter routines which are not available on the microcomputer. Therefore, plotting routines were created for driving a microcomputer compatible pen plotter. The Hewlett-Packard HP-7470A two-pen plotter was chosen since it is a low cost, high quality, pen plotter which is designed to interface with microcomputers. A plotter is optional and is not required for running PCSTABL4. The new plotting routines are provided for those users who desire report quality plots. Like previous versions of STABL, PCSTABL4 provides a character plot at the end of each output for aid in checking the accuracy of input data.

The PLOTIN subroutine of PCSTABL4 was revised extensively by removing the Calcomp/Versatec library calls and replacing them with statements which write control codes and coordinates to a separate disk file for subsequent

plotting using the HP-7470. This method of writing coordinates to a separate disk file during execution of PCSTABL4 allows the user to plot the results from only those runs desired.

The HP-7470 can only be driven using a BASIC program. Therefore a separate BASIC program was written which reads the plotting data written by PCSTABL4 program, emulates the commands used by a Calcomp/Versatec plotter, and drives the HP-7470 plotter. The name of the BASIC program developed for plotting PCSTABL4 output is PLOTSTBL.

The plotting routines in PCSTABL4 and PLOTSTBL simulate the routines in STABL4 and have some enhanced capabilities. If more than ten potential failure surfaces are generated by PCSTABL4, the plotter will plot all the surfaces generated, the screen will prompt the user for a new sheet of paper, and the plotter will plot the ten most critical potential failure surfaces starting with the most critical failure surface. The program permits specification of a title for the plot and specification of the units for the plot, either in feet or meters. The program also provides the user with the option of having the plot drawn with various line thicknesses or colors. If pen prompts are specified, the program will prompt the user during execution to change pens for profile boundaries, ground water tables, failure surfaces, etc.

### Program Characteristics

PCSTABL4 is a microcomputer version of the mainframe slope stability program, STABL4, and contains all the capabilities of STABL4, including: analysis of potential failure surfaces by the Simplified Janbu or Bishop method of slices; isotropic and anisotropic soil parameters; piezometric water surfaces; specific surface or random search surface generation; circular, random or block potential failure surfaces; and, tieback, surcharge and earthquake loads. The program requires 256 kilobytes of random access memory and is available for all versions of IBM and MS-DOS disk operation systems (DOS), including DOS 1.0 through DOS 3.0.

Input files for PCSTABL4 utilize free-format data entry, as used by previous mainframe versions of STABL. Input files may be created using a line editor, text editor, or a word processor.

### Versions

Two versions of PCSTABL4 are available for IBM compatible microcomputers. Version 1.87 utilizes the Intel 8087 Math Co-Processor for enhanced execution speed. The 8087 is an optional processor chip which performs real number calculations approximately 30 times faster than the standard 8086 processor in an IBM compatible microcomputer. Version 1.87 of PCSTABL4 requires the Intel 8087 Math Co-

Processor and will not run on IBM compatible machines without the 8087 math coprocessor.

Version 1.88 is also available for microcomputers without an optional Intel 8087 Math Co-Processor. This version will run on any IBM compatible machine, however it is significantly slower than version 1.87 and since it does not utilize the Intel 8087 Math Co-Processor.

Version 1.87 is strongly recommended since it will run 3 to 5 times faster than Version 1.88. For example, a moderately complex problem which generates and analyzes 100 potential failure surfaces takes approximately 4 minutes to run using the 8087 version (version 1.87), while the same problem takes approximately 12 minutes to run using the non-8087 version (version 1.88).

Detailed information on PCSTABL4's and PLOTSTBL's capabilities, and hardware and software requirements are found in the PCSTABL4 User Manual (Carpenter, 1985a).



## CHAPTER VI. ADDITION OF SPENCER'S METHOD OF SLICES - STABL5 AND PCSTABL5

In order to increase the versatility of STABL, Spencer's method of slices has been implemented in the program. Spencer's method was chosen since it satisfies complete equilibrium of the sliding mass; i.e. equilibrium with respect to moment and force equilibrium. In contrast, the Simplified Janbu method satisfies only vertical and horizontal force equilibrium and not moment equilibrium, while the Simplified Bishop method satisfies only vertical force and overall moment equilibrium but not horizontal force equilibrium. These methods are easily solved and typically give conservative values for the FOS when compared to the more accurate methods of slices satisfying complete equilibrium such as the Spencer or Morgenstern and Price methods (Wright et. al., 1973; Sharma and Lovell, 1983).

Spencer's method of slices is especially well suited for handling horizontal or inclined loads such as tieback loads since the method satisfies complete equilibrium. Spencer's method distributes the force from a load such as a tieback between slices through the interaction of the interslice side forces. Therefore, there is no need to use a technique such as the Load Distribution Method to account

for the presence of horizontal or inclined loads. The LDM was developed for use in conjunction with the Simplified Bishop or Simplified Janbu methods which do not consider the interaction of the interslice side forces.

Spencer's method is not used as frequently as the simplified methods since it requires more computation time and also since convergence of the solution is also often a problem. However, for problems with horizontal or inclined loads, Spencer's method is more appropriate than the simplified methods. Convergence problems have been avoided using the Linear Approximation Method of solution which will be described later.

The addition of Spencer's method complements the Simplified Janbu and Simplified Bishop methods existing in STABL. Implementation of this method allows the STABL user to search for critical potential failure surfaces using either the Simplified Janbu or Simplified Bishop methods and reanalyze any critical potential failure surface with Spencer's method to obtain a more accurate value of the FOS.

#### Stability Equations

Spencer (1967) developed a limiting equilibrium method of slices which satisfies complete equilibrium for circular failure surfaces assuming a constant ratio of the interslice normal and shear forces. This assumption leads to the formation of parallel interslice side forces inclined at a constant angle,  $\theta$ , on each slice. Spencer (1973) found that

a reasonably reliable value for the FOS can be obtained by assuming parallel interslice forces. The method was later extended to potential failure surfaces of a general or irregular shape (Wright, 1969; Spencer, 1973).

The slice forces considered in the derivation of Spencer's method of slices are shown in Figure 48. As with other limiting equilibrium methods, the factor of safety on each slice is assumed to be the same such that all slices of the the sliding mass will fail simultaneously. For all slices of a sliding mass to fail simultaneously, the load from one slice must be transmitted to the next slice through the interslice side forces. The interslice forces  $Z_l$  and  $Z_r$  are inclined from the horizontal at an angle  $\theta$ . The interslice forces acting on both sides of each slice can be replaced with a single statically equivalent resultant interslice force,  $QF$ , acting through the midpoint of the base of the slice and inclined at an angle  $\theta$  (Figure 49).

Summing the forces normal and tangential to the base of each slice provides two equations of force equilibrium:

$$\Delta N' + \Delta U_{\alpha} + QF \sin(\alpha - \theta) + \Delta W(k_h \sin \alpha - (1 - k_v) \cos \alpha) - \Delta U_{\beta} \cos(\alpha - \beta) - \Delta Q \cos(\alpha - \delta) - \Delta T \sin(\alpha - i) = 0 \quad \dots (18a)$$

$$\Delta S_r - QF \cos(\alpha - \theta) - \Delta W((1 - k_v) \sin \alpha - k_h \cos \alpha) + \Delta U_{\beta} \sin(\alpha - \beta) + \Delta Q \sin(\alpha - \delta) + \Delta T \cos(\alpha - i) = 0 \quad \dots (18b)$$

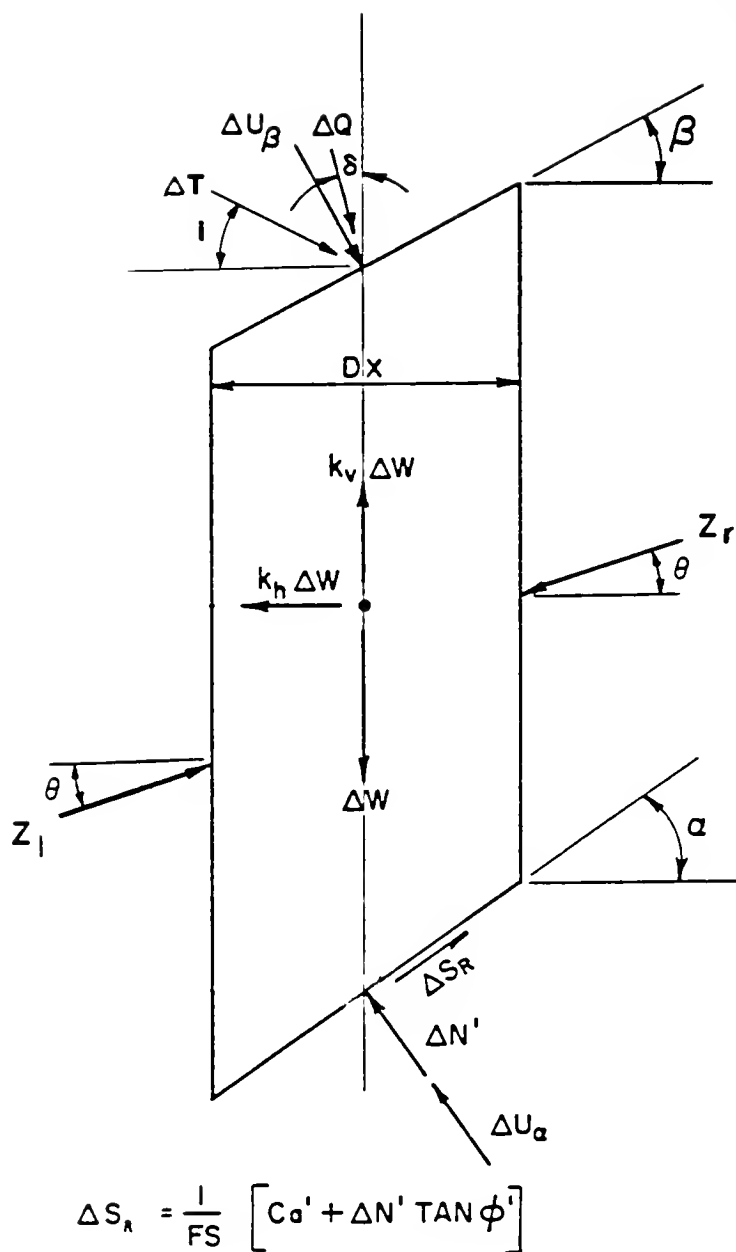


FIGURE 48. Slice Forces Considered for Spencer's Method of Slices

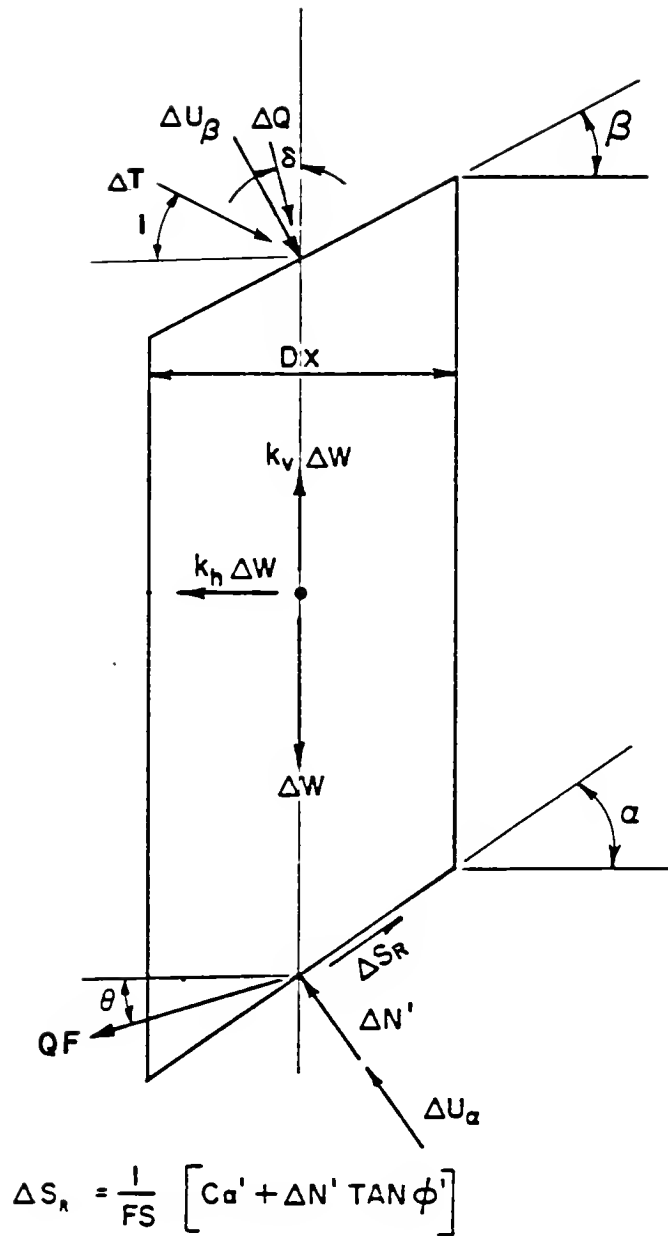


FIGURE 49. Slice Forces Considered in Derivation of Stability Equations for Spencer's Method of Slices

The expression for the effective normal force on the base of each slice may be obtained from equation 18a:

$$\begin{aligned} \Delta N' = & \Delta W((1-k_v)\cos\alpha - k_h\sin\alpha) - \Delta U_\alpha + \Delta U_\beta \cos(\alpha-\beta) \\ & + \Delta Q\cos(\alpha-\delta) - QF\sin(\alpha-\theta) + \Delta T\sin(\alpha-i) \dots (19) \end{aligned}$$

The expression for the mobilized resisting shear force at the base of a slice is given by:

$$\Delta S_r = \frac{[C_a' + \Delta N'\tan\phi']}{FS} \dots (20)$$

where:

FS = Factor of safety: assumed equivalent on all slices

$C_a'$  = Cohesion force =  $c' \cdot (dx)/\cos\alpha$

$\Delta N'$  = Effective normal force acting on the base of a slice

$\phi'$  = Effective angle of shearing resistance

Substituting equation 19 for the effective normal force into the expression for the resisting shear force at the base of each slice (Eqn. 20), and substituting the resulting expression into equation 18b yields the expression for the resultant of the interslice side forces on each slice:

$$QF = \frac{[S_1/FS + S_2]}{\cos(\alpha-\theta)[1 + S_3/FS]} \dots (21)$$

where:

$$S_1 = C_a' + \tan\phi' [\Delta W((1-k_v)\cos\alpha - k_h\sin\alpha) - \Delta U_\alpha + \Delta U_\beta \cos(\alpha-\beta) + \Delta Q \cos(\alpha-\delta) + \Delta T \sin(\alpha-i)]$$

$$S_2 = \Delta U_\beta \sin(\alpha-\beta) - \Delta W((1-k_v)\sin\alpha + k_h\cos\alpha) + \Delta Q \sin(\alpha-\delta) + \Delta T \cos(\alpha-i)$$

$$S_3 = \tan\phi' \tan(\alpha-\theta)$$

FS = Factor of safety: assumed equivalent on all slices

$$C_a' = \text{Cohesion force} = c' \cdot (dx) / \cos\alpha$$

If the overall moment produced about an arbitrary point by all external forces is zero, then the overall moment of the internal forces must also be zero, thus:

$$\sum_{i=1}^n QF[R\cos(\alpha-\theta)] = 0 \quad . . . . . (22)$$

where R is the distance from the center of rotation about which moments are summed to the center of each slice. For circular potential failure surfaces, the value of R is constant and may be taken out of the summation:

$$\sum_{i=1}^n [QF\cos(\alpha-\theta)] = 0 \quad . . . . . (23)$$

For surfaces of a general shape where no common axis exists, moments may be taken about a different axis for each

slice in turn. It is often convenient to take moments about the center of the base of each slice for irregular surfaces rather than about an arbitrary center of rotation. The approach adopted in obtaining the equilibrium equations does not affect the final solution to a given problem (Spencer, 1970).

If overall force equilibrium is satisfied, then the summation of the internal forces in two mutually exclusive directions must be zero. Hence, for force equilibrium in the horizontal and vertical directions:

$$\sum_{i=1}^n [QF \cos \theta] = 0 \quad . . . . . (24a)$$

$$\sum_{i=1}^n [QF \sin \theta] = 0 \quad . . . . . (24b)$$

The inclination of the resultant side forces can be expressed as:

$$\theta_i = \theta f(x) \quad . . . . . (25)$$

where  $\theta$  is a scaling angle of inclination and  $f(x)$  is an arbitrary function which defines how  $\theta_i$  varies with the  $x$  position of a slice. Parallel side forces occur when  $f(x) = 1$  for all values of  $x$ . The assumption of parallel resultant side forces is equivalent to the Morgenstern and Price Method (1965) when  $f(x) = 1$ , thus making Spencer's  $\tan \theta$  equivalent to Morgenstern and Price's  $\lambda$  (Spencer, 1973).

If the slope of the resultant interslice side forces is assumed to be parallel; i.e.,  $\theta_i = \text{constant}$ , equations 24a and 24b become identical and can be expressed as:

$$\sum_{i=1}^n [QF] = 0 \quad . . . . . (26)$$

Two factors of safety are obtained when equations 22 and 26 are solved assuming a value of  $\theta$ . Equation 22 yields a FOS satisfying moment equilibrium ( $F_m$ ), while equation 26 yields a FOS satisfying force equilibrium ( $F_f$ ). There is a unique value of the FOS and corresponding value of  $\theta$  which satisfies both force and moment equilibrium (Figure 50b). Equations 22 and 26 are solved using values of  $\theta$  until  $F_m$  and  $F_f$  are equal corresponding to equilibrium of forces and moments for the sliding mass.

It should be noted that at  $\theta = 0$ , the FOS with respect to moment equilibrium ( $F_m$ ) corresponds to the Simplified Bishop FOS, while the FOS with respect to force equilibrium ( $F_f$ ) corresponds to the Simplified Janbu FOS. It can be seen from Figure 50b that the FOS with respect to moment equilibrium ( $F_m$ ) is much less sensitive to the side force assumption (value of  $\theta$ ), than the FOS with respect to force equilibrium ( $F_f$ ). From this figure it can also be seen that the Simplified Bishop FOS yields rather accurate values of FOS when compared to complete equilibrium methods. This is

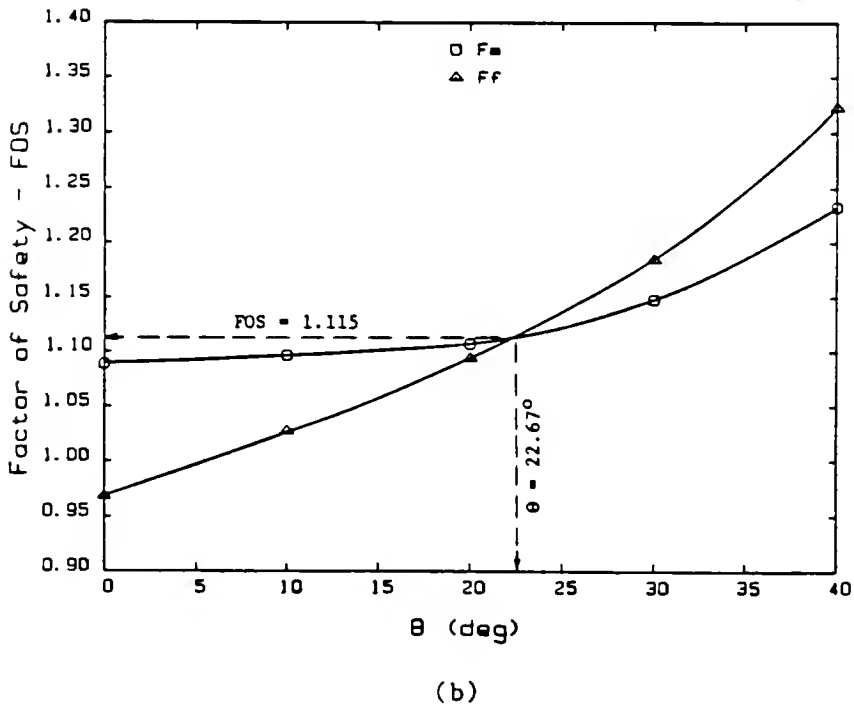
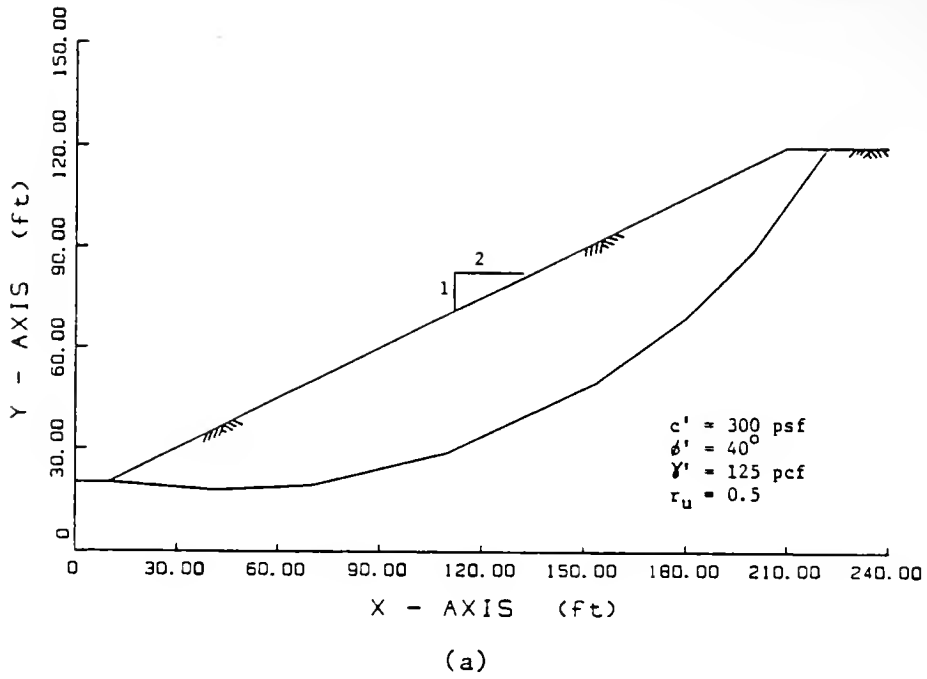


FIGURE 50. Variation of  $F_m$  and  $F_f$  with  $\theta$

due to the insensitivity of the  $F_m$  curve to the assumption of the slope of the interslice forces.

Reasonableness of the solution can be judged by examining the position of the line of thrust and the magnitude of the interslice shear stresses. Both are obtained from the moment equilibrium equations for the individual slices. This topic will be addressed later in this chapter.

#### STABL Method of Solution - Linear Approximation Method

Numerous iterative schemes have been used to solve for the FOS satisfying complete equilibrium. It is important to use an iterative scheme that readily converges and also minimizes the number of iterations required to produce a solution. Techniques have included: 1) mathematically sophisticated analyses such as the Newton-Raphson numerical technique (Wright, 1969; Boutrup, 1977); 2) arbitrarily assuming several values of  $\theta$ , calculating the corresponding values of  $F_m$  and  $F_f$ , and using a regression analysis to find the intersection of the  $F_m$  and  $F_f$  curves (Fredlund, 1974); 3) assuming a value of  $\theta$ , calculating  $F_m$  and  $F_f$ , and choosing a new value of  $\theta$  based on the relative magnitude of  $F_m$  and  $F_f$  for a given  $\theta$  (Fredlund, 1981); and 4) assuming a value of  $\theta$  and FOS, calculating  $F_f$ , setting  $F_m$  equal to  $F_f$ , solving for the new value of  $\theta$ , and substituting that value into the  $F_m$  equation (Spencer, 1973; Maksimovic, 1979).

None of the iterative schemes outlined above complemented the routines already present in STABL. Therefore, a new iterative method has been developed which rapidly and accurately determines the FOS satisfying complete equilibrium while avoiding problems of non-convergence. The new method is called the Linear Approximation Method (LAM), and utilizes the INTSCT routines in STABL which calculate the intersection of two straight lines. The method uses values of  $F_m$ ,  $F_f$  and  $\theta$  to approximate the  $F_m$  and  $F_f$  curves with straight lines and calculates their intersection. An accurate value of the FOS satisfying complete equilibrium is obtained by successive approximations of the  $F_m$  and  $F_f$  curves with straight lines for several values of  $\theta$ . Due to the shape of the  $F_m$  and  $F_f$  curves, convergence is rapid and often occurs within three iterations. Unlike some of the iterative techniques outlined previously, the LAM is easily comprehended and minimizes the number of iterations required for solution.

Equations 21 and 25 are first solved with initial estimates of  $\theta$  and FOS. The initial value of  $\theta$  is taken as one half the approximate slope angle, which is input by the user. Spencer (1967) found that the angle of the resultant interslice side forces satisfying complete equilibrium was less than the slope angle. Therefore, STABL utilizes a user input estimate of the slope angle to begin iteration for the FOS and corresponding angle of the resultant interslice side

forces. The solution is not sensitive to the value input for the slope angle; however, a reasonable estimate will minimize iteration time. The initial estimate of the FOS is obtained by first calculating the FOS by either the Simplified Bishop or Simplified Janbu method depending on the type of analysis being performed.

Using the initial estimates of  $\theta$  and FOS, equations 25 and 21 are solved for the sum of the resultant interslice forces and their corresponding moments. Based on the relative magnitude of the sum of the forces and the sum of the moments, a second value of FOS is chosen and the sum of the forces and moments are recalculated. The factor of safety satisfying force equilibrium for the given value of  $\theta$  is found by calculating the intersection of the line through the sum of the forces previously calculated with the  $\Sigma QF = 0$  axis as shown in Figure 51a. The value of  $F_f$  satisfying force equilibrium for the given  $\theta$  is checked by using that value of FOS to calculate the sum of the forces. The value of  $F_f$  is recalculated using a straight line intersection of the two previous values of the sum of the forces with the  $\Sigma QF = 0$  axis. Normally three trials are all that are required to find the value of  $F_f$  within a tolerance of 0.001. The value of  $F_m$  for a given  $\theta$  is found in the same manner.

The calculation of the sum of the resultant interslice forces and moments for a given value of  $\theta$  requires little

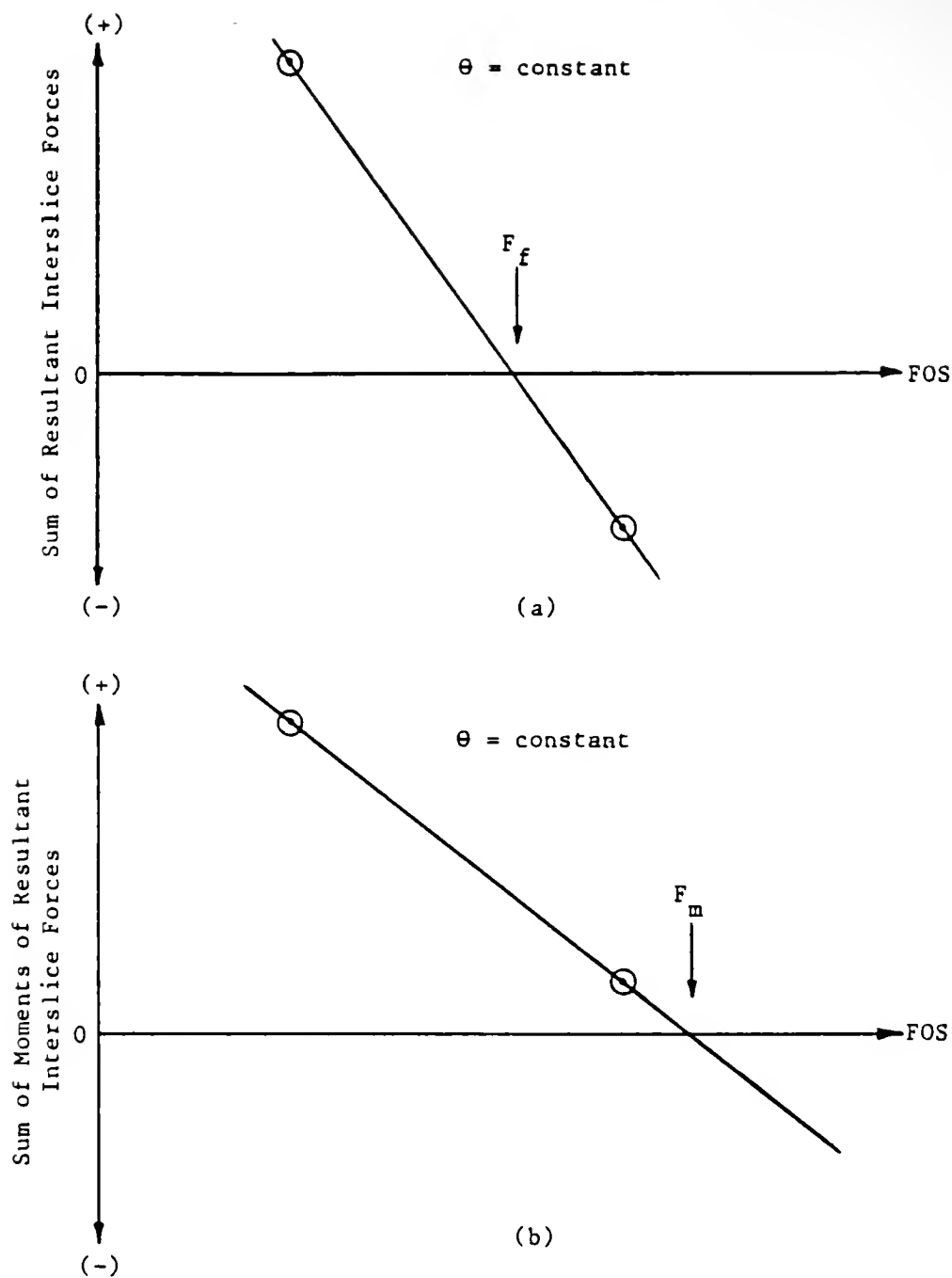


FIGURE 51. Determination of  $F_f$  and  $F_m$  for a Given Value of  $\theta$  by the Linear Approximation Method

calculation time. In addition, calculation of the intersection of two straight lines is simple and also requires very little computation time. The combination of these two facts leads to a very efficient procedure for accurately and rapidly determining the values of  $F_f$  and  $F_m$ .

A second value of  $\theta$  is taken as three-fourths the input slope angle. The force and moment equations are again solved for new values of  $F_f$  and  $F_m$  corresponding to the new value of  $\theta$ . A second value of  $\theta$  equal to three-fourths the input slope angle was found to lead to rapid solution of the FOS by the LAM, and was thus chosen.

After two iterations, the  $F_m$  and  $F_f$  curves are approximated by straight lines and the intersection of the these lines is calculated ( $(\theta_{int}, F_{int})$ ; Figure 52a). It can be seen from Figure 52a that the intersection of the approximation of the  $F_f$  and  $F_m$  curves by straight lines leads to a very accurate estimate of the value of  $\theta$  satisfying complete equilibrium and a rather good estimate of the FOS. The difference between  $\theta_{int}$  and the nearest value of  $\theta$  used (in this case  $\theta_2$ ) is calculated and another value of  $\theta$  is selected such that  $\theta_3 = \theta_{int} + (\theta_{int} - \theta_2)$ . The value of  $\theta_3$  is used along with  $F_{int}$  to calculate  $F_m$  and  $F_f$  corresponding to  $\theta_3$ . Using the new and previous values of  $F_m$ ,  $F_f$  and  $\theta$ , the intersection of the two curves is again approximated by the intersection of the straight lines representing the  $F_m$  and  $F_f$  curves (Figure 52b). This

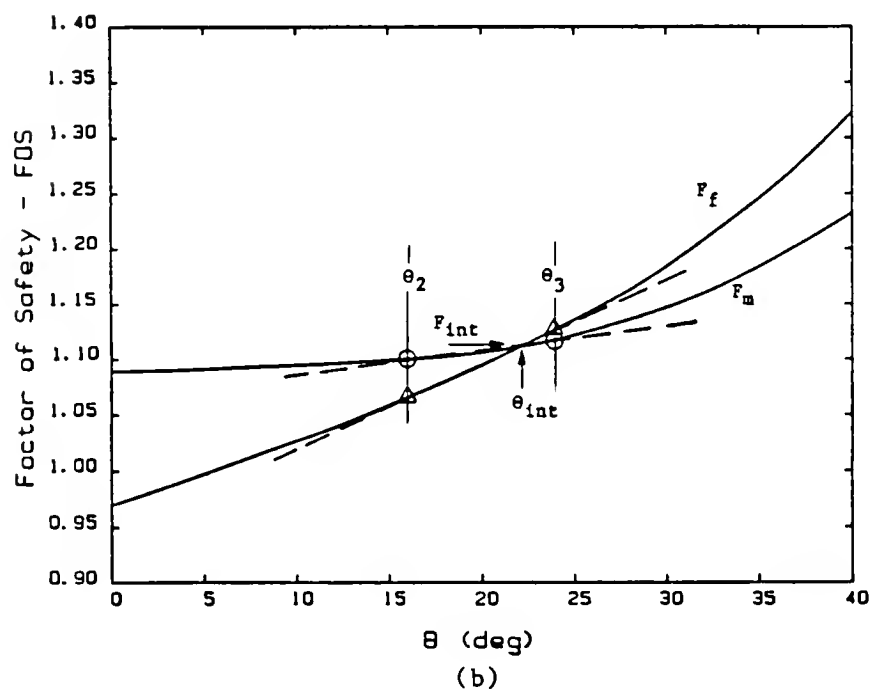
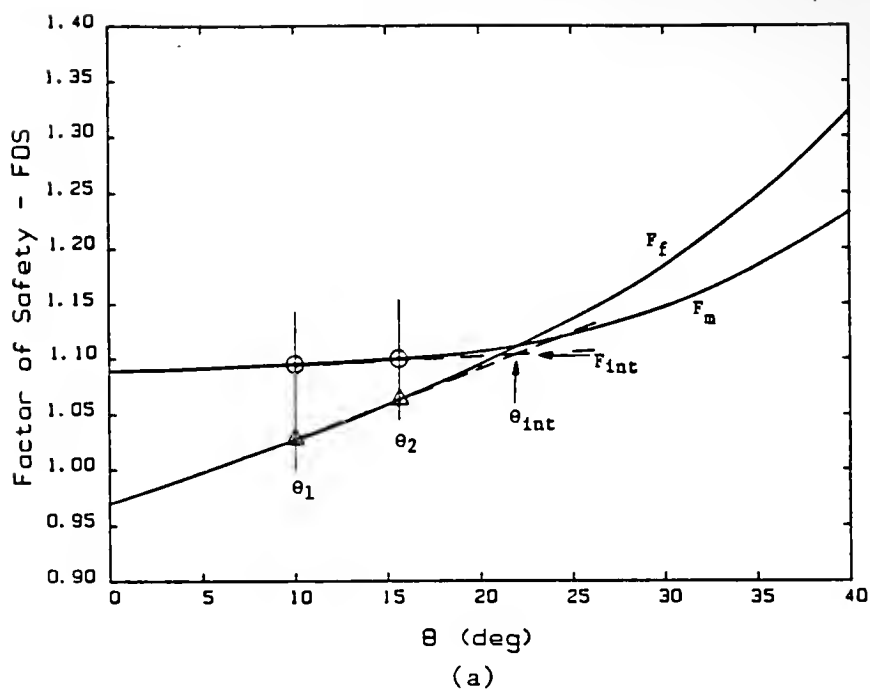


FIGURE 52. Determination of the FOS and  $\theta$  Satisfying Complete Equilibrium Using the Linear Approximation Method

process is repeated until the difference between the current FOS and the previous FOS is less than 0.001 and the difference between the last two values of  $\theta$  is less than 0.001 radians, or the difference between  $F_f$  and  $F_m$  is less than 0.001 for a given  $\theta$ . This avoids unnecessary calculations when the value of  $\theta$  being used happens to correspond to the value of  $\theta$  satisfying complete equilibrium. The program is structured such that a new value of  $\theta$  will be determined if  $\theta_{int}$  lies to the left of  $\theta_1$  or between  $\theta_1$  and  $\theta_2$ .

Due to the shape of the curves, convergence is rapid and often occurs within three iterations. No problems have been indicated with respect to non-convergence of a solution using the LAM. It is believed that STABL is the only known slope stability program to contain the Linear Approximation Method.

#### Line of Thrust

As mentioned previously, attention should be paid to the position of the line of thrust (location of the line of action, or points of application, of the interslice side forces on the slices) to check the reasonableness of the solution. A satisfactory solution is one in which the line of thrust passes through the middle third of the slices. Tensile forces are indicated within the slope if the line of thrust lies outside the middle third of the slice. The

location of a satisfactory line of thrust is shown in Figure 53 for the example problem shown in Figure 50a.

Once the slope of the interslice forces  $\theta$  and the FOS satisfying complete equilibrium have been determined, the line of thrust may be calculated. The values of the resultant interslice forces,  $(Z_1, Z_r)$ , for each slice are calculated by substituting the values of FOS and  $\theta$  satisfying complete equilibrium into equation 21. Working from the first slice to the last, the points of action of the interslice forces are found by taking moments about the center of the base of each slice in turn.

Spencer (1973) indicated that suitable lines of thrust can be obtained assuming that a tension crack filled with water exists at the upper end of the slip surface. The depth of the tension crack may initially be taken as the depth of zero active effective stress:

$$z_o = \frac{2c'}{\gamma FS(1-r_u)} \sqrt{\frac{1 + \sin\phi'_m}{1 - \sin\phi'_m}} \dots \dots \dots (27)$$

Spencer demonstrated that reliable factors of safety can be obtained assuming the slope of the interslice forces are parallel. However, he recommended that the slope of the interslice forces should be reduced at the upper end of the slip surface in order to obtain reasonable positions of the line of thrust. Spencer's method as programmed in STABL follows these recommendations.

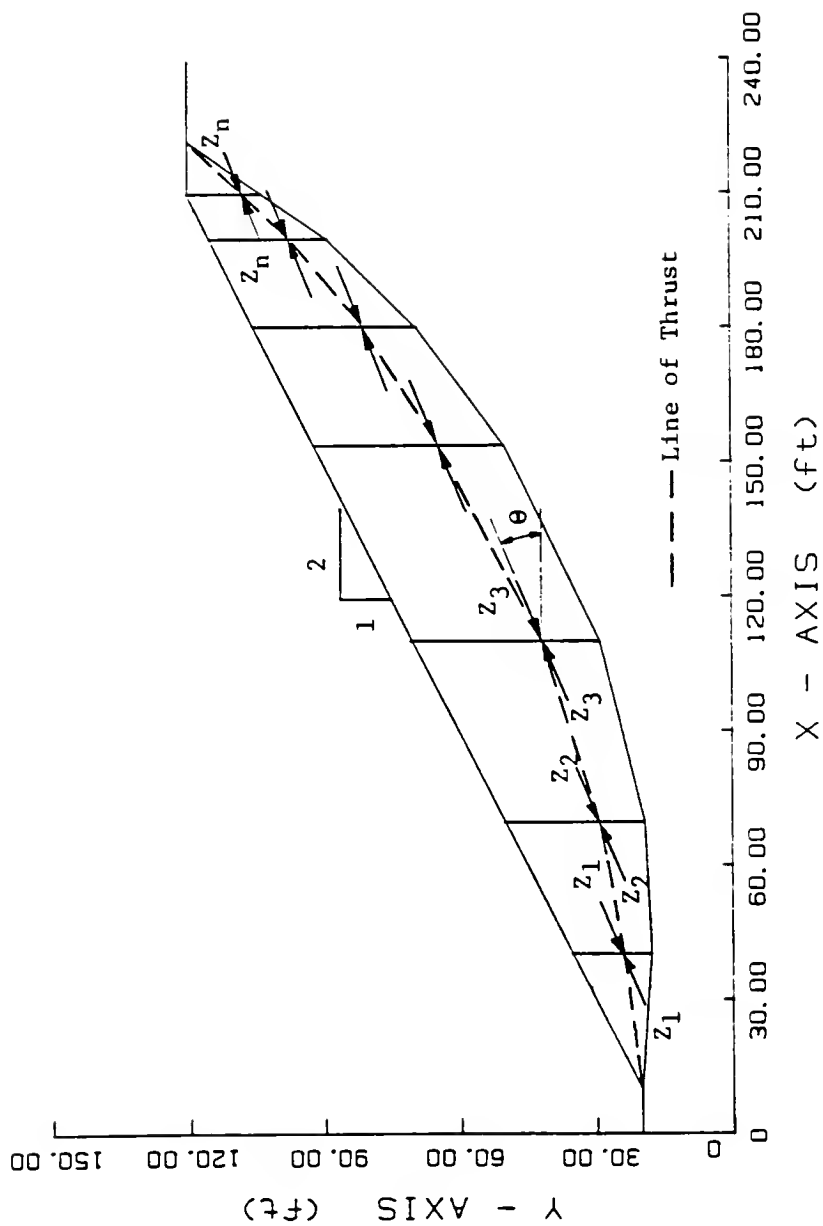


FIGURE 53. Line of Thrust

### Spencer Options in STABL

The Spencer option may be invoked by specifying the command "SPENCR" and an estimate of the slope angle. The SPENCR command precedes specification of the surface type and method of solution; i.e., SURFAC, SURBIS, CIRCLE, CIRCL2, RANDOM, BLOCK or BLOCK2.

Spencer's method has been implemented in the STABL program for the primary purpose of obtaining a more accurate value of the FOS and line of thrust for specific surfaces of interest. For critical surfaces, the Spencer method of slices is preferred over the Simplified Janbu or Simplified Bishop methods since it satisfies complete equilibrium of the sliding mass and yields a slightly more accurate FOS. Since determination of the FOS by Spencer's method requires approximately six times more calculation time, it is intended that only specific surfaces of interest will be analyzed utilizing Spencer's method. However, Spencer's method may be used for analysis of either user input specific surfaces, or randomly generated surfaces.

The most efficient use of STABL's capabilities will be realized if the user investigates a number of potential failure surfaces using one of STABL's random surface generation techniques and determines the FOS by either the Simplified Janbu or Simplified Bishop method of slices. Once critical potential failure surfaces have been identified, they may be analyzed using the SPENCR option in

conjunction with either the SURFAC or SURBIS option to obtain a more accurate value of the FOS and to gain insight into the reasonableness of the solution through examination of the line of thrust.

When a user input potential failure surface is analyzed, the program will output the values of  $F_f$ ,  $F_m$  and  $\theta$  calculated during iteration along with the value of FOS and  $\theta$  satisfying complete equilibrium. The user may use this information to construct a graph similar to that of Figure 50b. When analyzing a user input potential failure surface, the coordinates of the line of thrust, the ratio of the height of the line of thrust above the sliding surface to the slice height for each slice, and the values of the interslice forces are all output. This information allows the user to quickly determine whether or not the line of thrust, and hence the solution, is satisfactory.

The Spencer option may also be used with the STABL options that generate surfaces randomly. However, when the Spencer option is used in conjunction with randomly generated surfaces, only the FOS and angle of the interslice forces satisfying complete equilibrium are output for the ten most critical surfaces. Information regarding the line of thrust, interslice forces or values of  $F_f$ ,  $F_m$  and  $\theta$  calculated during iteration is not output for randomly generated surfaces; hence the reasonableness of the solution obtained for a randomly generated surface will not be

apparent. When the reasonableness of the solution of a randomly generated surface is desired, the surface must be analyzed using the SPENCR option in conjunction with either the SURBIS or SURFAC options.

The STABL5/PCSTABL5 User Manual (Carpenter, 1986), further describes the Spencer options, input format, restrictions, and error codes. This document also describes some minor program enhancements and provides an example problem using the Spencer option.

## CHAPTER VII. SUMMARY, CONCLUSIONS AND RECOMMENDATIONS

Summary

1. The primary purpose of this study was to develop a rational and convenient method for assessing the internal and overall stability of tiedback and anchored retaining structures, especially those used for landslide control. As a result, two methods were implemented in the STABL slope stability program to assess the stability of tiedback retaining structures. The stability of tiedback structures may be analyzed using the Load Distribution Method (LDM), (contained in STABL4, PCSTABL4, STABL5 and PCSTABL5), or Spencer's method of slices, (contained in STABL5 and PCSTABL5). The Spencer's method is the preferred technique of the two methods implemented.

2. Existing methods for determining the stability of tiedback structures were reviewed and investigated in the development of the LDM. It was found that some methods did not satisfy the laws of statics, while most methods were limited to a single row of tiebacks or homogeneous soil conditions. In addition, none of the existing methods properly accounted for the distribution of stresses throughout a soil mass caused by the presence of a tieback load.

3. The Load Distribution Method was developed in an attempt to account for the diffusion of stresses through a soil mass caused by the presence of a tieback load. The LDM was developed for use with the simplified methods of slices which do not satisfy complete equilibrium or transfer the load from one slice to another. This method was implemented in the slope stability computer programs, STABL4 and PCSTABL4. The distribution of stresses determined by the Load Distribution Method along the potential failure surface was presented along with applications of the method. The effect of tieback load, inclination, position, multiple tiedback structures and soil properties on the factor of safety of tiedback slopes was investigated.

4. Parametric studies were performed during development of the Load Distribution Method to determine the reasonableness of applying a stress distribution based on a semi-infinite elastic half space to the solution of tiedback slopes and retaining walls. These studies revealed that the method generally gives reasonable results; however, at large applied loads and for some slope models, the method may not yield conservative results since the problem modelled does not totally conform to a semi-infinite elastic half space. Recommendations for further research into modifying the stress distribution used in the LDM have been discussed so that the method can account for problems which do not

conform the the semi-infinite elastic half space assumption used in the method.

5. A microcomputer version of STABL4 was created for IBM compatible microcomputers in the program, PCSTABL4. PCSTABL4 was developed to meet the needs of today's engineering practice and the trend toward the use of micro-based computers. Plotting routines were also developed for a Hewlett-Packard plotter for plotting graphical output from PCSTABL4.

6. Finally, Spencer's method of slices was implemented in the programs STABL5 and PCSTABL5 to provide additional versatility to the STABL programs. Spencer's method of slices satisfies complete equilibrium and is capable of transferring the load from one slice to another through the interaction of the interslice shear and normal side forces. Therefore, Spencer's method of slices is particularly well suited for analysis of slopes and retaining walls subjected to tieback loads since it distributes the load from a tieback between slices. The development of Spencer's method was reviewed and its implementation in STABL5 and PCSTABL5 was presented. A new iterative technique was developed by the author for determining the factor of safety and angle of the interslice forces satisfying complete equilibrium of a sliding mass computed by Spencer's method. The new iterative technique is called the Linear Approximation Method (LAM).

### Conclusions

1. The Load Distribution Method attempts to account for the increase in stress within a soil mass between an anchor and a retaining structure due to the presence of tiebacks or anchors. The method models the increase in normal stress along the base of the slices due to the presence of tieback loads. As a result, the increase in soil resistance due to large compressive stresses within a soil mass is accounted for on all slices of a sliding mass. The method also models the tangential resisting forces produced along the failure surface by a tieback load.

2. Modelling the distribution of stresses produced by a tieback load throughout a soil mass using the semi-infinite elastic half space solution contained in the LDM, for analysis of tiedback slopes and walls, generally gives reasonable results. However, in some cases, and for large applied loads, the results obtained using the LDM may not be conservative since the problem being modelled does not conform to a semi-infinite elastic half space. Therefore, care should be exercised when interpreting the FOS obtained using the LDM.

3. The Load Distribution Method can be used with the Simplified Bishop method of analysis for circular failure surfaces, and the Simplified Janbu method of analysis for non-circular failure surfaces. The tieback option may be

used with random or specific failure surface generation methods for irregular, block or circular failure surfaces.

4. The tieback option in STABL4, PCSTABL4, STABL5 and PCSTABL5 can be used to model braced excavations, tiedback slopes and walls, and for determining the stability of such structures.

5. It was found that the soil parameters used in the stability analysis have the greatest effect on the overall stability of tiedback slopes and walls. A small change in the soil parameters input produces a significant change in the factor of safety obtained for a given failure surface.

6. The resistance to sliding of tiedback slopes in frictional soils is increased due to 1) an increase in the normal force on the sliding surface, which thereby increases the resistance provided by the soil, and 2) tangential forces produced along the failure surface. The resistance to sliding of tiedback slopes in purely cohesive soils is due solely to the presence of the tangential forces produced along the failure surface.

7. The FOS for a given trial failure surface will increase with an increase in tieback load for soils with either purely cohesive characteristics or frictional characteristics. However, more resistance to sliding is gained in soils with frictional characteristics than in purely cohesive soils. The increase in FOS for a given increase in tieback load will be greater for a slope with frictional

soil characteristics than for the same slope with purely cohesive soil characteristics.

8. The inclination and length of tiebacks have an effect on the overall stability of a wall or slope. Both the inclination and length of tiebacks may be optimized or varied to produce the desired stability, i.e., factor of safety.

9. In general, tiebacks are an efficient means of stabilizing retaining walls or slopes. The LDM provides a rapid and versatile tool for sequentially modelling the construction procedure of a tiedback or anchored retaining structure.

10. The Spencer method of slices, contained in STABL5 and PCSTABL5, is preferred for analysis of tiedback slopes and walls over the simplified methods using the LDM since it satisfies complete equilibrium and accounts for the interaction of the interslice side forces between slices. The FOS obtained by Spencer's method is typically slightly higher than the FOS obtained by the less rigorous Simplified Bishop or Simplified Janbu methods. Since Spencer's method satisfies complete equilibrium of the sliding mass, it is especially well suited for analysis of tiedback slopes and walls. Spencer's solution is more rigorous than the simplified methods and requires more computation time.

11. The Linear Approximation Method provides a reliable method for determining the FOS satisfying complete

equilibrium. The method not only converges readily, it also searches for the FOS satisfying complete equilibrium, thus minimizing the number of iterations required to obtain a solution. It is believed that the LAM is unique to the STABL5 and PCSTABL5 programs.

### Recommendations

1. Since Spencer's method of slices satisfies complete equilibrium, this method should be used to analyze the stability of tiedback slopes and retaining structures whenever possible.

2. It has been shown that the LDM solution is affected by the fact that most slopes do not conform to a semi-infinite half space. Therefore, additional research should be performed to modify the LDM to account for slopes which do not satisfy the semi-infinite half space assumption used in the method.

3. A conservative approach should be used to select a suitable FOS for tiedback slopes and retaining structures since little is actually known about the factor of safety which should be used for tiedback slopes and retaining structures. This recommendation is especially important when using the results obtained from the simplified methods of slices using the LDM due to the assumptions used in the formulation of these methods.

4. The effect of soil layers with varying stiffnesses on the factor of safety obtained by the Load Distribution

Method is worthy of further study. It may be desirable to conduct finite element studies on the stability of slopes composed of soil layers of varying stiffness and compare the results with the factor of safety obtained using the LDM. It may then be possible to modify the LDM routines to account for the distribution of load through soil layers of varying stiffness.

5. Since Spencer's method of slices requires more computer time to arrive at a solution, it is recommended that Spencer's method be used to analyze only those critical potential failure surfaces found by analysis of randomly generated surfaces using the Simplified Bishop or Simplified Janbu method of slices. Following this recommendation will lead to the most efficient utilization of STABL's capabilities and the engineer's time.

6. It is strongly recommended that the new Spencer routines be thoroughly tested prior to public release of the STABL5 and PCSTABL5 programs.

7. Once the new Spencer routines have been thoroughly tested, the results obtained from analysis of tiedback slopes and walls using the Load Distribution Method should be verified against those obtained using Spencer's method.

## LIST OF REFERENCES



## LIST OF REFERENCES

References Cited

- Anderson, W.F., Hanna, T.H., and Abdel-Malek, M.N. (1983), "Overall Stability of Anchored Retaining Walls", Journal, Geotechnical Engineering Division, ASCE, GT Vol. 109, No. 11, November, 1983, pp. 1416-1433.
- Baladi, G.Y. (1968), "Distribution of Stresses and Displacements Within and Under Long Elastic and Viscoelastic Embankments", Ph.D. Thesis, Purdue University, West Lafayette, Indiana, 1968.
- Bendel, H. and Weber, E. (1966), "Erdanker System Stump Bohr A.G. Schweiz", Bauztung, 6, 1966.
- Bishop, A.W. (1955), "The Use of Slip Circles in the Stability Analysis of Slopes", Geotechnique, Vol. 5, No. 1, March, 1955, pp. 7-17.
- Boussinesq, M.J. (1885), "Application Des Potentiels, a l'Etude de l'Equilibre et du Mouvement Des Solides Elastiques", Gauthier-Villars, Paris, 1885.
- Boutrup, E. (1977), "Computerized Slope Stability Analysis for Indiana Highways", MSCE Thesis, Purdue University, West Lafayette, Indiana, 1977.
- Broms, B.B. (1968), "Swedish Tie-back Anchor System for Sheetpile Walls", Proceedings, 3rd Budapest Conference on Soil Mechanics and Foundation Engineering, 1968, pp. 391-403.
- Carpenter, J.R. (1985a), "PCSTABL4 User Manual", Joint Highway Research Project No. 85-7, School of Civil Engineering, Purdue University, West Lafayette, Indiana, May, 1985.
- Carpenter, J.R. (1986), "STABL5/PCSTABL5 User Manual", Joint Highway Research Project No. 86-14, School of Civil Engineering, Purdue University, West Lafayette, Indiana, May, 1986.

- Carter, R.K. (1971), "Computer Oriented Slope Stability Analysis by Method of Slices", MSCE Thesis, Purdue University, West Lafayette, Indiana, 1971.
- Cheney, R.S. (1984), Permanent Ground Anchors, FHWA-DP-68-1, Demonstration Projects Division, Federal Highway Administration, U.S. Department of Transportation, Washington, D.C., January, 1984.
- Flamant, A. (1886), "Stabilite des Constructions: Resistance des Matériaux", Paris, 1886.
- Fredlund, D.G. (1974), "Slope Stability Analysis User's Manual", Computer Documentation CD-4, Transportation and Geotechnical Group, Department of Civil Engineering, University of Saskatchewan, Saskatoon, Canada, December, 1974.
- Fredlund, D.G. (1981), "SLOPE-II Computer Program", User's Manual S-10, Geo-Slope Programming Ltd., Calgary Canada, 1981.
- French Code of Practice (1972), "Recommendation Concernant la Conception, le Calcul, l'Execution et le Control des Tirants d'Ancrage", Recommendation T.A. 72, Bureau Securitas, 1st ed, Paris, 1972.
- Hanna, T.H. (1978), "Ground Anchors" contained in Developments In Soil Mechanics - 1, edited by Scott, C.R., Applied Science Publishers, Ltd, London, 1978.
- Harr, M.E. (1977), Mechanics of Particulate Media, McGraw-Hill Book Company, New York, 1977.
- Krantz, E. (1953), Über die Verankerung von Spundwände, 2nd edition, Wilhelm Ernst and Son, Berlin, 1953.
- Hobst, L. and Zajic, J. (1983), Anchoring In Rock And Soil, Elsevier Scientific Publishing Company, New York, 1983.
- Janbu, N. (1954), "Application of Composite Slip Surfaces for Stability Analysis", Proceedings of the European Conference on Stability of Earth Slopes, Stockholm, Vol. 3, 1954, pp. 43-49.
- Littlejohn, G.S. (1972), "Anchored Diaphragm Walls in Sand - Anchor Design", Ground Engineering, Vol. 5, No. 1, 1972, pp. 12-17.

- Lovell, C.W., Sharma, S.S., and Carpenter, J.R. (1984), "Introduction to Slope Stability Analysis with STABL4", Joint Highway Research Project No. 84-19, School of Civil Engineering, Purdue University, West Lafayette, Indiana, July, 1984.
- Maksimovic, M. (1979), "Limit Equilibrium for Nonlinear Failure Envelope and Arbitrary Slip Surface", Third International Conference on Numerical Methods in Geomechanics, Aachen, April, 1979, pp. 769-777.
- Morgenstern, N.R. and Price, V.E. (1965), "The Analysis of the Stability of General Slip Surfaces", Geotechnique, Vol. 15, No. 1, March, 1965, pp. 79-93.
- Newmark, N.M. (1942), "Influence Charts for Computation of Stresses in Elastic Foundations", University of Illinois Engineering Experiment Station, Bulletin No. 338, University of Illinois, 1942.
- Ostermayer, H. (1977), "Practice in the Detail Design Applications of Anchorages", A Review of Diaphragm Walls, Institution of Civil Engineers, London, 1977, pp. 55-61.
- Ranke, A. and Ostermayer, H. (1968), "Beitrag zur Stabilitätsuntersuchung mehrfach verankerter Baugrubenumschließungen", ("A Contribution to the Stability Calculations of Multiple Tiedback Walls"), Die Bautechnik, Vol. 45, No. 10, 1968, pp. 341-349.
- "Recommendations of the Committee for Waterfront Structures", EAU 1980, German Society for Soil Mechanics and Foundation Engineering, 4th English ed., W. Ernst & Sohn, Berlin-Munich, 1980.
- Sangrey, D.A. (1982), "Evaluation of Landslide Properties", Application of Walls to Landslide Control Problems, edited by Reeves, R.B., ASCE, Las Vegas, Nevada, 1982, pp. 30-43.
- Schnabel, Jr., H. (1982), Tiebacks In Foundation Engineering and Construction, McGraw-Hill Book Company, New York, 1982.
- Schnabel, Jr., H. (1984), "Discussion: Overall Stability of Anchored Retaining Walls", Journal, Geotechnical Engineering Division, ASCE, GT Vol. 110, No. 12, December, 1984, pp. 1817-1818.

- Schulz, H. (1976), "The Definition of the Factor of Safety of Multi-tied Back Walls", Proceedings, 6th European Conference on Soil Mechanics and Foundation Engineering, Paris, Vol. 2, 1976, pp. 189-196.
- Sharma, S.S. and Lovell, C.W. (1983), "Strengths and Weaknesses of Slope Stability Analysis", Proceedings, 34th Annual Highway Geology Symposium, Atlanta, Georgia, 1983, pp. 215-232.
- Siegel, R.A. (1975), "Computer Analysis of General Slope Stability Problems", MSCE Thesis, Purdue University, West Lafayette, Indiana, 1975.
- Spencer, E. (1967), "A Method of Analysis of the Stability of Embankments Assuming Parallel Inter-Slice Forces", Geotechnique, Vol. 17, No. 1, March, 1967, pp. 11-26.
- Spencer, E. (1970), "The Analysis of the Stability of Embankments by the Method of Slices", Ph.D. Thesis, University of Manchester, 1970.
- Spencer, E. (1973), "Thrust Line Criterion in Embankment Stability Analysis", Geotechnique, Vol. 23, No. 1, March, 1973, pp. 85-100.
- Tenier, P. and Morlier, P. (1982), "Influence de Surcharges Concentrees sur la Stabilité des Talus", ("Influence of Concentrated Loads on Slope Stability"), Canadian Geotechnical Journal, Vol. 19, February, 1982, pp. 396-400.
- Weatherby, D.E. (1982), Tiebacks, FHWA/RD-82/047, Office of Research and Development, Federal Highway Administration, U.S. Department of Transportation, Washington, D.C., July, 1982.
- Wright, S.G. (1969), "A Study of Slope Stability and the Undrained Shear Strength of Clay Shales", Ph.D. Thesis, University of California, Berkeley, 1969.
- Wright, S.G., Kulhawy, F.H., and Duncan, J.M. (1973), "Accuracy of Equilibrium Slope Stability Analysis", Journal of the Soil Mechanics and Foundation Division, ASCE, Vol. 99, No. SM10, October, 1973, pp. 783-792.

### General References

- Carpenter, J.R. (1985b), "STABL5...The Spencer Method of Slices: Final Report", Joint Highway Research Project No. 85-17, School of Civil Engineering, Purdue University, West Lafayette, Indiana, August, 1985.
- Chen, R.H. (1981), "Three-Dimensional Slope Stability Analysis", Ph.D. Thesis, Purdue University, West Lafayette, Indiana, 1981.
- Fredlund, D.G. and Krahn, J. (1977), "Comparison of Slope Stability Methods of Analysis", Canadian Geotechnical Journal, Vol. 14, 1977, pp. 429-439.
- Goodman, M.J., Chameau, J.L., and Lovell, C.W. (1983), "Design of Compacted Clay Embankments for Improved Stability and Settlement Performance", Joint Highway Research Project No. 83-12, School of Civil Engineering, Purdue University, Indiana, August, 1983.
- Fredlund, D.G., Krahn, J., and Pufahl, D.E. (1981), "The Relationship Between Limit Equilibrium Slope Stability Methods", Proceedings of the Tenth International Conference on Soil Mechanics and Foundation Engineering, Stockholm, Sweden, Vol. 3, pp. 409-416.
- Hanna, T.H. (1982), Foundations In Tension - Ground Anchors, McGraw-Hill Book Company, New York, 1982.
- Morgenstern, N.R. and Sangrey, D.A. (1976), "Methods of Stability Analysis", contained in Landslides Analysis and Control, edited by Schuster, R.L. and Krizek, R.J., TRB Special Report No. 176, Transportation Research Board, National Academy of Sciences, Washington, D.C., 1978, pp. 155-171.
- Morgenstern, N.R. (1982), "The Analysis of Walls and Supports to Stabilize Slopes", Application of Walls to Landslide Control Problems, edited by Reeves, R.B., ASCE, Las Vegas, Nevada, 1982, pp. 19-39.
- Pfister, P., et. al. (1982), Permanent Ground Anchors - Soletanche Design Criteria, FHWA/RD-81/150, Offices of Research and Development, Federal Highway Administration, U.S. Department of Transportation, Washington, D.C., September, 1982.
- Tysinger, G.L. (1982), "Slide Stabilization 4th Rocky Fill, Clinchfield RR", Application of Walls to Landslide Control Problems, edited by Reeves, R.B., ASCE, Las Vegas, Nevada, 1982, pp. 93-107.

Weatherby, D.E. and Nicholson, P.J. (1982), "Tiebacks Used for Landslide Stabilization", Application of Walls to Landslide Control Problems, edited by Reeves, R.B., ASCE, Las Vegas, Nevada, 1982, pp. 44-60.

Whitman, R.V. and Bailey, W.A. (1967), "Use of Computers for Slope Stability Analysis", Journal of the Soil Mechanics and Foundation Division, ASCE, Vol. 93, No. SM4, July, 1967, pp. 475-498.

## APPENDIX



Derivation of Simplified Bishop Factor of Safety

1. Notation after Siegel (1975)

2.  $\Delta x, \Delta e$  are negligible (Figure A-1)

STEP I - Enforce overall moment equilibrium of sliding circular mass divided into  $n$  slices:

$$\begin{aligned}
 \Sigma M_O &= 0 \\
 &= \sum_{l=1}^n [(\Delta W(1-k_v) + \Delta U_{\beta} \cos \beta + \Delta Q \cos \delta)(R \sin \alpha)] - \sum_{l=1}^n [\Delta S_r + \Delta T \tan] R \\
 &\quad - \sum_{l=1}^n [(\Delta U_{\beta} \sin \beta + \Delta Q \sin \delta)(R \cos \alpha - h)] \\
 &\quad + \sum_{l=1}^n [\Delta W k_h (R \cos \alpha - h_{eq})] = 0
 \end{aligned} \tag{A.1}$$

where:

$R$  = Radius of the circle

$$\Delta S_r = \frac{1}{FS} [C_a' + \Delta N' \tan \phi_a'] \tag{A.2}$$

$$C_a' = \text{Cohesion force} = c' dx / \cos \alpha \tag{A.2a}$$

Dividing equation A.1 by  $R$  yields:

$$\begin{aligned}
 \Sigma M_O &= \sum_{l=1}^n [(\Delta W(1-k_v) + \Delta U_{\beta} \cos \beta + \Delta Q \cos \delta)(\sin \alpha)] - \sum_{l=1}^n [\Delta S_r + \Delta T \tan] \\
 &\quad - \sum_{l=1}^n [(\Delta U_{\beta} \sin \beta + \Delta Q \sin \delta)(\cos \alpha - \frac{h}{R})] \\
 &\quad + \sum_{l=1}^n [\Delta W k_h (\cos \alpha - \frac{h_{eq}}{R})] = 0
 \end{aligned} \tag{A.3}$$

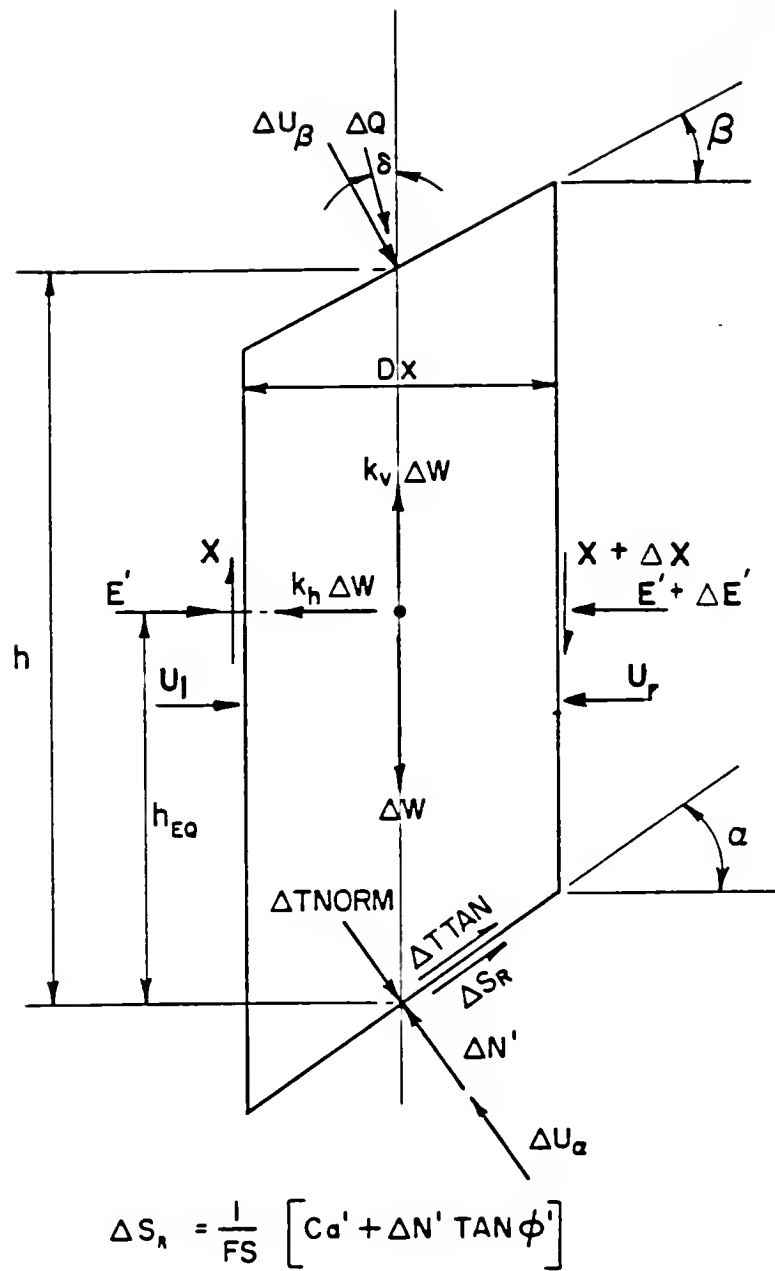


FIGURE A-1. Slice Forces Considered for Derivation of Simplified Bishop Method of Slices Using Load Distribution Method

STEP II - Substitute  $\Delta S_r$  into equation A.3, assume the factor of safety is equal for each slice, and solve for FS:

$$FS = \frac{\sum_1^n (C_a' + \Delta N' \tan \phi_a')}{\sum_1^n A_3 - \sum_1^n A_4 + \sum_1^n A_5 - \sum_1^n A_6} \quad (A.4)$$

where:

$$A_3 = (\Delta W(1-k_v) + \Delta U_\beta \cos \beta + \Delta Q \cos \delta) \sin \alpha \quad (A.4a)$$

$$A_4 = (\Delta U_\beta \sin \beta + \Delta Q \sin \delta) \left( \cos \alpha - \frac{h}{R} \right) \quad (A.4b)$$

$$A_5 = \Delta W k_h \left( \cos \alpha - \frac{h_{eq}}{R} \right) \quad (A.4c)$$

$$A_6 = \Delta TTAN \quad (A.4d)$$

STEP III - Sum forces in vertical direction for each slice:

$$\Sigma F_v = 0$$

$$\begin{aligned} &= \Delta U_\beta \cos \beta + \Delta Q \cos \delta + \Delta W(1-k_v) + (\Delta TNORM - \Delta N' - \Delta U_\alpha) \cos \alpha \\ &- (\Delta TTAN + \Delta S_r) \sin \alpha = 0 \end{aligned} \quad (A.5)$$

Substitute  $\Delta S_r$  into equation A.5:

$$\begin{aligned} \Sigma F_v &= \Delta U_\beta \cos \beta + \Delta Q \cos \delta + \Delta W(1-k_v) + (\Delta TNORM - \Delta N' - \Delta U_\alpha) \cos \alpha \\ &- \left( \Delta TTAN + \frac{1}{FS} (C_a' + \Delta N' \tan \phi_a') \right) \sin \alpha = 0 \end{aligned} \quad (A.6)$$

Solve equation A.6 for  $\Delta N'$ :

$$\begin{aligned} \Delta N' \left| \cos \alpha + \frac{\tan \phi_a' \sin \alpha}{FS} \right| &= \Delta U_\beta \cos \beta + \Delta Q \cos \delta + \Delta W(1-k_v) \\ &+ (\Delta TNORM - \Delta U_\alpha) \cos \alpha - \Delta TTAN \sin \alpha - \frac{C_a' \sin \alpha}{FS} \end{aligned} \quad (A.7)$$



Rearranging:

$$\Delta N' = \frac{\Delta W(1-k_v) - C_a'}{\quad} \quad (A.8)$$

STEP IV - Substitute equati

$$FS = \frac{\sum_{l=1}^n C_a' + \tan \phi'_a}{\quad} \quad (A.9)$$

Rearranging numerator yield

$$FS = \frac{\sum_{l=1}^n \left[ C_a' \cos \alpha + \frac{\tan \phi'_a}{\cos \alpha} \right]}{\quad} \quad (A.10)$$

Simplifying numerator and d

$$FS = \frac{\sum_{l=1}^n \left[ C_a' + \frac{\tan \phi'_a}{\cos \alpha} \right]}{\quad} \quad (A.11)$$



Rearranging:

$$\Delta N' = \frac{\Delta W(1-k_v) - C_a' \sin \alpha / FS - \Delta T \tan \alpha \sin \alpha + \Delta Q \cos \delta + \Delta U_\beta \cos \beta + (\Delta T \text{NORM} - \Delta U_\alpha) \cos \alpha}{\cos \alpha + \frac{\tan \phi'_a \sin \alpha}{FS}} \quad (\text{A.8})$$

STEP IV - Substitute equation A.8 into equation A.4 to yield:

$$FS = \frac{\sum_{l=1}^n \left| C_a' + \tan \phi'_a \right| \left| \frac{\Delta W(1-k_v) - C_a' \sin \alpha / FS - \Delta T \tan \alpha \sin \alpha + \Delta Q \cos \delta + \Delta U_\beta \cos \beta + (\Delta T \text{NORM} - \Delta U_\alpha) \cos \alpha}{\cos \alpha + \frac{\tan \phi'_a \sin \alpha}{FS}} \right|}{\sum_{l=1}^n A_3 - \sum_{l=1}^n A_4 + \sum_{l=1}^n A_5 - \sum_{l=1}^n A_6} \quad (\text{A.9})$$

Rearranging numerator yields:

$$FS = \frac{\sum_{l=1}^n \left| C_a' \left| \cos \alpha + \frac{\tan \phi'_a \sin \alpha}{FS} \right| + \tan \phi'_a \left| \Delta W(1-k_v) - C_a' \sin \alpha / FS - \Delta T \tan \alpha \sin \alpha + \Delta Q \cos \delta + \Delta U_\beta \cos \beta + (\Delta T \text{NORM} - \Delta U_\alpha) \cos \alpha \right| \right|}{\sum_{l=1}^n A_3 - \sum_{l=1}^n A_4 + \sum_{l=1}^n A_5 - \sum_{l=1}^n A_6} \quad (\text{A.10})$$

Simplifying numerator and dividing numerator by  $\cos \alpha$  yields:

$$FS = \frac{\sum_{l=1}^n \left| C_a' + \frac{\tan \phi'_a}{\cos \alpha} \right| \left| \Delta W(1-k_v) - \Delta T \tan \alpha \sin \alpha + \Delta Q \cos \delta + \Delta U_\beta \cos \beta + (\Delta T \text{NORM} - \Delta U_\alpha) \cos \alpha \right|}{\sum_{l=1}^n A_3 - \sum_{l=1}^n A_4 + \sum_{l=1}^n A_5 - \sum_{l=1}^n A_6} \quad (\text{A.11})$$



For simplicity in coding, equation A.11 may be written as:

$$FS = \frac{\sum_{l=1}^n A_3 - \sum_{l=1}^n A_4 + \sum_{l=1}^n A_5 - \sum_{l=1}^n A_6}{\sum_{l=1}^n \left| \frac{A_1}{1 + A_2/FS} \right|} \quad (A.12)$$

where:

$$A_1 = C_a' + \tan\phi_a' \sec\alpha(\Delta W(1-k_v) - \Delta TTANsina + \Delta Q\cos\delta + \Delta U_\beta\cos\beta + (\Delta TNORM - \Delta U_\alpha)\cos\alpha) \quad (A.12a)$$

$$A_2 = \tan\phi_a' \tan\alpha \quad (A.12b)$$

and where  $A_3$  through  $A_6$  are as defined earlier (see equations A.4a - A.4d).

Equation A.12 is programmed in STABL4, PCSTABL4, STABL5 and PCSTABL5.





COVER DESIGN BY ALDO GIORGINI